Non-adiabatic Mapping Dynamics in the Phase Space of the $SU(N)$ Lie Group

Duncan Bossion,[1, a)] Wenxiang Ying,[1] Sutirtha N. Chowdhury,[1, 2] and Pengfei Huo[1, 3, b)]
[1)] *Department of Chemistry, University of Rochester, 120 Trustee Road, Rochester, New York 14627, USA*
[2)] *Department of Chemistry, Duke University, 3236 French Science Center, 124 Science Drive, Durham, North Carolina 27708, USA*
[3)] *The Institute of Optics, Hajim School of Engineering, University of Rochester, Rochester, New York 14627, USA*

(Dated: 26 May 2022)

We present the rigorous theoretical framework of the generalized spin mapping representation for non-adiabatic dynamics. This formalism is based on the generators of the $\mathfrak{su}(N)$ Lie algebra to represent N discrete electronic states, thus preserving the size of the original Hilbert space in the state representation. The Stratonovich-Weyl transform is then used to map an operator in the Hilbert space to a continuous function on the $SU(N)$ Lie Group *manifold* which is a phase space of continuous variables. Wigner representation is used to describe the nuclear degrees of freedom. Using the above representations, we derived an exact expression of the time-correlation function as well as the exact quantum Liouvillian. Making the linearization approximation, this exact Liouvillian is reduced to the Liouvillian of the several recently proposed methods. These expressions lead to a self-consistent trajectory-based method to simulate non-adiabatic dynamics, which is based entirely on the generalized spin mapping formalism to treat the electronic states without the necessity of converting back to the cartesian Meyer-Miller-Stock-Thoss mapping variables. We envision that the theoretical work presented in this work provides a rigorous and unified framework to formally derive non-adiabatic quantum dynamics approaches with continuous variables.

I. INTRODUCTION

Studying non-adiabatic dynamics in quantum systems, particularly in condensed phase, is a central challenge for modern theoretical chemistry.[1] In this context, we are interested in the quantum dynamics of a system with N electronic states coupled to nuclear degrees of freedom (DOFs) as follows

$$\begin{aligned}\hat{H} =&\big[\hat{T}_R + U_0(\hat{R})\big]\hat{\mathcal{I}} + \hat{V}_{\mathrm{e}}(\hat{R}) \\ =&\big[\hat{T}_R + U_0(\hat{R})\big]\hat{\mathcal{I}} + \sum_n V_{nn}(\hat{R})|n\rangle\langle n| \\ &+ \sum_{n\neq m} V_{nm}(\hat{R})|n\rangle\langle m|,\end{aligned} \tag{1}$$

where $\hat{T}_R$ is the nuclear kinetic energy, $U_0(\hat{R})$ represents the state-independent part of the potential, and $\hat{V}_{\mathrm{e}}(\hat{R})$ is the state-dependent part of the potential. Further, $\hat{R}$ represents a nuclear DOF, $\{|n\rangle\}$ represents a set of diabatic electronic states, and $V_{nm}(\hat{R}) = \langle n|\hat{V}_{\mathrm{e}}(\hat{R})|m\rangle$ is the matrix element of $\hat{V}_{\mathrm{e}}(\hat{R})$ in this diabatic representation. The identity operator $\hat{\mathcal{I}} = \sum_{n=1}^{N}|n\rangle\langle n|$ represents the identity in the electronic Hilbert space. In order to avoid an exponential numerical scaling with the number of DOFs of the system, different approximate methods have been developed. Trajectory-based quantum-classical methods are among the most successful ones as

[a)] Electronic mail: dbossion@ur.rochester.edu
[b)] Electronic mail: pengfei.huo@rochester.edu

Non-adiabatic Mapping Dynamics in the Phase Space of the $SU(N)$ Lie Group

Duncan Bossion,[1, a)] Wenxiang Ying,[1] Sutirtha N. Chowdhury,[1, 2] and Pengfei Huo[1, 3, b)]
[1)] *Department of Chemistry, University of Rochester, 120 Trustee Road, Rochester, New York 14627, USA*
[2)] *Department of Chemistry, Duke University, 3236 French Science Center, 124 Science Drive, Durham, North Carolina 27708, USA*
[3)] *The Institute of Optics, Hajim School of Engineering, University of Rochester, Rochester, New York 14627, USA*

(Dated: 26 May 2022)

We present the rigorous theoretical framework of the generalized spin mapping representation for non-adiabatic dynamics. This formalism is based on the generators of the $\mathfrak{su}(N)$ Lie algebra to represent N discrete electronic states, thus preserving the size of the original Hilbert space in the state representation. The Stratonovich-Weyl transform is then used to map an operator in the Hilbert space to a continuous function on the $SU(N)$ Lie Group *manifold* which is a phase space of continuous variables. Wigner representation is used to describe the nuclear degrees of freedom. Using the above representations, we derived an exact expression of the time-correlation function as well as the exact quantum Liouvillian. Making the linearization approximation, this exact Liouvillian is reduced to the Liouvillian of the several recently proposed methods. These expressions lead to a self-consistent trajectory-based method to simulate non-adiabatic dynamics, which is based entirely on the generalized spin mapping formalism to treat the electronic states without the necessity of converting back to the cartesian Meyer-Miller-Stock-Thoss mapping variables. We envision that the theoretical work presented in this work provides a rigorous and unified framework to formally derive non-adiabatic quantum dynamics approaches with continuous variables.

they scale linearly with the number of DOFs and allow for a simple numerical propagation scheme. One of the most popular trajectory-based approach is the surface-hopping method,[2–6] where an ensemble of classical trajectories hop among electronic states upon non-adiabatic transitions, mimicking the wavepacket branching dynamics. The other widely used approach is the Ehrenfest trajectory dynamics where the nuclear DOFs feel a time-dependent mean field potential from the quantum subsystem's time evolution.

In a separate direction, the idea of mapping variables is proposed to represent quantum transitions among discrete electronic states as classical-like motion of continuous phase space variables,[7,8] thus treating all the DOFs on an equal footing. Historically, one of the most successful mapping theories in physical chemistry is the Meyer-Miller-Stock-Thoss (MMST) mapping formalism,[8–10] which maps a N-level system onto N singly excited harmonic oscillators, and thus can be viewed as a generalization of the Schwinger's bosonization approach.[10] The mapping variables of the MMST formalism are conjugate position and momentum of each mapping oscillator. This method, despite its great success and broad applications,[11–19] has known flaws.[20–22] This is because the MMST mapping operators belong to a larger Hilbert space that contains other states outside the singly excited oscillator (SEO) subspace of the mapping oscillators, whereas the MMST mapping procedure tries to map the original electronic subspace onto the SEO subspace. It thus requires a projection back to the singly excited mapping subspace to obtain accurate results.[20–22] As a consequence, the identity operator is not preserved through the MMST mapping and there is an ambiguity of how to evaluate it.[22] Related

to the problem of the non-conserving identity, the non-adiabatic dynamics is sensitive to the separation between the state-dependent and the state-independent Hamiltonian.[21,23] Moreover, projecting the Hilbert space to the SEO subspace also ruins the original simple commutation relations among the MMST mapping operators in their full Hilbert space,[24] making the mapping Hamiltonian potentially containing more terms that require additional approximations to parameterize.[25]

Mathematically, the idea of mapping relation is referred to as the generalized Weyl correspondence, in which Lie groups and Lie algebras are the central components.[26–28] Lie algebras are formed by commutation relations among generators with given structure constants; the elements of a connected matrix Lie group[29] can be expressed as the exponential of the Lie algebra generators, *i.e.*, the exponential map.[30] On the other hand, a Lie group is also a differentiable manifold, which is a phase space with continuous variables. The dual identity of Lie groups naturally construct a bijective map between operators described by the generators represented in the Hilbert space and continuous functions on the differentiable manifold.

Following this fundamental idea of mapping, one of the most natural ways to map a N-level quantum system is to respect its original symmetry, which is described by the special unitary symmetry group[31] $SU(N)$. For $N = 2$, it is well-known that the quantum dynamics of two electronic states can be mapped as the spin precession around a magnetic field (represented by the Hamiltonian) described by the motion of the Bloch vector on the Bloch sphere,[32,33] due to the $SU(2)$ symmetry shared by both problems. Thoss and Stock have developed a semiclassical initial-value representation of the corresponding propagator using the $SU(2)$ mapping.[10] Recently, Runeson and Richardson used this spin mapping approach to map a two-level system on a single spin-$\frac{1}{2}$ DOFs.[34] The same mapping formalism was also used to develop non-adiabatic path-integral approaches.[35]

One can, in principle, generalize this idea by mapping a N-level system with the generators of the $\mathfrak{su}(N)$ Lie algebra. The unique advantage of this mapping procedure compared to the MMST formalism is that the commutation relations among operators as well as the size of the Hilbert space are exactly preserved in the $SU(N)$ representation. The corresponding quantum equations of motion (EOMs) for the $SU(N)$ mapping were first introduced by Hioe and Eberly,[36] which can be viewed as the generalization of the spin precession to N-dimensions with $SU(N)$ symmetry.[36] The $SU(N)$ mapping has also been used recently for density matrix mapping.[37] Meyer, McCurdy, and Miller[7,38,39] also used a similar idea to map two-state or three-state systems with spin-$\frac{1}{2}$ and spin-1 operators, although the matrices of the spin-1 operators (which are not necessarily traceless) are different than the $\mathfrak{su}(N)$ generators (which are traceless).[40] Note that the $SU(N)$ mapping formalism is also different than the recent spin-mapping formalism introduced by Cot-

ton and Miller,[41] which maps N states onto N spin-$\frac{1}{2}$ particles,[42] hence having the symmetry of $\otimes_N SU(2)$ that is different than $SU(N)$.

Recently, Runeson and Richardson used the spin operators (which are equivalent to the generators of the $\mathfrak{su}(N)$ Lie algebra up to a constant) and the $SU(N)$ Lie group to perform the non-adiabatic mapping dynamics of a N-state vibronic Hamiltonian, and developed the spin-Linearized semi-classical (spin-LSC) approach.[43] In particular, the Stratonovich-Weyl (S-W) transform[27,28,44,45] is used to map an operator in the Hilbert space described by the generators (of the $\mathfrak{su}(N)$ Lie algebra) to a continuous function on the Lie group/manifold, resulting in a classical-like Hamiltonian. The S-W transform evaluates the expectation values of the spin operators under the generalized spin coherent states.[46,47] The generalized spin coherent states[48–50] are further expressed as a linear expansion of the diabatic electronic states, and the real and imaginary parts of the expansion coefficients are further defined as the conjugate position and momentum variables,[43] leading to an equivalence between the generalized spin-based mapping Hamiltonian and the MMST mapping Hamiltonian. Using the connection between these two Hamiltonians, Runeson and Richardson found the particular choice of zero-point energy parameter for the MMST Hamiltonian as well as an expression of the estimators. With a proposed sampling procedure of the initial conditions that constrains a total population equal to one, spin-LSC effectively propagates the EOMs with a total of $2N$ MMST variables ($2N-2$ independent mapping variables when considering the population constraint). This is a reasonable choice for constructing an algorithm for approximate quantum dynamics, as it avoids deriving the EOMs in the generalized Euler angles of the spin coherent state, which is highly non-trivial. However, this choice also brings the potential confusions[25] that the MMST mapping Hamiltonian is a necessary and essential ingredient in the $SU(N)$ mapping formalism.[43] Further, the EOMs of the spin-LSC approach[43] were not rigorously derived, and there is a lack a rigorous derivation of the time-correlation function as well. In a related direction, the Generalized Discrete Truncated Wigner Approximation (GDTWA) approach[51] is developed using the generators of the $\mathfrak{su}(N)$ Lie algebra. The EOMs for GDTWA were argued as the classical limit of the Heisenberg EOMs[51] of the corresponding operators and generators, where the classical variables for those generators (N^2-1 of them) obey the equations of the N-dimensional spin precession theory by Hioe and Eberly.[36] However, the EOMs are not rigorously derived in GDTWA approach,[51] and their connection with the MMST-type of EOMs used in spin-LSC[43] remains to be discovered.

In this work, we provide rigorous theoretical derivations of non-adiabatic mapping dynamics in the phase space of the $SU(N)$ Lie group. Thus, the current work can be viewed as a rigorous theoretical justification of the generalized spin mapping formalism by Rune-

The relations between SU(F) Stratonovich phase space and Meyer-Miller mapping model are first proposed in Appendix 3 of WIREs. Comput. Mol. Sci. e1619 (2022), especially the EOMs of SU(F) angle variables with an evolving global phase are also listed in this appendix, which is identical to those of Meyer-Miller mapping variables. However, this manuscript intentionally ignore the contributions of WIREs. Comput. Mol. Sci. e1619 (2022) and cite it nowhere.

son and Richardson.[43] We will not distinguish between the nomenclature of generalized spin mapping and the $SU(N)$ mapping in this paper when we mention this mapping formalism. In Sec. II, we briefly review the generators of the $\mathfrak{su}(N)$ Lie algebra which are used as the operator basis to represent the Hamiltonian and any operators in the electronic Hilbert space, and derive the analytic expression of the structure constants of the $\mathfrak{su}(N)$ Lie algebra (presented in Appendix A). In Sec. III we briefly review some basic properties of the S-W transform[27,44,50] which effectively constructs a mapping relation between an operator described by the generators in the Hilbert space to a continuous function on the Lie group/manifold. Note that Sec. II and Sec. III are used to set up the theoretical background for our work presented in this paper, where similar expressions/discussions can be found in part in the previous works.[43,51]

Sec. IV to Sec. VI present our *main theoretical contributions* in this work. In Sec. IV, we present a mixed Wigner/S-W representation that performs Wigner transform on the nuclear DOFs and S-W transform on the electronic DOFs, and derive the exact expressions of the time-correlation function (TCF). In Sec. V, we derive the exact quantum Liouvillian expression (Eq. 85-89). under the mixed Wigner/S-W representation. Using this exact expression, we can explore approximate forms of the Liouvillian under the linearization approximation, which gives the EOMs with the variables of the spin coherent state expectation values (Eq. 98). These EOMs are identical to those proposed in the GDTWA approach,[51] which can also be viewed as a generalization of the Hioe-Eberly theory[36] of the N-dimensional spin precession with the explicit presence of the nuclear DOFs.

The "derivation" of eq (98) is still not so clear to us. From eqs (94) and (96) we arrive at eq (98), which coincides with equations of motion in J. Chem. Phys. 155, 024111 (2021). However, there is no explanation why they do not use eq (97).

The EOMs under the linearization approximation (Eq. 98) are shown to have three equivalent forms, documented in Sec. VI with (1) the conjugated action-angle type variables (Eq. 102), (2) the generalized Euler angles on multi-dimensional Bloch sphere (Eq. 113), and (3) the MMST Cartesian phase space variables (Eq. 117). The TCF and the EOMs under the linearized approximation are used as a trajectory-based non-adiabatic method in the mixed Wigner/S-W formalism. We perform numerical simulations to demonstrate the accuracy of this method by simulating non-adiabatic population dynamics of challenging model systems. We emphasize that despite that our work is inspired by the recent spin mapping formalism,[34,43,51] we have made several unique theoretical contributions in the current work, which are detailed in the Conclusion section.

We envision that the theoretical work presented in this work provides a rigorous and unified framework to formally derive non-adiabatic quantum dynamics approaches with continuous variables.

II. GENERATORS OF THE $\mathfrak{su}(N)$ LIE ALGEBRA

In this section, we review how to use the generators of the $\mathfrak{su}(N)$ Lie algebra[36,43] to represent a Hamiltonian operator. The $\mathfrak{su}(N)$ Lie algebra and its corresponding Lie group are widely used in fundamental physics, particularly in the Standard Model of particle physics.[31,52,53] For example, the $\mathfrak{su}(2)$ Lie algebra is used to describe the spin-$\frac{1}{2}$ system. The generators of $\mathfrak{su}(2)$ are the spin operators $\hat{\mathcal{S}}_j = \frac{\hbar}{2}\sigma_j$ with the two-dimensional represented Pauli matrices defined as follows

$$\sigma_1 = \begin{pmatrix} 0 & 1 \\ 1 & 0 \end{pmatrix},\ \sigma_2 = \begin{pmatrix} 0 & -i \\ i & 0 \end{pmatrix},\ \sigma_3 = \begin{pmatrix} 1 & 0 \\ 0 & -1 \end{pmatrix}.$$

The generators of the $\mathfrak{su}(3)$ Lie algebra are $\hat{\mathcal{S}}_j = \frac{\hbar}{2}\lambda_j$, where three-dimensional represented λ_j are the well-known Gell-Mann $\lambda-$matrices[54] defined as follows

$$\lambda_1 = \begin{pmatrix} 0 & 1 & 0 \\ 1 & 0 & 0 \\ 0 & 0 & 0 \end{pmatrix},\ \lambda_2 = \begin{pmatrix} 0 & -i & 0 \\ i & 0 & 0 \\ 0 & 0 & 0 \end{pmatrix},\ \lambda_3 = \begin{pmatrix} 1 & 0 & 0 \\ 0 & -1 & 0 \\ 0 & 0 & 0 \end{pmatrix},$$

$$\lambda_4 = \begin{pmatrix} 0 & 0 & 1 \\ 0 & 0 & 0 \\ 1 & 0 & 0 \end{pmatrix},\ \lambda_5 = \begin{pmatrix} 0 & 0 & -i \\ 0 & 0 & 0 \\ -i & 0 & 0 \end{pmatrix},\ \lambda_6 = \begin{pmatrix} 0 & 0 & 0 \\ 0 & 0 & 1 \\ 0 & 1 & 0 \end{pmatrix},$$

$$\lambda_7 = \begin{pmatrix} 0 & 0 & 0 \\ 0 & 0 & -i \\ 0 & i & 0 \end{pmatrix},\ \lambda_8 = \frac{1}{\sqrt{3}}\begin{pmatrix} 1 & 0 & 0 \\ 0 & 1 & 0 \\ 0 & 0 & -2 \end{pmatrix}.$$

They are widely used in quantum chromodynamics as an approximate symmetry of the strong interaction between quarks and gluons.[54] The generators of an algebra can be obtained in different ways, but the most commonly used ones in physics are based on a generalization of the Pauli matrices of $\mathfrak{su}(2)$ and of the Gell-Mann matrices[54] of $\mathfrak{su}(3)$, which are what we use in this work. This specific way of representing the generators is commonly referred to as the Generalized Gell–Mann matrix (GGM) basis.[50,53] In the following, we briefly review the general expressions of these GGM generators. The commutation (and anti-commutation) relations among these generators are defined in the $\mathfrak{su}(N)$ Lie algebra, whereas the exponential functions of these generators construct the elements of the $SU(N)$ Lie group via the exponential map.[29,31]

The elements of the GGM basis are denoted as $\hat{\mathcal{S}}_i$ with $i \in \{1, \cdots, N^2-1\}$. There are $N(N-1)/2$ symmetric matrices

$$\hat{\mathcal{S}}_{\alpha_{nm}} = \frac{\hbar}{2}\big(|m\rangle\langle n| + |n\rangle\langle m|\big), \tag{2}$$

$N(N-1)/2$ anti-symmetric matrices,

$$\hat{\mathcal{S}}_{\beta_{nm}} = -i\frac{\hbar}{2}\big(|m\rangle\langle n| - |n\rangle\langle m|\big), \tag{3}$$

and $N-1$ diagonal matrices,

$$\hat{\mathcal{S}}_{\gamma_n} = \frac{\hbar}{\sqrt{2n(n-1)}}\Big(\sum_{l=1}^{n-1}|l\rangle\langle l| + (1-n)|n\rangle\langle n|\Big), \tag{4}$$

where we introduced the indices α_{nm} related to the symmetric matrices, β_{nm} related to the anti-symmetric matrices, and γ_n related to the diagonal matrices as follows

$$\alpha_{nm} = n^2 + 2(m-n) - 1, \tag{5a}$$
$$\beta_{nm} = n^2 + 2(m-n), \tag{5b}$$
$$\gamma_n = n^2 - 1. \tag{5c}$$

Note that in the above definitions, $1 \leq m < n \leq N$ and $2 \leq n \leq N$, and the generators are ordered according to the conventions.[53,55] Another commonly used notation[55] is $\hat{\Lambda}$, where $\hat{\mathcal{S}}_i = \frac{\hbar}{2}\hat{\Lambda}_i$.

These generators are traceless,

$$\mathrm{Tr_e}[\hat{\mathcal{S}}_i] = 0, \tag{6}$$

and are orthonormal to each other as

$$\mathrm{Tr_e}\big[\hat{\mathcal{S}}_i\hat{\mathcal{S}}_j\big] = \frac{\hbar^2}{2}\delta_{ij}. \tag{7}$$

The commutation and anti-commutation relations among the generators of the $\mathfrak{su}(N)$ *Lie algebra* are presented as follows

$$\big[\hat{\mathcal{S}}_i, \hat{\mathcal{S}}_j\big] = i\hbar \sum_{k=1}^{N^2-1} f_{ijk}\hat{\mathcal{S}}_k, \tag{8a}$$

$$\big\{\hat{\mathcal{S}}_i, \hat{\mathcal{S}}_j\big\}_+ = \frac{\hbar^2}{N}\delta_{ij}\hat{\mathcal{I}} + \hbar \sum_{k=1}^{N^2-1} d_{ijk}\hat{\mathcal{S}}_k, \tag{8b}$$

where $\{\hat{\mathcal{S}}_i, \hat{\mathcal{S}}_j\}_+$ represents the anti-commutator between $\hat{\mathcal{S}}_i$ and $\hat{\mathcal{S}}_j$, the indices $i, j, k \in \{\alpha_{nm}, \beta_{nm}, \gamma_n\}$, and f_{ijk} and d_{ijk} are the totally anti-symmetric and totally symmetric *structure constants*, respectively. Using Eqs. 8a-8b, one can obtain the following well-known expressions for these structure constants

$$f_{ijk} = -i\frac{2}{\hbar^3}\mathrm{Tr}\Big[\big[\hat{\mathcal{S}}_i, \hat{\mathcal{S}}_j\big]\hat{\mathcal{S}}_k\Big], \tag{9a}$$

$$d_{ijk} = \frac{2}{\hbar^3}\mathrm{Tr}\Big[\big\{\hat{\mathcal{S}}_i, \hat{\mathcal{S}}_j\big\}_+\hat{\mathcal{S}}_k\Big]. \tag{9b}$$

Despite the extensive usage and the crucial role these structure constants play in modern physics, there is no analytic expression (closed formulas) of f_{ijk} and d_{ijk}. Here, we derive these analytic formulas for these structure constants in Appendix A, with their analytic expressions listed in Eq. A5 for f_{ijk} and in Eq. A14 for d_{ijk}.

One can express the Hamiltonian in Eq. 1 through the generators as $\hat{H} = C_0\hat{\mathcal{I}} + \sum_{k=1}^{N^2-1} C_k\hat{\mathcal{S}}_k$ due to the completeness of the generators. To figure out C_j, we perform $\mathrm{Tr_e}[\hat{H}\cdot\hat{\mathcal{S}}_j] = C_0\mathrm{Tr_e}[\hat{\mathcal{S}}_j] + \sum_{k=1}^{N^2-1} C_k\mathrm{Tr_e}[\hat{\mathcal{S}}_k\cdot\hat{\mathcal{S}}_j] = \hbar^2 C_j/2$, thus $C_j = (2/\hbar^2)\cdot\mathrm{Tr_e}[\hat{H}\cdot\hat{\mathcal{S}}_j]$, where we have used the property of Eq. 6 and Eq. 7. Here, we explicitly indicate the trace over the electronic DOFs by using $\mathrm{Tr_e}$. Further, we have $\mathrm{Tr_e}[\hat{H}] = C_0\mathrm{Tr_e}[\hat{\mathcal{I}}] + \sum_{k=1}^{N^2-1} C_k\mathrm{Tr_e}[\hat{\mathcal{S}}_k] = C_0 N$, thus $C_0 = (1/N)\cdot\mathrm{Tr_e}[\hat{H}]$. Putting these together, one can

represent the Hamiltonian in Eq. 1 using the generators as follows[36,43]

$$\hat{H} = \mathcal{H}_0(\hat{R}) \cdot \hat{\mathcal{I}} + \frac{1}{\hbar} \sum_{k=1}^{N^2-1} \mathcal{H}_k(\hat{R}) \cdot \hat{\mathcal{S}}_k, \tag{10}$$

where the elements $\mathcal{H}_0(\hat{R})$ and $\mathcal{H}_k(\hat{R})$ are expressed as

$$\mathcal{H}_0(\hat{R}) = \frac{1}{N}\mathrm{Tr}_\mathrm{e}\big[\hat{H} \cdot \hat{\mathcal{I}}\big] = \hat{T}_R + U_0(\hat{R}) + \frac{1}{N}\sum_{n=1}^{N} V_{nn}(\hat{R}), \tag{11a}$$

$$\mathcal{H}_k(\hat{R}) = \frac{2}{\hbar}\mathrm{Tr}_\mathrm{e}\big[\hat{H} \cdot \hat{\mathcal{S}}_k\big] = \frac{2}{\hbar}\mathrm{Tr}_\mathrm{e}\big[\hat{V}_\mathrm{e}(\hat{R}) \cdot \hat{\mathcal{S}}_k\big]. \tag{11b}$$

This expansion can also be easily verified using the relation between $|n\rangle\langle m|$ and the GMM matrices in Eq. 2-Eq. 4. Note that Eq. 11 has an explicit separation of the trace and traceless parts of the potential, due to the traceless generators in Eqs. 2-4 where $\mathrm{Tr}_\mathrm{e}[\hat{\mathcal{S}}_i] = 0$. Enforcing this separation in the MMST mapping formalism can significantly improve the stability and accuracy of the dynamics.[21,23,35] In the $SU(N)$ mapping formalism, this is intrinsically enforced.

Using the generators defined in Eqs. 2-4, we can explicitly write $\mathcal{H}_k(\hat{R})$ in Eq. 11b as

$$\mathcal{H}_{\alpha_{nm}}(\hat{R}) = V_{mn}(\hat{R}) + V_{nm}(\hat{R}), \tag{12a}$$

$$\mathcal{H}_{\beta_{nm}}(\hat{R}) = i\big(V_{mn}(\hat{R}) - V_{nm}(\hat{R})\big), \tag{12b}$$

$$\mathcal{H}_{\gamma_n}(\hat{R}) = \sum_{l=1}^{n-1}\sqrt{\frac{2}{n(n-1)}}V_{ll}(\hat{R}) - \sqrt{\frac{2(n-1)}{n}}V_{nn}(\hat{R}), \tag{12c}$$

with $1 \leq m < n \leq N$ and $2 \leq n \leq N$ as previously introduced.

In the special case where the system does not have any nuclear (or other) DOF, we can write down the exact quantum Liouville equation for this closed system as

$$i\hbar\frac{\partial\hat{\rho}}{\partial t} = \big[\hat{H}, \hat{\rho}\big], \tag{13}$$

where the commutator is taken within the electronic subspace. The $\mathfrak{su}(N)$ representation of the density operator is

$$\hat{\rho} = \frac{1}{N}\hat{\mathcal{I}} + \frac{1}{\hbar}\sum_{k=1}^{N^2-1} \mathcal{S}_k \cdot \hat{\mathcal{S}}_k, \tag{14}$$

where $\mathcal{S}_k = \frac{2}{\hbar}\mathrm{Tr}[\hat{\rho}\hat{\mathcal{S}}_k]$, as well as the corresponding expression for $\hat{H} = \mathcal{H}_0 \cdot \hat{\mathcal{I}} + \frac{1}{\hbar}\sum_{k=1}^{N^2-1}\mathcal{H}_k \cdot \hat{\mathcal{S}}_k$, the quantum Liouville equation is equivalently expressed as[36]

$$\frac{\mathrm{d}}{\mathrm{d}t}\mathcal{S}_i = \frac{1}{\hbar}\sum_{j,k=1}^{N^2-1} f_{ijk}\mathcal{H}_j\mathcal{S}_k, \tag{15}$$

which can be viewed as the generalization of the spin precession (see Eq. E7) to N dimensions, originally discovered by Hioe and Eberly.[36] This relation was suggested as the time development of the N-level coherence vector. In the following sections, we will generalize this formalism and develop the corresponding theory when the Hamiltonian explicitly contains nuclear DOFs.

III. STRATONOVICH-WEYL TRANSFORM AND THE SPIN MAPPING FORMALISM

The S-W transform constructs a mapping between an operator in the Hilbert space to a continuous function on the Lie group/manifold. Here, we present the properties of this transformation for a general N-level system.

A. Spin Coherent States

For a spin (or equivalently, a two-level system), one can use the following spin coherent states[46]

$$|\mathbf{u}\rangle = \cos\frac{\theta}{2}|1\rangle + \sin\frac{\theta}{2}\cdot e^{i\varphi}|2\rangle \tag{16}$$

as a basis to describe the quantum dynamics,[34,35] where θ and φ are the angles defining the Bloch vector, with the radius of the Bloch sphere being fixed.[56]

The spin coherent states $|\mathbf{u}\rangle$ can be generalized for a N-level system, denoted as $|\mathbf{\Omega}\rangle$, through a rigorous procedure with Lie groups and Lie algebras. Mathematically, these generalized spin-coherent states $|\mathbf{\Omega}\rangle$ are introduced by acting a parametrized unitary transformation operator on a given diabatic basis $|n\rangle$, *i.e.*, $|\mathbf{\Omega}\rangle = \hat{U}(\boldsymbol{\theta},\boldsymbol{\varphi})|n\rangle$, where the unitary transformation operator $\hat{U}(\boldsymbol{\theta},\boldsymbol{\varphi})$ is an exponential function to linear order of the generators $\hat{\mathcal{S}}$ (Eq. 2-Eq. 4) associated with real parameters $\{\boldsymbol{\theta},\boldsymbol{\varphi}\}$. The detailed expression of $\hat{U}(\boldsymbol{\theta},\boldsymbol{\varphi})$ can be found in Eq. (2.6) of Ref. 50. This particular expression is referred to as the generalized Euler angle parametrization of $\mathfrak{su}(N)$,[49] which gives rise to a continuous phase space. Actually, one can regard $\hat{U}(\boldsymbol{\theta},\boldsymbol{\varphi})$ as a unitary representation[26,31] of the $SU(N)$ Lie group.[57]

The generalized spin coherence state can be expressed as

$$|\mathbf{\Omega}\rangle = \sum_{n=1}^{N} |n\rangle\langle n|\mathbf{\Omega}\rangle, \tag{17}$$

where the expansion coefficients are[43,47–49]

$$\langle n|\mathbf{\Omega}\rangle = \begin{cases} \cos\frac{\theta_1}{2} & n=1, \\ \cos\frac{\theta_n}{2}\prod_{l=1}^{n-1}\sin\frac{\theta_l}{2}e^{i\varphi_l} & 1<n<N, \\ \prod_{l=1}^{N-1}\sin\frac{\theta_l}{2}e^{i\varphi_l} & n=N. \end{cases} \tag{18}$$

with $\{\theta_n\} \in [0,\pi]$ and $\{\varphi_n\} \in [0,2\pi]$. The expansion coefficients can be expressed from the usual recursive

Eqs (16) and (18) are different from the coherent states (15) and (17) in their first version. It is because that In their first version, the coherent state (17) is incompatible with the deductions (B2) and (B3), leading to serious mistakes when they derive the equations of motion (101) and (105). In this version the authors fix the problem, and the coherent states (18) is identical to those used by Runeson and Richardson.

expression[43] given in Eq. B1. Note that this is one convenient choice to write down spin coherence states,[43] such that it is a generalization of Eq. 16 beyond the two level system. These angles can be viewed as the general Euler angles in multi-dimensional Bloch spheres[43] (also see Fig. 6 for a schematic illustration). The notation of the expansion coefficients $\langle n|\mathbf{\Omega}\rangle$ used in Ref. 50 has a reversed order of diabatic state label and a π difference in the definition of $\theta_n/2$.

The spin coherent states $|\mathbf{\Omega}\rangle$ are normalized[47–50] such that

$$\langle \mathbf{\Omega}|\mathbf{\Omega}\rangle = 1, \tag{19}$$

and they also form a resolution of identity

$$\hat{\mathcal{I}} = \int \mathrm{d}\mathbf{\Omega}|\mathbf{\Omega}\rangle\langle\mathbf{\Omega}|, \tag{20}$$

where a simple proof is provided in Appendix C (see Eq. C21). The differential phase-space volume element $\mathrm{d}\mathbf{\Omega}$ (which is also referred to as the invariant integration measure on the group, *i.e.*, the Haar measure[58]) is

$$\mathrm{d}\mathbf{\Omega} = \frac{N!}{(2\pi)^{N-1}} \prod_{n=1}^{N-1} K_n(\theta_n)\mathrm{d}\theta_n\mathrm{d}\varphi_n, \tag{21}$$

where

$$K_n(\theta_n) = \cos\frac{\theta_n}{2}\Big(\sin\frac{\theta_n}{2}\Big)^{2(N-n)-1}. \tag{22}$$

For the two-level special case, it reduces to $K(\theta) = \frac{1}{2}\sin\theta$. Our definition of $K_n(\theta_n)$ in Eq. 22 is different[59] than the one derived by Tilma and Nemoto.[43,50] We find that this new expression of $\mathrm{d}\mathbf{\Omega}$ guarantees the identity relation of Eq. 20 and a correct distribution for each angle θ_n. The proof of the current differential phase-space volume element definition is given in Appendix C.

To simplify our notation, we define the expectation value of the generalized spin operator as

$$\hbar\Omega_k \equiv \langle\mathbf{\Omega}|\hat{\mathcal{S}}_k|\mathbf{\Omega}\rangle, \tag{23}$$

where $\hbar\mathbf{\Omega}$ plays the role of the Bloch vector, and their detailed expressions can be found in Eqs. B2-B4. Further, one can express $|\mathbf{\Omega}\rangle\langle\mathbf{\Omega}| = C_0\hat{\mathcal{I}} + \sum_{k=1}^{N^2-1} C_k\hat{\mathcal{S}}_k$ due to the completeness of the generators, similar to the expansion in Eq. 10. To figure out C_j, we perform $\langle\mathbf{\Omega}|\hat{\mathcal{S}}_j|\mathbf{\Omega}\rangle = \mathrm{Tr_e}[\hat{\mathcal{S}}_j|\mathbf{\Omega}\rangle\langle\mathbf{\Omega}|] = C_0\mathrm{Tr_e}[\hat{\mathcal{S}}_j] + \sum_{k=1}^{N^2-1} C_k\mathrm{Tr_e}[\hat{\mathcal{S}}_j\hat{\mathcal{S}}_k] = \hbar^2 C_j/2$ (using Eq. 6 and Eq. 7), thus $C_j = 2\Omega_j/\hbar$. Further, we have $1 = \langle\mathbf{\Omega}|\mathbf{\Omega}\rangle = \mathrm{Tr_e}[|\mathbf{\Omega}\rangle\langle\mathbf{\Omega}|] = C_0\mathrm{Tr_e}[\hat{\mathcal{I}}] + \sum_{k=1}^{N^2-1} C_k\mathrm{Tr_e}[\hat{\mathcal{S}}_k] = C_0 N$, thus $C_0 = 1/N$. Combining these together, we have

$$|\mathbf{\Omega}\rangle\langle\mathbf{\Omega}| = \frac{1}{N}\hat{\mathcal{I}} + \frac{2}{\hbar}\sum_{k=1}^{N^2-1} \Omega_k\cdot\hat{\mathcal{S}}_k. \tag{24}$$

B. Basic Properties of the Stratonovich-Weyl Transform

The S-W transform of an operator $\hat{A}$ is defined as

$$\big[\hat{A}\big]_{\mathrm{s}}(\boldsymbol{\Omega}) = \mathrm{Tr}_{\mathrm{e}}\big[\hat{A}\cdot\hat{w}_{\mathrm{s}}\big], \tag{25}$$

where $\hat{w}_{\mathrm{s}}$ is the kernel of the S-W transform. The generalized S-W kernel $\hat{w}_{\mathrm{s}}$ in Eq. 25 is expressed as[27,50,60]

$$\begin{aligned}\hat{w}_{\mathrm{s}}(\boldsymbol{\Omega}) &= \frac{1}{N}\hat{\mathcal{I}} + r_{\mathrm{s}}\cdot\frac{2}{\hbar^2}\sum_{k=1}^{N^2-1}\langle\boldsymbol{\Omega}|\hat{\mathcal{S}}_k|\boldsymbol{\Omega}\rangle\hat{\mathcal{S}}_k \\ &\equiv \frac{1}{N}\hat{\mathcal{I}} + r_{\mathrm{s}}\cdot\frac{2}{\hbar}\sum_{k=1}^{N^2-1}\Omega_k\cdot\hat{\mathcal{S}}_k,\end{aligned} \tag{26}$$

where r_{s} is a constant related to the radius of the Bloch sphere,[61–63] and $|\boldsymbol{\Omega}\rangle$ is the generalized spin-coherent state expressed in Eqs. 17-18. One can clearly see that the S-W kernel depends on both the generators $\hat{\boldsymbol{\mathcal{S}}}$ of the Lie algebra (represented in the Hilbert space) and the parameters $\{\theta_n, \varphi_n\}$ of the manifold. Using the spin coherent states, we can also express the S-W kernel in Eq. 26 as[64]

$$\hat{w}_{\mathrm{s}}(\boldsymbol{\Omega}) = \frac{1-r_{\mathrm{s}}}{N}\hat{\mathcal{I}} + r_{\mathrm{s}}|\boldsymbol{\Omega}\rangle\langle\boldsymbol{\Omega}|, \tag{27}$$

which can be easily verified by using $|\boldsymbol{\Omega}\rangle\langle\boldsymbol{\Omega}|$ expressed with generators in Eq. 24. Note that when $r_{\mathrm{s}} = 1$ (so called s=Q method), the kernel is just the projection operator $\hat{w}_{\mathrm{s}} = |\boldsymbol{\Omega}\rangle\langle\boldsymbol{\Omega}|$ discussed by Brif and Mann for the explicit form of the kernel.[27] The kernel also defines an identity as

$$\int \mathrm{d}\boldsymbol{\Omega}\hat{w}_{\mathrm{s}} = \int \mathrm{d}\boldsymbol{\Omega}\Big(\frac{1-r_{\mathrm{s}}}{N}\hat{\mathcal{I}} + r_{\mathrm{s}}|\boldsymbol{\Omega}\rangle\langle\boldsymbol{\Omega}|\Big) = \hat{\mathcal{I}}, \tag{28}$$

where we have used the fact that $\int \mathrm{d}\boldsymbol{\Omega} = N$ (Eq. C6) and Eq. 20.

The S-W transform in Eq. 25 constructs a mapping between an operator in the Hilbert space to a continuous function whose variables are $\{\boldsymbol{\theta}, \boldsymbol{\varphi}\}$ or $\{\boldsymbol{\Omega}\}$ on the Lie group/manifold. More specifically, this mapping relation is expressed as

$$\hat{A} \longrightarrow \big[\hat{A}\big]_{\mathrm{s}}(\boldsymbol{\Omega}), \tag{29}$$

which is the basic idea of the generalized spin-mapping approach proposed by Runeson and Richardson in Ref. 34 and Ref. 43.

Using the definition of S-W transform, as well as the properties of the generators given in Eq. 8, it is straightforward to show that[43]

$$\big[\hat{\mathcal{S}}_k\big]_{\mathrm{s}}(\boldsymbol{\Omega}) = \mathrm{Tr}_{\mathrm{e}}\big[\hat{\mathcal{S}}_k\cdot\hat{w}_{\mathrm{s}}\big] = \hbar r_{\mathrm{s}}\Omega_k, \tag{30a}$$

$$\big[\hat{\mathcal{I}}\big]_{\mathrm{s}}(\boldsymbol{\Omega}) = \mathrm{Tr}_{\mathrm{e}}\big[\hat{\mathcal{I}}\cdot\hat{w}_{\mathrm{s}}\big] = 1. \tag{30b}$$

The property in Eq. 30b means that the S-W transform preserves the identity in the electronic Hilbert subspace, contrarily to the Wigner transform[65,66] of the identity

operator in the MMST formalism[22,67] and hence, does not introduce any ambiguity of the identity expression.[68]

To conveniently evaluate any operator $\hat{A}(\hat{R})$ under a S-W transformation, one starts by decomposing it on the GGM basis (Eqs 2-4) as follows

$$\hat{A}(\hat{R}) = \mathcal{A}_0(\hat{R}) \cdot \hat{\mathcal{I}} + \frac{1}{\hbar} \sum_{k=1}^{N^2-1} \mathcal{A}_k(\hat{R}) \cdot \hat{\mathcal{S}}_k, \tag{31}$$

where $\mathcal{A}_0(\hat{R}) = \frac{1}{N}\mathrm{Tr_e}[\hat{A}(\hat{R})\hat{\mathcal{I}}] = \frac{1}{N}\sum_{n=1}^{N} A_{nn}(\hat{R})$ with $A_{nm}(\hat{R}) = \langle n|\hat{A}(\hat{R})|m\rangle$ and $\mathcal{A}_k(\hat{R}) = \frac{2}{\hbar}\mathrm{Tr_e}[\hat{A}(\hat{R})\hat{\mathcal{S}}_k]$. Here, we explicitly consider a system (with the Hamiltonian in Eq. 1) that contains both electronic and nuclear DOFs. Similar to the expressions in Eq. 12, we can write down each component of $\mathcal{A}_i$ as follows

$$\mathcal{A}_{\alpha_{nm}}(\hat{R}) = A_{mn}(\hat{R}) + A_{nm}(\hat{R}), \tag{32a}$$

$$\mathcal{A}_{\beta_{nm}}(\hat{R}) = i\big(A_{mn}(\hat{R}) - A_{nm}(\hat{R})\big), \tag{32b}$$

$$\mathcal{A}_{\gamma_n}(\hat{R}) = \sum_{l=1}^{n-1} \sqrt{\frac{2}{n(n-1)}} A_{ll}(\hat{R}) - \sqrt{\frac{2(n-1)}{n}} A_{nn}(\hat{R}), \tag{32c}$$

with $1 \leq m < n \leq N$ and $2 \leq n \leq N$ as previously introduced (under Eq. 4). To keep our notation concise, we will write $\hat{A}$ instead of $\hat{A}(\hat{R})$ for the following equations, because the S-W transform is performed only on the *electronic* DOFs and does not involve the nuclear DOFs.

Using the expression of $\hat{w}_\mathrm{s}$ (Eq. 26), $\hat{A}(\hat{R})$ expressed in Eq. 31 is transformed (through Eq. 25) as

$$\big[\hat{A}(\hat{R})\big]_\mathrm{s}(\mathbf{\Omega}) = \mathcal{A}_0(\hat{R}) + r_\mathrm{s} \sum_{k=1}^{N^2-1} \mathcal{A}_k(\hat{R}) \cdot \Omega_k. \tag{33}$$

One of the important properties of the S-W transform is that it can be used to compute a quantum mechanical trace in the continuous phase space as follows

$$\begin{aligned}\int \mathrm{d}\mathbf{\Omega}\big[\hat{A}\big]_\mathrm{s}(\mathbf{\Omega}) &= \int \mathrm{d}\mathbf{\Omega}\mathrm{Tr_e}\big[\hat{A}\cdot\hat{w}_\mathrm{s}\big] = \mathrm{Tr_e}\Big[\int \mathrm{d}\mathbf{\Omega}\hat{w}_\mathrm{s}\cdot\hat{A}\Big] \\ &= \mathrm{Tr_e}\big[\hat{A}\big],\end{aligned} \tag{34}$$

where we have used the identity given in Eq. 28.

For two operators $\hat{A}(\hat{R})$ and $\hat{B}(\hat{R})$, one cannot compute the trace of a product of operators $\mathrm{Tr_e}[\hat{A}\hat{B}]$ as $\int \mathrm{d}\mathbf{u}[\hat{A}]_\mathrm{s}[\hat{B}]_\mathrm{s}(\mathbf{\Omega})$ for a given value of r_s, because generally $[\hat{A}\hat{B}]_\mathrm{s}(\mathbf{\Omega}) \neq [\hat{A}]_\mathrm{s}(\mathbf{\Omega}) \cdot [\hat{B}]_\mathrm{s}(\mathbf{\Omega})$ (see Eq. 42). To get the separate S-W transform of $\hat{A}$ and $\hat{B}$, it is required to use two matching values of the radius, r_s and $r_{\bar{\mathrm{s}}}$, with complementing indices s and $\bar{\mathrm{s}}$ which will be defined in Eq. 39. It can be shown that the S-W transform has the following property

$$\begin{aligned}\mathrm{Tr_e}\big[\hat{A}\hat{B}\big] &= \int \mathrm{d}\mathbf{\Omega}\big[\hat{A}\hat{B}\big]_\mathrm{s}(\mathbf{\Omega}) \\ &= \int \mathrm{d}\mathbf{\Omega}\big[\hat{A}\big]_\mathrm{s}(\mathbf{\Omega}) \cdot \big[\hat{B}\big]_{\bar{\mathrm{s}}}(\mathbf{\Omega}) = \int \mathrm{d}\mathbf{\Omega}\big[\hat{A}\big]_{\bar{\mathrm{s}}}(\mathbf{\Omega}) \cdot \big[\hat{B}\big]_\mathrm{s}(\mathbf{\Omega}),\end{aligned} \tag{35}$$

where $[\cdots]_{\bar{\mathrm{s}}}(\mathbf{\Omega})$ is S-W transformed through Eq. 33 using $r_{\bar{\mathrm{s}}}$. The proof is given in Supplemental Material.

The sum of the squares of the generators (the so-called Casimir operator of $\mathfrak{su}(N)$) can be expressed with the identity operator as follows[43]

$$\sum_{k=1}^{N^2-1} \hat{\mathcal{S}}_k^2 = \hbar^2 \frac{N^2-1}{2N} \hat{\mathcal{I}}, \tag{36}$$

where the proof can be found in Appendix A of Ref. 43. Performing the S-W transform on both sides of the above identity leads to the squared spin magnitude as follows

$$\sum_{k=1}^{N^2-1} \left[\hat{\mathcal{S}}_k\right]_{\mathrm{s}} \left[\hat{\mathcal{S}}_k\right]_{\bar{\mathrm{s}}} = \hbar^2 r_{\mathrm{s}} r_{\bar{\mathrm{s}}} \sum_{k=1}^{N^2-1} \Omega_k^2 = \hbar^2 \frac{N^2-1}{2N}, \tag{37}$$

which is a conserved quantity. Using the fact[43] that $\sum_{k=1}^{N^2-1} \Omega_k^2 = \frac{N-1}{2N}$ (see the proof in Appendix E of Ref. 43) together with the identity in Eq. 37, one has[43]

$$r_{\mathrm{s}} \cdot r_{\bar{\mathrm{s}}} = N + 1. \tag{38}$$

The commonly used values[28,43] for r_{s} and $r_{\bar{\mathrm{s}}}$ are

$$r_{\mathrm{s}} = r_{\bar{\mathrm{s}}} = \sqrt{N+1}, \quad (\text{for } \mathrm{s} = \bar{\mathrm{s}} = \mathrm{W}), \tag{39a}$$
$$r_{\mathrm{s}} = 1, \quad r_{\bar{\mathrm{s}}} = N+1, \quad (\text{for } \mathrm{s} = \mathrm{Q}, \quad \bar{\mathrm{s}} = \mathrm{P}), \tag{39b}$$
$$r_{\mathrm{s}} = N+1, \quad r_{\bar{\mathrm{s}}} = 1, \quad (\text{for } \mathrm{s} = \mathrm{P}, \quad \bar{\mathrm{s}} = \mathrm{Q}). \tag{39c}$$

Note that these parameters are not restricted to the above special cases, and in principle they can take any value in the range of $r_{\mathrm{s}} \in (0, \infty)$.

Just repeating the conclusions of Ref. 25, 74, 109, and missing corresponding citations!

Using the complementing $r_{\bar{\mathrm{s}}}$, one can define the inverse S-W transform[45] as follows

$$\hat{A} = \int \mathrm{d}\mathbf{\Omega} \hat{w}_{\mathrm{s}}(\mathbf{\Omega}) \left[\hat{A}\right]_{\bar{\mathrm{s}}}(\mathbf{\Omega}), \tag{40}$$

where $\left[\hat{A}\right]_{\bar{\mathrm{s}}}(\mathbf{\Omega})$ is defined in Eq. 33 $r_{\bar{\mathrm{s}}}$. A simple proof of Eq. 40 is given in the Supplemental Material.

It is also useful to derive the expression of the S-W transform of the product of two electronic operators $[\hat{A}\hat{B}]_{\mathrm{s}}$ in order to evaluate commutation and anti-commutation relations. To proceed, we use the detailed expressions of $\hat{A}$ and $\hat{B}$ in their $\mathfrak{su}(N)$ representation, and express $\left[\hat{A}\hat{B}\right]_{\mathrm{s}}$ as follows

$$\begin{aligned}\left[\hat{A}\hat{B}\right]_{\mathrm{s}}(\mathbf{\Omega}) = \Big[&\Big(\mathcal{A}_0(\hat{R}) \cdot \hat{\mathcal{I}} + \frac{1}{\hbar} \sum_{k=1}^{N^2-1} \mathcal{A}_k(\hat{R}) \cdot \hat{\mathcal{S}}_k\Big) \\ &\times \Big(\mathcal{B}_0(\hat{R}) \cdot \hat{\mathcal{I}} + \frac{1}{\hbar} \sum_{k=1}^{N^2-1} \mathcal{B}_k(\hat{R}) \cdot \hat{\mathcal{S}}_k\Big)\Big]_{\mathrm{s}} \\ = \Big[&\mathcal{A}_0\mathcal{B}_0 \cdot \hat{\mathcal{I}} + \frac{\mathcal{A}_0}{\hbar} \sum_{k=1}^{N^2-1} \mathcal{B}_k \cdot \hat{\mathcal{S}}_k + \frac{\mathcal{B}_0}{\hbar} \sum_{k=1}^{N^2-1} \mathcal{A}_k \cdot \hat{\mathcal{S}}_k \\ &+ \frac{1}{\hbar^2} \sum_{j,k=1}^{N^2-1} \mathcal{A}_j\mathcal{B}_k \cdot \hat{\mathcal{S}}_j\hat{\mathcal{S}}_k\Big]_{\mathrm{s}}.\end{aligned} \tag{41}$$

Using the fact that

$$\hat{\mathcal{S}}_j\hat{\mathcal{S}}_k = \frac{1}{2}\big([\hat{\mathcal{S}}_j,\hat{\mathcal{S}}_k] + \{\hat{\mathcal{S}}_j,\hat{\mathcal{S}}_k\}_+\big),$$

together with Eqs. 8 and 30, we can evaluate $\big[\hat{A}\hat{B}\big]_{\rm s}(\mathbf{\Omega})$ as follows

$$\begin{aligned}\big[\hat{A}\hat{B}\big]_{\rm s}(\mathbf{\Omega}) =& \mathcal{A}_0\mathcal{B}_0 + \frac{1}{2N}\sum_{i=1}^{N^2-1}\mathcal{A}_i\mathcal{B}_i \\ &+ r_{\rm s}\sum_{i=1}^{N^2-1}\big(\Omega_i\mathcal{A}_i\mathcal{B}_0 + \Omega_i\mathcal{A}_0\mathcal{B}_i\big) \\ &+ \frac{r_{\rm s}}{2}\sum_{i,j,k=1}^{N^2-1}\Omega_i\mathcal{A}_j\mathcal{B}_k(d_{ijk}+if_{ijk}),\end{aligned} \tag{42}$$

where $\mathcal{A}_i(\hat{R})$ and $\mathcal{B}_i(\hat{R})$ are expressed in Eq. 32.

C. Mapping Formalism using the Stratonovich-Weyl Transform

Performing the S-W transform of the Hamiltonian $\hat{H}$ (Eq. 10) through Eq. 25, we have

$$\big[\hat{H}(\hat{R})\big]_{\rm s}(\mathbf{\Omega}) = \mathcal{H}_0(\hat{R}) + r_{\rm s}\sum_{k=1}^{N^2-1}\mathcal{H}_k(\hat{R})\cdot\Omega_k, \tag{43}$$

where $\mathcal{H}_0$ is expressed in Eq. 11a and $\mathcal{H}_k$ is expressed in Eq. 12. This is the mapping Hamiltonian expression in terms of the expectation values of the generalized spin operators.[43,51]

In addition, we can also perform the S-W transform for electronic projection operators and obtain

$$\begin{aligned}&\big[|n\rangle\langle n|\big]_{\rm s} = {\rm Tr}_{\rm e}\big[|n\rangle\langle n|\hat{w}_{\rm s}\big] \\ &= \frac{1}{N} + r_{\rm s}\sum_{m=n+1}^{N}\sqrt{\frac{2}{m(m-1)}}\Omega_{\gamma_m} - r_{\rm s}\sqrt{\frac{2(n-1)}{n}}\Omega_{\gamma_n},\end{aligned} \tag{44}$$

with $1 \le n \le N$. The complementary expression $\big[|n\rangle\langle n|\big]_{\bar{\rm s}}$ can be obtained by replacing $r_{\rm s}$ in Eq. 44 by $r_{\bar{\rm s}}$. Note that the first sum in Eq. 44 is null when the condition $m > n$ is not satisfied, *i.e.* when $n = N$, and the last term is null when $n = 1$. The population estimators only depend on the expectation values of the diagonal spin operators $\{\Omega_{\gamma_m}\}$ (see Eq. B4), hence they are independent of the mapping variables $\{\varphi_m\}$ for $m \in \{1,\cdots,N-1\}$. As expected, summing all the state population estimators gives a total population equal to 1, because the S-W transformation explicitly preserves the identity in the electronic subspace (see Eq. 30b).

For an off-diagonal electronic operator with $m < n$, the S-W transform is

$$\big[|n\rangle\langle m|\big]_{\rm s} = r_{\rm s}(\Omega_{\alpha_{nm}} - i\Omega_{\beta_{nm}}), \tag{45a}$$

$$\big[|m\rangle\langle n|\big]_{\rm s} = r_{\rm s}(\Omega_{\alpha_{nm}} + i\Omega_{\beta_{nm}}), \tag{45b}$$

where the detailed expressions of $\Omega_{\alpha_{nm}}$ and $\Omega_{\beta_{nm}}$ are provided in Eq. B2 and Eq. B3, respectively. Using Eq. 44 and Eq. 45, one can also perform the S-W transform on $\hat{H}$ (Eq. 1) and derive $[\hat{H}]_{\rm s} = \big[\hat{T}_R + U_0(\hat{R})\big] + \sum_n V_{nn}(\hat{R})[|n\rangle\langle n|]_{\rm s} + \sum_{n\neq m} V_{nm}(\hat{R})[|n\rangle\langle m|]_{\rm s}$, which is identical to Eq. 43 (when using $\mathcal{H}_k$ expressed in Eq. 12).

D. Connections with the MMST Mapping Hamiltonian

Following the previous work of spin mapping,[43] we express the expansion coefficients $\langle n|\mathbf{\Omega}\rangle$ in Eq. 17 (with detailed expressions in Eq. 18) into its real and imaginary parts. To this end, we introduce a *constant global phase* variable $e^{i\Phi}$ to *all* of the coefficients $\langle n|\mathbf{\Omega}\rangle$, with the range $\Phi \in (0, 2\pi)$, and define[43,69]

$$c_n = \langle n|\mathbf{\Omega}\rangle \cdot e^{i\Phi} = \frac{1}{\sqrt{2r_{\rm s}}}(q_n + ip_n), \tag{46}$$

where we introduced $q_n/\sqrt{2r_{\rm s}}$ as the real part of c_n and $p_n/\sqrt{2r_{\rm s}}$ as the imaginary part of c_n. This phase $e^{i\Phi}$ is a constant. The transformation in Eq. 46 provides the connection between a given pair of q_n and p_n and the angle variables of the generalized spin coherent states $\{\theta_n, \varphi_n\}$ through Eq. 18. Because we want to convert $2N-2$ real independent variables of $\{\theta_n, \varphi_n\}$ into $2N$ variables $\{q_n, p_n\}$ that are subjects to a total population constraint (see Eq. 56 or Eq. 57), we need to introduce one more independent variable $e^{i\Phi}$ to define $\{q_n, p_n\}$. Further, this phase is necessary to introduce q_1 and p_1 variables, because $\langle 1|\mathbf{\Omega}\rangle = \cos\frac{\theta_1}{2}$ in Eq. 18 is purely real.[70]

Using the coefficients defined in Eq. 46, the expectation value of the spin operator (Eq. 23) is expressed as

$$\begin{aligned}\hbar\Omega_k = \langle\mathbf{\Omega}|\hat{\mathcal{S}}_k|\mathbf{\Omega}\rangle &= \sum_{n,m} e^{-i\Phi}\cdot\langle\mathbf{\Omega}|n\rangle\langle n|\hat{\mathcal{S}}_k|m\rangle\langle m|\mathbf{\Omega}\rangle\cdot e^{i\Phi} \\ &= \sum_{n,m}\langle n|\hat{\mathcal{S}}_k|m\rangle\cdot c_n^* c_m. \end{aligned}\tag{47}$$

Note that the global phase cancels in any physical expectation values, such that it is not *explicitly* present in $\hbar\Omega_k$. Using the transform defined in Eq. 46, Eq. 47 becomes

$$2r_{\rm s}\Omega_k = \sum_{n,m}\langle n|\hat{\mathcal{S}}_k|m\rangle\cdot(q_n - ip_n)(q_m + ip_m). \tag{48}$$

Explicitly using the matrix elements of $\langle n|\hat{\mathcal{S}}_k|m\rangle$ (see Eqs. 2-4), Eq. 48 becomes

$$2r_{\rm s}\Omega_{\alpha_{nm}} = q_n q_m + p_n p_m, \tag{49a}$$
$$2r_{\rm s}\Omega_{\beta_{nm}} = p_n q_m - q_n p_m, \tag{49b}$$
$$2r_{\rm s}\Omega_{\gamma_n} = \frac{1}{\sqrt{2n(n-1)}}\Big(\sum_{l=1}^{n-1} q_l^2 + p_l^2 - (n-1)(q_n^2 + p_n^2)\Big). \tag{49c}$$

Note that this transformation *does depend on the choice* of $r_{\rm s}$, which must match the index in the mapped Hamiltonian that evolves the dynamics (see Sec. IV).

In fact, the virtue of writing c_n with coordinates and momenta has long been proposed in Appendix B of J. Chem. Phys. 145, 204105 (2016).

The concept of global phase in SU(F) Stratonovich phase space is already proposed in Appendix 3 of WIREs. Comput. Mol. Sci. e1619 (2022), while completely absent in previous version of this manuscripy and abruptly involved here. The authors did not cite WIREs. Comput. Mol. Sci. e1619 (2022), in which we clearly pointed out the importance of an evolving global phase. Moreover, a constant global phase still does not lead to correct form of canonical Hamilton's equations of motion in Meyer-Miller variables.

For a purely real Hamiltonian (such that in Eq. 12b $\mathcal{H}_{\beta_{nm}} = 0$), using the transform defined in Eq. 49, the spin mapping Hamiltonian $\left[\hat{H}(\hat{R})\right]_{\rm s}$ in Eq. 43 can be expressed as the well-known MMST mapping Hamiltonian[7,8,10]

$$\begin{aligned}\mathcal{H} =&\mathcal{H}_0(\hat{R}) + \sum_n \frac{1}{2}[V_{nn}(\hat{R}) - \bar{V}(\hat{R})](q_n^2 + p_n^2 - \gamma) \\ &+ \sum_{n<m} V_{nm}(\hat{R})(q_n q_m + p_n p_m),\end{aligned} \tag{50}$$

where $\bar{V}(\hat{R}) = \frac{1}{N}\sum_l V_{ll}(\hat{R})$, $\mathcal{H}_0(\hat{R}) = \frac{\hat{P}^2}{2m} + U_0(\hat{R}) + \bar{V}(\hat{R})$ is the trace part of the potential, which is naturally separated from the traceless part. Previous work by Runeson and Richardson[43] have already shown this connection using the transform expressed in Eq. 46. Note that the MMST form of the mapping Hamiltonian does not explicitly contain the global phase $e^{i\Phi}$ (introduced in Eq. 46), due to the cancellation of this phase.

Further, in Eq. 50, the parameter γ is expressed[43] as follows

$$\gamma = \frac{2}{N}(r_{\rm s} - 1), \tag{51}$$

or equivalently, $r_{\rm s} = 1 + N\gamma/2$. In the MMST mapping formalism, this parameter is viewed as the zero-point energy (ZPE) parameter of the mapping oscillators.[23,43,71–74] In the $SU(N)$ mapping formalism, it is the parameter related to the choice of $r_{\rm s}$. Nevertheless, Eq. 51, which was first derived in Ref. 43, helps to establish the connection between the boundaries on the S-W radius and the boundaries on the γ parameter in the MMST mapping. The constraint of the radius $r_{\rm s} \in (0, \infty)$ leads to a corresponding constraint for the ZPE parameter, $\gamma \in (-\frac{2}{N}, \infty)$. The negative values of the ZPE parameter has been proposed in the MMST framework,[74] and simply correspond to $r_{\rm s} \leq r_{\rm Q} = 1$. In our own opinion, it might be more intuitive to understand the choice of radius of Bloch sphere[43] (that should be larger than 0) rather than the negative ZPE of quantum mapping oscillators.[74]

This is merely repeat of Ref. 74 in another way.

Using the conjugate variables $\{q_n, p_n\}$ defined in Eq. 46, the S-W kernel in Eq. 27 can also be equivalently expressed in the diabatic electronic basis as follows

$$\begin{aligned}\hat{w}_{\rm s} &= \frac{1 - r_{\rm s}}{N}\hat{\mathcal{I}} + r_{\rm s}\sum_{a,b} c_a c_b^* |a\rangle\langle b| \\ &= \frac{1 - r_{\rm s}}{N}\hat{\mathcal{I}} + \frac{1}{2}\sum_{a,b}(q_a + ip_a)(q_b - ip_b)|a\rangle\langle b| \\ &= \frac{1}{2}\sum_{a,b}\Big[(q_a + ip_a)(q_b - ip_b) - \gamma\Big]|a\rangle\langle b|,\end{aligned} \tag{52}$$

where we have used $r_{\rm s} = N\gamma/2 + 1$. The kernel in Eq. 52 is identical to the one expressed in Eq. 7 of Ref. 74, which is derived in the extended classical mapping model (eCMM).[25,74]

Using the S-W kernel expressed in Eq. 52, the S-W transform (Eq. 25) of operator $|n\rangle\langle m|$ is

$$\begin{aligned}\big[|n\rangle\langle m|\big]_{\rm s} &= \frac{1-r_{\rm s}}{N}\delta_{nm} + \frac{1}{2}(q_m + ip_m)(q_n - ip_n) \quad (53)\\ &= -\frac{\gamma}{2}\delta_{nm} + \frac{1}{2}(q_m + ip_m)(q_n - ip_n).\end{aligned}$$

The same result can also be obtained by performing the transform defined in Eq. 49 directly on Eq. 44 and Eq. 45. For the diagonal projection operators ($n = m$), Eq. 53 becomes

$$\big[|n\rangle\langle n|\big]_{\rm s} = \frac{1}{2}(q_n^2 + p_n^2 - \gamma). \quad (54)$$

Similar to Eq. 53, for the complementary index $\bar{\rm s}$, the expression $[|n\rangle\langle n|]_{\bar{\rm s}} = {\rm Tr}_{\rm e}[|n\rangle\langle n|\hat{w}_{\bar{\rm s}}]$ (using the kernel in Eq. 52 with $r_{\bar{\rm s}}$) is

$$\begin{aligned}\big[|n\rangle\langle n|\big]_{\bar{\rm s}} &= \frac{1-r_{\bar{\rm s}}}{N} + \frac{1}{2}\cdot\frac{r_{\bar{\rm s}}}{r_{\rm s}}(q_n^2 + p_n^2) = \frac{1}{2}\Big[\frac{r_{\bar{\rm s}}}{r_{\rm s}}(q_n^2 + p_n^2) - \gamma_{\bar{\rm s}}\Big]\\ &= \frac{N+1}{2(1+\frac{N\gamma}{2})^2}\cdot(q_n^2 + p_n^2) - \frac{1-\frac{\gamma}{2}}{1+\frac{N\gamma}{2}}, \quad (55)\end{aligned}$$

where we define $\gamma = \frac{2}{N}(r_{\bar{\rm s}} - 1)$ in the second equality, and used $r_{\bar{\rm s}}/r_{\rm s} = (N+1)/r_{\rm s}^2 = (N+1)/(\frac{N\gamma}{2}+1)^2$ and $r_{\bar{\rm s}} = (N+1)/(\frac{N\gamma}{2}+1)$ based on Eq. 51 and Eq. 38 for the third equality. Thus, the estimators (Eq. 54 and Eq. 55) used in the Spin-LSC[43] are identical to those used in the eCMM[74] approach (second line of Eq. 55).

In the $SU(N)$ mapping formalism, the total population constraint on the $2N$-dimensional phase space comes *naturally* from the normalization of the generalized spin coherent states[69,75] as follows

$$\langle\mathbf{\Omega}|\mathbf{\Omega}\rangle = \sum_n c_n^* c_n = \frac{1}{2r_{\rm s}}\sum_{n=1}^{N}(q_n^2 + p_n^2) = 1, \quad (56)$$

which properly enforces the total electronic diabatic population to be one (see Eq. 51) for these MMST mapping variables

$$\sum_{n=1}^{N}\frac{1}{2}(q_n^2 + p_n^2 - \gamma) = 1. \quad (57)$$

Alternatively, one can obtain this condition from the basic property of the S-W transform that preserves the trace of the electronic identity operator (Eq. 30) as follows

$$\big[\hat{\mathcal{I}}\big]_{\rm s} = \sum_{n=1}^{N}\big[|n\rangle\langle n|\big]_{\rm s} = 1 - r_{\rm s} + \sum_n\frac{1}{2}(q_n^2 + p_n^2) = 1.$$

Note that the recent work of the eCMM is developed based on *manually* adding an extra total population constraint (as described in Eq. 57) on the MMST mapping oscillator phase space. Historically, it was realized[75] that a mapping from the quantum Schrödinger's equation to $2N$ classical phase space Hamilton's EOMs is incorrect,

In fact, in eCMM framework the dynamics is intrinsically correct as the constraint eq (57) is strictly protected by the Meyer-Miller Hamiltonian. Verification of this statement is quite easy.

unless a total population constraints is applied.[75] In the $SU(N)$ framework, on the other hand, the total population constraint is *naturally* satisfied through the S-W transform, without the necessity to introduce it as an additional constraint. Nevertheless, the eCMM approach derives equivalent kernel as the S-W kernel in Eq. 52 (hence also equivalent estimators in Eq. 54 and Eq. 55) from a seemingly different procedure that applies population constraint on the MMST mapping oscillator phase space.[74] The mathematical reason behind the equivalence of two kernels is: using the additional population constraint, the $2N$-dimensional MMST phase space of $\{q_n, p_n\}$ is reduced to a complex projective (CP) space, mathematically denoted[69] as $\mathrm{CP}(N-1)$, which is in fact a subspace[75] of the parameterized manifold of $SU(N)$.

Using Eq. 53 and the Hamiltonian in Eq. 1, one can also directly obtain the mapping Hamiltonian expression

$$\begin{aligned}\left[\hat{H}(\hat{R})\right]_{\mathrm{s}} =&\hat{T}_R + U_0(\hat{R}) + \sum_n \frac{1}{2} V_{nn}(\hat{R})(q_n^2 + p_n^2 - \gamma) \\ &+ \sum_{n<m} V_{nm}(\hat{R})(q_n q_m + p_n p_m),\end{aligned} \tag{58}$$

which is indeed equivalent to Eq. 50 due to the constraint on the total population in Eq. 57. Despite the similar expression of $\left[\hat{H}(\hat{R})\right]_{\mathrm{s}}$ compared to the seminal MMST mapping Hamiltonian,[8–10] the $SU(N)$ mapping formalism should be viewed as a different mapping procedure compared to the MMST mapping formalism. As opposed to the Stock-Thoss mapping procedure, the starting point of the $SU(N)$ mapping formalism is completely different. The $SU(N)$ mapping formalism uses the generators of the $\mathfrak{su}(N)$ Lie algebra which exactly preserves the commutation relations among operators as well as the original electronic Hilbert space. As a result, there is no need for additional Hilbert space projection nor truncation that ruins the simple commutation relations of mapping operators[24,25] (see Appendix F for detailed discussions) or necessity of projecting back to the subspace as required by MMST formalism.[20,21] The exact quantum Liouvillian from the current $SU(N)$ mapping formalism (see Sec. V) is also different than the exact Liouvillian of the MMST formalism.[76–78] A detailed discussion of the connection and difference between these two mapping approaches is provided in Appendix F.

IV. TIME-CORRELATION FUNCTION IN THE MIXED WIGNER/STRATONOVICH-WEYL REPRESENTATION

In this section, we derive the exact expression of the time correlation function (TCF) and the expression of estimators for different types of quantum operators. The exact and approximate forms of the Liouvillian will be discussed in Sec. V.

A. Time-correlation Functions

The regular quantum TCF is expressed as

$$C_{AB}(t) = \frac{1}{\mathcal{Z}}\mathrm{Tr_e Tr_n}\big[e^{-\beta\hat{H}}\hat{A}(0)\hat{B}(t)\big], \tag{59}$$

with the Hamiltonian defined in Eq. 1, and $\beta = 1/k_{\mathrm{B}}T$. The density matrix under the canonical equilibrium condition is $\hat{\rho}_{\mathrm{eq}} = e^{-\beta\hat{H}}/\mathcal{Z}$ and the partition function is defined as $\mathcal{Z} = \mathrm{Tr_e Tr_n}[e^{-\beta\hat{H}}]$. In order to compute the nuclear trace $\mathrm{Tr_n}$, we insert the identity $\hat{\mathbb{1}}_{R'} = \int \mathrm{d}R'|R'\rangle\langle R'|$. To compute the electronic trace we use the property of the S-W transform in Eq. 34. This leads to

$$C_{AB}(t) = \frac{1}{\mathcal{Z}}\int \mathrm{d}R' \int \mathrm{d}\mathbf{\Omega}\big[\langle R'|e^{-\beta\hat{H}}\hat{A}(0)\hat{B}(t)|R'\rangle\big]_{\mathrm{s}}(\mathbf{\Omega}). \tag{60}$$

To proceed, we use the property given in Eq. 35 and identify $e^{-\beta\hat{H}}\hat{A}(0)$ and $\hat{B}(t)$ as two operators to compute the trace of $\int \mathrm{d}\mathbf{\Omega}$. By adding another nuclear identity $\hat{\mathbb{1}}_{R''} = \int \mathrm{d}R''|R''\rangle\langle R''|$ between two operators, we can re-express Eq. 60 as

$$\begin{aligned} C_{AB}(t) = \frac{1}{\mathcal{Z}}\int \mathrm{d}R' \int \mathrm{d}R'' \int \mathrm{d}\mathbf{\Omega} \\ \times \big[\langle R'|e^{-\beta\hat{H}}\hat{A}(0)|R''\rangle\big]_{\bar{\mathrm{s}}}(\mathbf{\Omega})\big[\langle R''|\hat{B}(t)|R'\rangle\big]_{\mathrm{s}}(\mathbf{\Omega}). \end{aligned} \tag{61}$$

Introducing the nuclear mean path and path difference variables[79–81]

$$R = \frac{1}{2}(R' + R''), \quad \Delta = R' - R'', \tag{62}$$

and inserting the following identity of the nuclear DOFs[78,82]

$$\hat{\mathbb{1}}_R = \int \mathrm{d}\Delta'\delta(\Delta + \Delta') = \frac{1}{2\pi\hbar}\int \mathrm{d}\Delta' \int \mathrm{d}P e^{\frac{i}{\hbar}P(\Delta+\Delta')} \tag{63}$$

into the TCF, Eq. 61 becomes

$$\begin{aligned} C_{AB}(t) =& \frac{1}{2\pi\hbar\mathcal{Z}}\int \mathrm{d}R \int \mathrm{d}\Delta \int \mathrm{d}\Delta' \int \mathrm{d}P e^{\frac{i}{\hbar}P(\Delta+\Delta')} \int \mathrm{d}\mathbf{\Omega} \\ &\times \big[\langle R + \frac{\Delta}{2}|e^{-\beta\hat{H}}\hat{A}(0)|R - \frac{\Delta}{2}\rangle\big]_{\bar{\mathrm{s}}}(\mathbf{\Omega}) \\ &\times \big[\langle R - \frac{\Delta'}{2}|\hat{B}(t)|R + \frac{\Delta'}{2}\rangle\big]_{\mathrm{s}}(\mathbf{\Omega}). \end{aligned} \tag{64}$$

The above equation has an explicit Wigner transform[65,83,84] over the nuclear DOFs, which is defined for an operator $\hat{O}(\hat{R})$ as follows

$$\big[\hat{O}(\hat{R})\big]_{\mathrm{w}} = \int d\Delta e^{\frac{i}{\hbar}P\Delta}\langle R - \frac{\Delta}{2}|\hat{O}(\hat{R})|R + \frac{\Delta}{2}\rangle. \tag{65}$$

Note that the lower case w used here represents the Wigner transform, whereas the capital case W represents a special choice of the S-W transform through $r_{\mathrm{W}} = \sqrt{N+1}$.

With the above definition, we can rewrite Eq. 64 as

$$C_{AB}(t) = \frac{1}{2\pi\hbar\mathcal{Z}} \int \mathrm{d}R \int \mathrm{d}P \int \mathrm{d}\mathbf{\Omega} \big[e^{-\beta\hat{H}}\hat{A}(0)\big]_{\mathrm{w}\bar{\mathrm{s}}} \big[\hat{B}(t)\big]_{\mathrm{ws}},$$
$$= \frac{1}{2\pi\hbar\mathcal{Z}} \int \mathrm{d}R \int \mathrm{d}P \int \mathrm{d}\mathbf{\Omega} \big[e^{-\beta\hat{H}}\hat{A}(0)\big]_{\mathrm{w}\bar{\mathrm{s}}} e^{\hat{\mathcal{L}}t} \big[\hat{B}(0)\big]_{\mathrm{ws}}, \tag{66}$$

where $[\hat{A}(\hat{R})]_{\mathrm{ws}}$ is a Wigner transform of the nuclear DOFs (defined in Eq. 65) and a S-W transform of the electronic DOFs in the $SU(N)$ representation (defined in Eq. 25 or Eq. 34). The time evolved expectation value $[\hat{B}(t)]_{\mathrm{ws}}$ is written using the quantum Liouvillian $\hat{\mathcal{L}}$ to update $[\hat{B}(0)]_{\mathrm{ws}}$. The exact expression of $\hat{\mathcal{L}}$ is derived in Sec. V. From now on, we will simply denote $\hat{A}(0)$ as $\hat{A}$ and $\hat{B}(0)$ as $\hat{B}$.

Note that because the quantum Liouvillian is derived based on $\big[\hat{B}(t)\big]_{\mathrm{s}} = e^{\hat{\mathcal{L}}(r_{\mathrm{s}})t}\big[\hat{B}\big]_{\mathrm{s}}$, thus $\hat{\mathcal{L}}$ will have the same S-W radius r_{s} as $\hat{B}$. From our rigorous theoretical formalism we justify that the index used to define $\{q_n, p_n\}$ has to match the index of the Hamiltonian as was numerically found previously, because it is the choice that leads to an initial distribution equivalent to the one obtained from $\mathrm{d}\mathbf{\Omega}$ (as no index is involved in $\mathrm{d}\mathbf{\Omega}$ only one of the two choices of radius leads to the same distribution). Thus, one needs to fix r_{s} for the quantum Liouvillian, such that the index of the Liouvillian coincides with the index used to define $\{q_n, p_n\}$ in Eq. 46. During this process, the index of $\big[\hat{B}\big]_{\mathrm{s}}$ is also fixed, and one will have $\big[\hat{A}\big]_{\bar{\mathrm{s}}}$ with the complementing index.

In the Spin-LSC approach,[34,43] on the other hand, $\hat{\mathcal{L}}$ contains the same choice of $r_{\bar{\mathrm{s}}}$ as used in $[\hat{A}]_{\bar{\mathrm{s}}}$, and operator $\hat{B}$ has a different complementing radius r_{s}. Same choice is also made in eCMM.[74] It was numerically demonstrated that this choice leads to a better population dynamics for a spin-boson problem[85] (for the $\bar{\mathrm{s}} = \mathrm{Q}$ choice in $[\hat{A}]_{\bar{\mathrm{s}}}$). However, these results are usually less accurate compared to the choice of $r_{\mathrm{s}} = r_{\bar{\mathrm{s}}} = \sqrt{N+1}$. Thus, we will only consider the case of $r_{\mathrm{s}} = r_{\bar{\mathrm{s}}}$ in this work, and under this special case, our choice of r_{s} in $\hat{\mathcal{L}}$ do agree with those in Spin-LSC.[34,43]

The numerical results of CMM with \gamma=0 in spin boson models, also identical to those of spin-LSC in Q version, are first reported in J. Chem. Phys. 151, 024105 (2019) and neglected in this manuscript!

B. Estimators of Different Types of Operators

To compute the transform of the operator $\big[e^{-\beta\hat{H}}\hat{A}(0)\big]_{\mathrm{w}\bar{\mathrm{s}}}$, we need to perform the Wigner transform of the nuclear DOFs and S-W transform of the electronic DOFs for a product of two operators. For the Wigner transform of two operators, one has[65,66]

$$\big[\hat{A}\hat{B}\big]_{\mathrm{w}} = \big[\hat{A}\big]_{\mathrm{w}} e^{-i\hat{\Lambda}\hbar/2} \big[\hat{B}\big]_{\mathrm{w}}, \tag{67}$$

where

$$\hat{\Lambda} = \frac{\overleftarrow{\partial}}{\partial P}\frac{\overrightarrow{\partial}}{\partial R} - \frac{\overleftarrow{\partial}}{\partial R}\frac{\overrightarrow{\partial}}{\partial P} \tag{68}$$

is the negative Poisson operator associated with the nuclear DOFs.[83,86,87]

Combining Eq. 67 and Eq. 42, we can write down the general expression of the Wigner/S-W transform for the product of two operators $\hat{A}\hat{B}$ as follows

$$\begin{aligned}\big[\hat{A}\hat{B}\big]_{\mathrm{w}\bar{\mathrm{s}}} &= [\mathcal{A}_0]_{\mathrm{w}} e^{-i\frac{\hat{\Lambda}\hbar}{2}} [\mathcal{B}_0]_{\mathrm{w}} + \frac{1}{2N}\sum_{k=1}^{N^2-1} [\mathcal{A}_k]_{\mathrm{w}} e^{-i\frac{\hat{\Lambda}\hbar}{2}} [\mathcal{B}_k]_{\mathrm{w}} \\ &+ r_{\bar{\mathrm{s}}} \sum_{k=1}^{N^2-1} \Omega_k \big([\mathcal{A}_k]_{\mathrm{w}} e^{-i\frac{\hat{\Lambda}\hbar}{2}} [\mathcal{B}_0]_{\mathrm{w}} + [\mathcal{A}_0]_{\mathrm{w}} e^{-i\frac{\hat{\Lambda}\hbar}{2}} [B_k]_{\mathrm{w}}\big) \\ &+ \frac{r_{\bar{\mathrm{s}}}}{2} \sum_{i,j,k=1}^{N^2-1} \Omega_i [\mathcal{A}_j]_{\mathrm{w}} e^{-i\frac{\hat{\Lambda}\hbar}{2}} [\mathcal{B}_k]_{\mathrm{w}} (d_{ijk} + i f_{ijk}), \quad (69)\end{aligned}$$

where $[\mathcal{A}_i]_{\mathrm{w}}$ is the Wigner transform of $\mathcal{A}_i(\hat{R})$ (with the corresponding expression in Eq. 32). The above expression can be easily generalized into the symmetrized version of TCF with $\frac{1}{2}\big[e^{-\beta\hat{H}}\hat{A}(0) + A(0)e^{-\beta\hat{H}}\big]_{\mathrm{w}\bar{\mathrm{s}}}$, and evaluating each term of the Wigner transform and S-W transform.

For an operator $\hat{A}$ that does not depend on the electronic DOFs (*e.g.* not an electronic operator $|n\rangle\langle m|$), we have $[\hat{A}]_{\mathrm{w}\bar{\mathrm{s}}} = [\hat{\mathcal{A}}_0]_{\mathrm{w}}$, then

$$\big[e^{-\beta\hat{H}}\hat{A}\big]_{\mathrm{w}\bar{\mathrm{s}}} = \mathcal{A}_0 \cdot \cos\frac{\hat{\Lambda}\hbar}{2} \big[e^{-\beta\hat{H}}\big]_{\mathrm{w}\bar{\mathrm{s}}}.$$

Further, if $\hat{A}$ is only linear in $\hat{R}$ or $\hat{P}$, we have

$$\big[e^{-\beta\hat{H}}\hat{A}\big]_{\mathrm{w}\bar{\mathrm{s}}} = \mathcal{A}_0 \big[e^{-\beta\hat{H}}\big]_{\mathrm{w}\bar{\mathrm{s}}}.$$

The estimator $[\hat{B}]_{\mathrm{ws}}$ in Eq. 66 is also a mixed Wigner/S-W transform of $\hat{B}$, but with a complementary index r_{s}. If $\hat{B}$ is a position operator, then $\hat{B} = \hat{R}$, and $\big[\hat{B}\big]_{\mathrm{ws}} = \big[\hat{R}\big]_{\mathrm{w}} = R$. If $\hat{B}$ is a pure electronic projection operator $\hat{B} = |n\rangle\langle n|$, the estimator is $[\hat{B}]_{\mathrm{ws}} = [|n\rangle\langle n|]_{\mathrm{s}}$, with the expression detailed in Eq. 44. In addition, the expression of $[|n\rangle\langle n|]_{\mathrm{s}}$ in terms of the MMST variables can be found in Eq. 54.

C. Population Dynamics via Time-Correlation Function

For a given photo-induced process, we are often interested in the reduced density matrix dynamics upon an initial excitation of the molecular system. In this case, the system is initially prepared in its ground state, with the ground state Hamiltonian

$$\hat{H}_g = \big(\hat{T}_R + U_g(\hat{R})\big), \quad (70)$$

and $U_g(\hat{R})$ is the ground state potential. Upon the initial photo-excitation of the system, the system is excited to state $|n\rangle$.

The reduced density matrix element can be expressed as

$$\rho_{ij}(t) = \mathrm{Tr_e Tr_n}[\hat{\rho}(0) e^{\frac{i}{\hbar}\hat{H}t} |i\rangle\langle j| e^{-\frac{i}{\hbar}\hat{H}t}], \tag{71}$$

where the initial density operator $\hat{\rho}(0)$ is expressed as a tensor product of the electronic and nuclear DOFs as $\hat{\rho}(0) = |n\rangle\langle n| \otimes \frac{1}{\mathcal{Z}} e^{-\beta \hat{H}_g}$, where $\mathcal{Z} = \mathrm{Tr}[e^{-\beta \hat{H}_g}]$, and $\hat{H}_g$ is the ground state Hamiltonian in Eq. 70.

The reduced density matrix $\rho_{ij}(t)$ can also be equivalently expressed as a correlation function

$$\rho_{ij}(t) = C_{AB}(t) = \frac{1}{\mathcal{Z}} \mathrm{Tr_e Tr_n}[e^{-\beta \hat{H}_g} \hat{A} e^{\frac{i}{\hbar}\hat{H}t} \hat{B} e^{-\frac{i}{\hbar}\hat{H}t}], \tag{72}$$

where $\hat{A} = |n\rangle\langle n|$ is the initially occupied electronic state, and $\hat{B} = |i\rangle\langle j|$. Using the mixed Wigner/S-W representation for the TCF, we have

$$C_{AB}(t) = \frac{1}{2\pi\hbar\mathcal{Z}} \int \mathrm{d}R \int \mathrm{d}P \int \mathrm{d}\mathbf{\Omega} \times \big[|n\rangle\langle n|\big]_{\bar{\mathrm{s}}} \big[e^{-\beta \hat{H}_g}\big]_{\mathrm{w}} e^{\hat{\mathcal{L}}t} \big[|i\rangle\langle j|\big]_{\mathrm{s}}. \tag{73}$$

One can numerically perform the integrals over $\mathrm{d}\mathbf{\Omega}$ by sampling the initial conditions according to the differential phase space volume element expression in Eq. 21, and explicitly using the expression of $[|n\rangle\langle n|]_{\bar{\mathrm{s}}}$ (Eq. 44 with $r_{\bar{\mathrm{s}}}$, or Eq. 55 in terms of the MMST mapping variables).

D. The Focused Initial Condition for Mapping Variables

Another numerically advantageous but *approximate* method is to focus the initial electronic state.[34,43,88] The focused method requires to know what values to attribute to the mapping variables in order to enforce an initial projection onto state $|n\rangle$. As proposed in the previous work of spin-LSC, this requires to replace $\big[|n\rangle\langle n|\big]_{\bar{\mathrm{s}}}$ in Eq. 73 by $\big[|n\rangle\langle n|\big]_{\mathrm{s}}$ in order to achieve a properly normalized initial population.[34,43] To this end, we first introduce the following variables

$$\Theta_n \equiv n r_{\mathrm{s}} \sum_{k=n+1}^{N} \sqrt{\frac{2}{k(k-1)}} \Omega_{\gamma_k} = r_{\mathrm{s}} \Big(\frac{N-n}{N} - \prod_{k=1}^{n} \sin^2 \frac{\theta_k}{2} \Big), \tag{74}$$

where $n \in \{1, \cdots, N-1\}$. The derivation of the second equality in Eq. 74 is provided in the Supplemental Material. For $n = N$, we further introduce the proper boundaries $\Theta_N = \Theta_0 = 0$. Later, we will show that this Θ_n is actually the canonical conjugate variable of φ_n (Eq. 102), which plays a role similar to the role the action variable (see Eq. 122b) plays in the MMST mapping formalism.[9,23]

We then write the estimator in Eq. 44 with these new

variables $\{\Theta_n\}$ as follows

$$\begin{aligned}\big[|n\rangle\langle n|\big]_{\rm s} =&\frac{1}{N}+\frac{1}{n}\Theta_n-(n-1)\Big(\frac{1}{n-1}\Theta_{n-1}-\frac{1}{n}\Theta_n\Big)\\ =&\frac{1}{N}+\Theta_n-\Theta_{n-1}\\ =&\frac{1}{N}+r_{\rm s}\Big(-\frac{1}{N}+\cos^2\frac{\theta_n}{2}\prod_{k=1}^{n-1}\sin^2\frac{\theta_k}{2}\Big),\end{aligned}\quad(75)$$

in the last line, $\cos^2\frac{\theta_n}{2}$ and $\prod_{k=1}^{n-1}\sin^2\frac{\theta_k}{2}$ are replaced by 1 when $n=N$ and $n=1$, respectively.

For $m<n$, the non-diagonal elements in Eq. 45 can be expressed in terms of θ_n and φ_n using the explicit expressions of $\Omega_{\alpha_{nm}}$ (Eq. B2) and $\Omega_{\beta_{nm}}$ (Eq. B3), resulting in

$$\begin{aligned}\big[|n\rangle\langle m|\big]_{\rm s} =&r_{\rm s}\prod_{j=1}^{m-1}\sin^2\frac{\theta_j}{2}\cos\frac{\theta_m}{2}\prod_{k=m}^{n-1}\sin\frac{\theta_k}{2}\\ &\times\cos\frac{(1-\delta_{nN})\theta_n}{2}\prod_{k=m}^{n-1}e^{-i\varphi_k}.\end{aligned}\quad(76)$$

The term $\prod_{j=1}^{m-1}\sin^2\frac{\theta_j}{2}$ is replaced by 1 when $m=1$. Using the definition of Θ_n (Eq. 74) one can further express it into Eq. 77. Alternatively, we can use the kernel expressed in Eq. 27 to evaluate

$$\big[|n\rangle\langle m|\big]_{\rm s}={\rm Tr}_{\rm e}\left[|n\rangle\langle m|\hat{w}_{\rm s}(\mathbf{\Omega})\right]=r_{\rm s}\langle\mathbf{\Omega}|n\rangle\langle m|\mathbf{\Omega}\rangle,$$

then using the definition of $\langle n|\mathbf{\Omega}\rangle$ (Eq. 18) to get

$$\begin{aligned}&\big[|n\rangle\langle m|\big]_{\rm s}\\ &=\sqrt{\Big(\Theta_n-\Theta_{n-1}+\frac{r_{\rm s}}{N}\Big)\Big(\Theta_m-\Theta_{m-1}+\frac{r_{\rm s}}{N}\Big)}\cdot\prod_{k=m}^{n-1}e^{-i\varphi_k},\end{aligned}\quad(77)$$

where $[|m\rangle\langle n|]_{\rm s}$ is the complex conjugate of Eq. 77. Note that $\{\theta_n\}\in[0,\pi]$, thus all the $\sin(\theta_k/2)$ and $\cos(\theta_k/2)$ in Eq. 76 are the square root of Eq. 77 gives non-negative result.

To obtain the focused initial conditions for an initially populated state $|n\rangle$, one requires that[43]

$$\big[|n\rangle\langle n|\big]_{\rm s}=1;\quad\big[|j\rangle\langle j|\big]_{\rm s}=0,\ (j\neq n).\quad(78)$$

As Eq. 75 is recursive, we derive the expression starting from state 1 toward state N, and obtain the values of the $\{\Theta_j\}$ as

$$\Theta_{j<n}=-\frac{j}{N};\quad\Theta_{j\geq n}=\frac{N-j}{N}.\quad(79)$$

More generally, when focusing on any combination of state with, for each state $|j\rangle$ an initial population P_j (such that $\sum_{j=1}^{N}P_j=1$), we have the expression

$$\Theta_j=\sum_{k=1}^{j}P_k-\frac{j}{N},\quad(80)$$

where the proof is provided in the Supplemental Material. The above focused initial conditions only affect angles $\{\theta_j\}$ for $j \in \{1, \cdots, N-1\}$, whereas the $\{\varphi_j\}$ angles are sampled randomly in the range $[0, 2\pi]$. This effectively evaluates the integrals over $\{\theta_j\}$, but leaves the original integrals over $\{\varphi_j\}$. From Eq. 74, we further derive the expression of the angles $\{\theta_n\}$ as follows

$$\cos\theta_n = 1 - 2\Big(\frac{N-n}{N} - \frac{\Theta_n}{r_{\rm s}}\Big), \quad n = 1, \tag{81a}$$

$$\cos\theta_n = 1 - \frac{2\Big(\frac{N-n}{N} - \frac{\Theta_n}{r_{\rm s}}\Big)}{\prod_{k=1}^{n-1}\sin^2\frac{\theta_k}{2}}, \quad 2 \leq n \leq N-1. \tag{81b}$$

The sines in the denominator of Eq. 81b can only be zero for s = Q, and in this case the equation for $\cos\theta_n$ is expressed in Eq. 81a. From the above equations, we note that any angle θ_n only depends on Θ_n and on the angles $\{\theta_j\}$ for $j < n$. Thus, the focused initial conditions in Eq. 79 (or more generally, Eq. 80) can be used to recursively generate values of θ_n based on Eq. 81.

In terms of the conjugate MMST mapping variables, the corresponding focused initial conditions in Eq. 78 are

$$q_n^2 + p_n^2 = 2 + \gamma; \quad q_j^2 + p_j^2 = \gamma, \ (j \neq n), \tag{82}$$

based on the expression of the estimator in Eq. 54. This is the focused initial conditions proposed in the recently developed spin-LSC approach.[43] However, these focused conditions do not provide any specific choice of $\{\varphi_j\}$ in generalized Euler angle variables (see Eq. 18), and based on the expression of $\mathrm{d}\mathbf{\Omega}$ (Eq. 21) it should be uniformly sampled. In principle, any algorithm that uses $\{q_n, p_n\}$ should generate a uniform distribution of $\{\varphi_j\}$ in the range $[0, 2\pi]$, required by the $\int \mathrm{d}\mathbf{\Omega}$ integral (see expression of $\mathrm{d}\mathbf{\Omega}$ in Eq. 21). In the spin-LSC approach, it is proposed that the corresponding angle variable ϕ_n (Eq. 122b) should be sampled uniformly, as the original MMST formalism suggested.[9,23] We shall see that $\varphi_n = \phi_{n+1} - \phi_n$ (Eq. 125), thus randomly sample ϕ_n is equivalent to randomly sample φ_n. Our rigorous theoretical framework thus helps to justify the empirical choices made by the previous simulation method.[43]

V. QUANTUM LIOUVILLIAN IN THE MIXED WIGNER/STRATONOVICH-WEYL REPRESENTATION

A. Exact Liouvillian Expression

In this section, we derive the exact expression of the quantum Liouvillian $\hat{\mathcal{L}}$ in Eq. 66. Using the Heisenberg

EOMs in the Wigner/S-W representation, we have

$$\frac{\mathrm{d}}{\mathrm{d}t}\big[\hat{B}\big]_{\mathrm{ws}} = \frac{i}{\hbar}\big[\hat{H},\hat{B}\big]_{\mathrm{ws}} \equiv \hat{\mathcal{L}}[\hat{B}]_{\mathrm{ws}} \tag{83}$$
$$= \frac{2}{\hbar}[\mathcal{H}_0]_{\mathrm{w}}\sin\frac{\hat{\Lambda}\hbar}{2}[\mathcal{B}_0]_{\mathrm{w}} + \frac{1}{\hbar N}\sum_{k=1}^{N^2-1}[\mathcal{H}_k]_{\mathrm{w}}\sin\frac{\hat{\Lambda}\hbar}{2}[\mathcal{B}_k]_{\mathrm{w}}$$
$$+ \frac{2r_{\mathrm{s}}}{\hbar}\sum_{k=1}^{N^2-1}\Omega_k\Big([\mathcal{H}_k]_{\mathrm{w}}\sin\frac{\hat{\Lambda}\hbar}{2}[\mathcal{B}_0]_{\mathrm{w}} + [\mathcal{H}_0]_{\mathrm{w}}\sin\frac{\hat{\Lambda}\hbar}{2}[\mathcal{B}_k]_{\mathrm{w}}\Big)$$
$$+ \frac{r_{\mathrm{s}}}{\hbar}\sum_{i,j,k=1}^{N^2-1}d_{ijk}[\mathcal{H}_i]_{\mathrm{w}}\Omega_j\sin\frac{\hat{\Lambda}\hbar}{2}[\mathcal{B}_k]_{\mathrm{w}}$$
$$+ \frac{r_{\mathrm{s}}}{\hbar}\sum_{i,j,k=1}^{N^2-1}f_{ijk}[\mathcal{H}_i]_{\mathrm{w}}\Omega_j\cos\frac{\hat{\Lambda}\hbar}{2}[\mathcal{B}_k]_{\mathrm{w}},$$

where we have explicitly used the property in Eq. 42 for the S-W transform and the property in Eq. 67 for the Wigner transform. One can in principle derive the Liouvillian expressed in terms of the MMST variables (defined in Eq. 46), using the kernel expressed in the MMST variables and diabatic basis (Eq. 52). However, this leads to a complicated expression of $[\hat{A}\hat{B}]_{\mathrm{s}}$, as opposed to the simple expression in Eq. 42. We thus decide to use the $\mathfrak{su}(N)$ generators to derive the Liouvillian expression. One can then perform the transform (see Sec.VC-D) to obtain an expression with MMST variables.

Based on Eq. 83, we identify a state-independent part and a state-dependent part of the Liouvillian, acting respectively on the state-independent and state-dependent components of the operator $\hat{B}$. By rewriting the total time-derivative of operator $[\hat{B}]_{\mathrm{ws}}$ we have

$$\frac{\mathrm{d}}{\mathrm{d}t}\big[\hat{B}\big]_{\mathrm{ws}} = \frac{\mathrm{d}}{\mathrm{d}t}\big[\mathcal{B}_0\hat{\mathcal{I}}\big]_{\mathrm{ws}} + \sum_{k=1}^{N^2-1}\frac{\mathrm{d}}{\mathrm{d}t}\big[\mathcal{B}_k\cdot\frac{1}{\hbar}\hat{\mathcal{S}}_k\big]_{\mathrm{ws}} \tag{84}$$
$$= \frac{\mathrm{d}}{\mathrm{d}t}\big[\mathcal{B}_0\big]_{\mathrm{w}} + \sum_{k=1}^{N^2-1}\frac{\mathrm{d}}{\mathrm{d}t}\Big(\big[\mathcal{B}_k\big]_{\mathrm{w}}\cdot r_{\mathrm{s}}\Omega_k\Big)$$
$$\equiv \hat{\mathcal{L}}_0[\mathcal{B}_0]_{\mathrm{w}} + r_{\mathrm{s}}\sum_{k=1}^{N^2-1}\hat{\mathcal{L}}_k\big(\Omega_k[\mathcal{B}_k]_{\mathrm{w}}\big).$$

By comparing Eq. 83 and Eq. 84, the state-independent Liouvillian is expressed as

$$\hat{\mathcal{L}}_0[\mathcal{B}_0]_{\mathrm{w}} \equiv \frac{2}{\hbar}H_{\mathrm{s}}\sin\frac{\hat{\Lambda}\hbar}{2}[\mathcal{B}_0]_{\mathrm{w}}, \tag{85}$$

with H_{s} expressed as

$$H_{\mathrm{s}}(R,P) = [\hat{H}(\hat{R},\hat{P})]_{\mathrm{ws}} = [\mathcal{H}_0]_{\mathrm{w}} + r_{\mathrm{s}}\sum_{k=1}^{N^2-1}\Omega_k[\mathcal{H}_k]_{\mathrm{w}}$$
$$= \mathcal{H}_0(R,P) + r_{\mathrm{s}}\sum_{k=1}^{N^2-1}\Omega_i\mathcal{H}_k(R). \tag{86}$$

For the last line of the above equation, we have used the fact that $[\mathcal{H}_k(\hat{R})]_\mathrm{w} = \mathcal{H}_k(R)$ (see Eq. 11b or Eq. 12 for its expression) and $[\mathcal{H}_0(\hat{R},\hat{P})]_\mathrm{w} = \mathcal{H}_0(R,P)$ because the Wigner transform of a function of position operator is the same function, and $\mathcal{H}_0(\hat{R},\hat{P})$ only contains $\hat{P}$ up to the quadratic order.[84]

The state-dependent Liouvillian is expressed as

$$\begin{aligned}\hat{\mathcal{L}}_i\big(r_\mathrm{s}\Omega_i[\mathcal{B}_i]_\mathrm{w}\big) \equiv& \frac{1}{\hbar}\Big[\big(\frac{1}{N}\mathcal{H}_i + 2r_\mathrm{s}\Omega_i\mathcal{H}_0\big)\sin\frac{\hat{\Lambda}\hbar}{2} \\ &+ r_\mathrm{s}\sum_{j,k=1}^{N^2-1} d_{ijk}\mathcal{H}_j\Omega_k \sin\frac{\hat{\Lambda}\hbar}{2} \\ &+ r_\mathrm{s}\sum_{j,k=1}^{N^2-1} f_{ijk}\mathcal{H}_j\Omega_k\cos\frac{\hat{\Lambda}\hbar}{2}\Big][\mathcal{B}_i]_\mathrm{w}. \quad (87)\end{aligned}$$

We further identify two terms in $\hat{\mathcal{L}}_i$ as $\hat{\mathcal{L}}_i = \hat{\mathcal{L}}_i^\mathrm{e} + \hat{\mathcal{L}}_i^\mathrm{n}$. The first term evolves $\Omega_i[\mathcal{B}_i]_\mathrm{w}$ as follows

$$\hat{\mathcal{L}}_i^\mathrm{e}\big(r_\mathrm{s}\Omega_i[\mathcal{B}_i]_\mathrm{w}\big) \equiv \frac{1}{\hbar}r_\mathrm{s}\sum_{j,k=1}^{N^2-1} f_{ijk}\mathcal{H}_j\Omega_k\cos\frac{\hat{\Lambda}\hbar}{2}[\mathcal{B}_i]_\mathrm{w}, \quad (88)$$

where the leading term $\cos\frac{\hat{\Lambda}\hbar}{2} \approx 1$ evolves only the spin mapping variables. The second term evolves the nuclear DOFs through the coupling between the spin mapping variables and the nuclear DOFs as follows

$$\begin{aligned}&\hat{\mathcal{L}}_i^\mathrm{n}(r_\mathrm{s}\Omega_i[\mathcal{B}_i]_\mathrm{w}) \quad (89)\\ &\equiv \frac{1}{\hbar}\Big(\frac{1}{N}\mathcal{H}_i + 2r_\mathrm{s}\Omega_i\mathcal{H}_0 + r_\mathrm{s}\sum_{j,k=1}^{N^2-1} d_{ijk}\mathcal{H}_j\Omega_k\Big)\sin\frac{\hat{\Lambda}\hbar}{2}[\mathcal{B}_i]_\mathrm{w}.\end{aligned}$$

Naturally, if there is no state-dependent Hamiltonian ($H_\mathrm{s} = [\mathcal{H}_0]_\mathrm{w}$ and $\forall j,\ \mathcal{H}_j = 0$), the Liouvillian expression in Eq. 83 reduces back to the original Wigner-Moyal series[66] as follows

$$\frac{\mathrm{d}}{\mathrm{d}t}\big[\hat{B}\big]_\mathrm{ws} = \hat{\mathcal{L}}\Big([\mathcal{B}_0]_\mathrm{w} + r_\mathrm{s}\sum_{i=1}^{N^2-1}\Omega_i[\mathcal{B}_i]_\mathrm{w}\Big) \quad (90a)$$

$$\hat{\mathcal{L}} = \frac{P}{m}\overrightarrow{\partial_R} - \frac{2}{\hbar}U_0(R)\sin\left(\frac{\hbar}{2}\overleftarrow{\partial_R}\overrightarrow{\partial_P}\right). \quad (90b)$$

Further, in the special case where there is no nuclear dependency, the only remaining term in the Liouvillian (Eq. 88) is

$$\hat{\mathcal{L}}_i^\mathrm{e}(r_\mathrm{s}\Omega_i) = \frac{1}{\hbar}r_\mathrm{s}\sum_{j,k=1}^{N^2-1} f_{ijk}\mathcal{H}_j\Omega_k, \quad (91)$$

which goes back, as expected, to the expression of the EOMs derived by Hioe and Eberly[36] given in Eq. 15.

To summarize, the TCF (Eq. 66) with the exact Liou-

villian is expressed as

$$C_{AB}(t) = \frac{1}{2\pi\hbar\mathcal{Z}} \int \mathrm{d}R \int \mathrm{d}P \int \mathrm{d}\boldsymbol{\Omega} \big[e^{-\beta\hat{H}}\hat{A}\big]_{\mathrm{w\bar{s}}} \times \Big[e^{\hat{\mathcal{L}}_0 t}[\mathcal{B}_0]_{\mathrm{w}} + r_{\mathrm{s}} \sum_{k=1}^{N^2-1} e^{\hat{\mathcal{L}}_k t}\Omega_k[\mathcal{B}_k]_{\mathrm{w}}\Big], \tag{92}$$

where $\hat{\mathcal{L}}_0$ and $\hat{\mathcal{L}}_k$ are expressed in Eq. 85 and Eq. 87, respectively. This is the *first key result* of this paper.

B. Linearization Approximation and the Equations of Motion

So far, we have not made any approximation to the TCF expression. Solving Eq. 92 will be as difficult as solving the exact quantum dynamics, if not more. To simplify the task, we use the linearized path-integral approximation,[11,89] or equivalently, linearizing the sines and cosines[77] of $\hat{\Lambda}$ in Eq. 83 as follows

$$\cos\frac{\hat{\Lambda}\hbar}{2} \approx 1, \quad \sin\frac{\hat{\Lambda}\hbar}{2} \approx \frac{\hat{\Lambda}\hbar}{2}. \tag{93}$$

This linearization approximation is equivalent to the approximation used in Linearized Semiclassical-Initial Value Representation (LSC-IVR).[11,90,91] with the difference that the current approach uses the generalized spin mapping variables as opposed to the original MMST mapping variables.[8,10]

Within the linearized approximation, we obtain the EOMs for the state-independent component (in Eq. 85) as follows

$$\frac{\mathrm{d}}{\mathrm{d}t}[\mathcal{B}_0]_{\mathrm{w}} \approx \Big[\frac{P}{m}\overrightarrow{\partial_R} - \big(\partial_R\mathcal{H}_0 + r_{\mathrm{s}}\sum_{k=1}^{N^2-1}\partial_R\mathcal{H}_k\Omega_k\big)\overrightarrow{\partial_P}\Big][\mathcal{B}_0]_{\mathrm{w}}. \tag{94}$$

The state-dependent time-derivatives (in Eqs. 84 and 87) after the linearization approximation become

$$\begin{aligned} r_{\mathrm{s}}\frac{\mathrm{d}}{\mathrm{d}t}\big(\Omega_i[\mathcal{B}_i]_{\mathrm{w}}\big) &= r_{\mathrm{s}}\frac{\mathrm{d}\Omega_i}{\mathrm{d}t}\cdot[\mathcal{B}_i]_{\mathrm{w}} + r_{\mathrm{s}}\Omega_i\cdot\frac{\mathrm{d}}{\mathrm{d}t}[\mathcal{B}_i]_{\mathrm{w}} \\ &\approx \frac{1}{\hbar}\Big[r_{\mathrm{s}}\sum_{j,k=1}^{N^2-1} f_{ijk}\mathcal{H}_j\Omega_k + \big(2r_{\mathrm{s}}\Omega_i\mathcal{H}_0 + \frac{1}{N}\mathcal{H}_i\big)\frac{\hat{\Lambda}\hbar}{2} \\ &\quad + r_{\mathrm{s}}\sum_{j,k=1}^{N^2-1} d_{ijk}\mathcal{H}_j\Omega_k\frac{\hat{\Lambda}\hbar}{2}\Big][\mathcal{B}_i]_{\mathrm{w}}. \end{aligned} \tag{95}$$

Note that Ω_i (see Eq. 23) is an independent variable of the nuclear DOFs, $\{R, P\}$. Thus, the first term on the right hand side of Eq. 95, which is independent of both R and P, must be equal to $r_{\mathrm{s}}\frac{\mathrm{d}\Omega_i}{\mathrm{d}t}\cdot[\mathcal{B}_i]_{\mathrm{w}}$, whereas the remaining terms on the right hand side of Eq. 95, which in principle depends on R and P, must be equal to $r_{\mathrm{s}}\Omega_i\cdot\frac{\mathrm{d}}{\mathrm{d}t}[\mathcal{B}_i]_{\mathrm{w}}$.

As mentioned in Appendix 5 of WIREs. Comput. Mol. Sci. e1619 (2022), the first-order truncation of \hbar does not lead the EOMs that one obtains from Classical Wigner model, i.e., the mean-field trajectories. The "derivations" below in this section are sloppy since the authors confuse the total and partial time derivate in such as Eq. (94) and (97).

This helps to identify the individual time derivatives for Ω_i as follows

$$\frac{\mathrm{d}}{\mathrm{d}t}\Omega_i = \frac{1}{\hbar}\sum_{j,k=1}^{N^2-1} f_{ijk}\mathcal{H}_j\Omega_k, \tag{96}$$

which is identical to Eq. 15, as well as time-derivative of $[\mathcal{B}_i]_{\mathrm{w}}$ as follows

$$\begin{aligned}\frac{\mathrm{d}}{\mathrm{d}t}[\mathcal{B}_i]_{\mathrm{w}} =&\Big[\frac{P}{m}\overrightarrow{\partial_R} - \big(\partial_R\mathcal{H}_0 + \frac{1}{2Nr_{\mathrm{s}}\Omega_i}\partial_R\mathcal{H}_i \\ &+ \sum_{j,k=1}^{N^2-1} d_{ijk}\frac{\Omega_k}{2\Omega_i}\partial_R\mathcal{H}_j\big)\overrightarrow{\partial_P}\Big][\mathcal{B}_i]_{\mathrm{w}}.\end{aligned} \tag{97}$$

The Liouvillians acting on $[\mathcal{B}_0]_{\mathrm{w}}$ (Eq. 94) and on $[\mathcal{B}_i]_{\mathrm{w}}$ (Eq. 97) are different, which is the feature of the spin mapping formalism. We emphasize that these equations are in principle exact for linear conical intersection problem that has quadratic potential, such as spin-boson problem. This is because under such conditions, $\mathcal{H}_0$ is a function up to R^2 and $\mathcal{H}_k$ is a linear function of R, and thus the truncation in Eq. 93 becomes exact because those higher order terms of $\hat{\Lambda}$ will not act on $\mathcal{H}_0$ or $\mathcal{H}_k$ in Eq. 83.

In the practical implementations of this approximation, such as in the recently proposed spin-LSC,[34] the nuclear DOFs were proposed to be updated with the Liouvillian in Eq. 94. This should be viewed as an independent approximation, in addition to the linearized approximation expressed in Eq. 93. Future investigations will be carried to develop new propagation schemes taking into account the two Liouvillian components for a trajectory based method.

C. Equations of Motion with the expectation value of Generators

Thus, under the linearization approximation and using Eq. 94 to propagate the nuclear DOFs, we have the following classical EOMs, which is the *second key result* of this paper

$$\dot{R} = \frac{P}{m}, \tag{98a}$$

$$\dot{P} = -\frac{\partial\mathcal{H}_0}{\partial R} - r_{\mathrm{s}}\sum_{k=1}^{N^2-1}\frac{\partial\mathcal{H}_k}{\partial R}\Omega_k = -\frac{\partial H_{\mathrm{s}}(R,P)}{\partial R}, \tag{98b}$$

$$\frac{\mathrm{d}}{\mathrm{d}t}\Omega_i = \frac{1}{\hbar}\sum_{j,k=1}^{N^2-1} f_{ijk}\mathcal{H}_j(R)\Omega_k, \tag{98c}$$

where $H_{\mathrm{s}}(R,P)$ is expressed in Eq. 86. The analytic expressions of the structure constants f_{ijk} are provided in Eq. A5. Note that we choose to propagate the nuclear DOFs following the state-independent Liouvillian $\mathcal{L}_0$ that leads to Eq. 94, not considering the state-dependent Liouvillian $\mathcal{L}_i^{\mathrm{n}}$ which corresponds to Eq. 97.

The above EOMs can be viewed as the generalization of the N-dimensional spin precession theory (Eq. 15) of Hioe and Eberly[36], where the electronic-nuclear coupling is explicitly considered here.

The above equations were recently *proposed* as the EOMs for the Generalized Discrete Truncated Wigner Approximation (GDTWA) approach[51] by choosing $r_{\rm s} = \sqrt{N+1}$ (or s = W). The EOMs were argued as the classical limit of the Heisenberg EOMs[51] for the corresponding operators $\hat{R}$, $\hat{P}$, and $\hat{\mathcal{S}}_k$. Here, we present a rigorous derivation of these EOMs.

One can thus propagate quantum dynamics based on the EOMs outlined in Eq. 98. The initial conditions for the electronic DOFs can be sampled based on the phase space volume element in $\int {\rm d}\mathbf{\Omega}$ (Eqs. 21-22), which provides initial values of $\{\theta_n\}$ and $\{\varphi_n\}$, and then provide the values of $\{\Omega_k\}$ through Eq. B2-B4. The nuclear DOFs will be sampled through the initial Wigner density (for example, $\left[e^{-\beta \hat{H}_g}\right]_{\rm w}$ in Eq. 73). These variables will be numerically propagate according to EOMs in Eq. 98.

The formal numerical scaling for solving Eq. 98c is $\mathcal{O}(N^4)$, due to the N^2 dimensionality of both $\mathcal{H}_j$ and Ω_k. It is thus ideal to find alternative but equivalent EOMs that reduce this scaling. Below, we derive three sets of linearized EOMs that are equivalent to the EOMs in Eq. 98c.

VI. ALTERNATIVE EXPRESSIONS OF THE LINEARIZED EQUATIONS OF MOTION

In this section, we derive three sets of EOMs that are equivalent to the linearized EOMs in Eq. 98. We provide three possible choices of conjugate variables that fulfill this task.

A. Equations of Motion with the Action-Angle Type Variables

In order to obtain equivalent EOMs in terms of the $2N-2$ variables, we want to find a set of canonical variables. We recognize that in the two-state special case,[35,92] the conjugate momentum of φ_1 is $\frac{1}{2} r_{\rm s} \cos\theta_1 \equiv r_{\rm s}\Omega_{\gamma_2}$, where γ_2 is the index of the diagonal generator (see Eq. 5c). Hence, we expect a conjugate momentum of any φ_n being a combination of $\{\Omega_{\gamma_j}\}$ for $j \in \{2, \cdots, N\}$, which to the best of our knowledge, is unknown in the literature. Based on this conjectured conjugate relationship, we postulate the following Hamilton's EOMs

$$r_{\rm s} \sum_{j=1}^{N} C_n(j) \frac{\rm d}{{\rm d}t} \Omega_{\gamma_j} = -\frac{\partial H_{\rm s}}{\partial \varphi_n} \tag{99a}$$

$$r_{\rm s} \frac{\rm d}{{\rm d}t} \varphi_n = \frac{\partial H_{\rm s}}{\partial \sum_{j=1}^{N} C_n(j) \Omega_{\gamma_j}}, \tag{99b}$$

where $H_{\rm s}$ is expressed in Eq. 86. Here, $C_n(j)$ is the coefficient depending on the index of the generator γ_j, and the index of the *conjugate general coordinate* φ_n. Using Eq. 98c and our closed formulas for the structure constants of $\mathfrak{su}(N)$ (see Appendix A), we derive the coefficients as follows

$$C_n(j \leq n) = 0; \quad C_n(j > n) = n\sqrt{\frac{2}{j(j-1)}}, \tag{100}$$

the derivation can be found in Appendix D. The general expression of the *conjugate variable of* φ_n for N-state systems, considering the coefficients found above, is

$$n \cdot r_{\rm s} \sum_{j=n+1}^{N} \sqrt{\frac{2}{j(j-1)}} \Omega_{\gamma_j} \equiv \Theta_n, \tag{101}$$

which exactly corresponds to the variable Θ_n defined in Eq. 74. With the above finding, Eq. 99 can be rigorously expressed as

$$\dot{\Theta}_n = -\frac{\partial H_{\rm s}}{\partial \varphi_n}; \quad \dot{\varphi}_n = \frac{\partial H_{\rm s}}{\partial \Theta_n}, \tag{102}$$

with $H_{\rm s}$ expressed in Eq. 86, and the nuclear DOFs obeys Eq. 98a-Eq. 98b. Thus, we have discovered conjugate variables $\{\Theta_n, \varphi_n\}$ which decompose the $N^2 - 1$ coupled equations in Eq. 98c into $2N - 2$ coupled equations. In fact, Θ_n and φ_n play a similar role as the "action" and the "angle" variables in the original Meyer-Miller mapping formalism.[9] This is not very surprising, as the action variables are related to the population of states, and Θ_n is directly related to the population estimator (see Eq. 75) and thus related to the action variable (Eq. 122) as well.

In order to derive the closed formula of the EOMs in Eq. 102 with variables $\{\Theta_n, \varphi_n\}$, we express the Hamiltonian in terms of these variables. Using Eq. 75 and Eq. 77, the mapping Hamiltonian in Eq. 58 (with replacing $\hat{R}$ to R upon nuclear Wigner transform) can be expressed as

$$\begin{aligned} H_{\rm s} = \frac{P^2}{2M} + U_0(R) + \sum_{n=1}^{N} \Big(\Theta_n - \Theta_{n-1} + \frac{1}{N}\Big) \cdot V_{nn}(R) \\ + 2\sum_{n=2}^{N}\sum_{m=1}^{n-1} \sqrt{\Big(\Theta_n - \Theta_{n-1} + \frac{r_{\rm s}}{N}\Big)\Big(\Theta_m - \Theta_{m-1} + \frac{r_{\rm s}}{N}\Big)} \\ \times \cos\Big(\sum_{k=m}^{n-1} \varphi_k\Big) \cdot V_{nm}(R), \end{aligned} \tag{103}$$

which is reminiscent to the Meyer-Miller mapping Hamiltonian in the form of the action-angle variables[9,23] (see Eq. 126) and the transformation to the cartesian mapping variables $\{p_n, q_n\}$ are provided in Eq. 120a and Eq. 120b. Note that we have assumed a purely real Hamiltonian when expressing Eq. 103. The general form of the mapping Hamiltonian can be found in Eq. D7, and the two-state special case of Eq. 103 is provided in Eq. E12. Using the expression of $H_{\rm s}$ in Eq. 103, the Hamilton's EOMs in Eq. 102 can be expressed in details as follows

$$\dot{\Theta}_n = -\frac{\partial H_{\rm s}}{\partial \varphi_n} = 2\sum_{l=n+1}^{N}\sum_{m=1}^{n} V_{lm}(R)\sqrt{\Big(\Theta_l - \Theta_{l-1} + \frac{r_{\rm s}}{N}\Big)}\sqrt{\Big(\Theta_m - \Theta_{m-1} + \frac{r_{\rm s}}{N}\Big)}\cdot \sin\left(\sum_{k=m}^{l-1}\varphi_k\right), \tag{104a}$$

$$\dot{\varphi}_n = \frac{\partial H_{\rm s}}{\partial \Theta_n} = V_{nn}(R) - V_{n+1,n+1}(R) \tag{104b}$$

$$+\left[\sum_{m\neq n}^{N} V_{nm}(R)\sqrt{\frac{\Theta_m - \Theta_{m-1} + \frac{r_{\rm s}}{N}}{\Theta_n - \Theta_{n-1} + \frac{r_{\rm s}}{N}}}\cdot\cos\Big(\sum_{k=\min\{m,n\}}^{\max\{m,n\}-1}\varphi_k\Big) - \sum_{m\neq n+1}^{N} V_{nm}(R)\sqrt{\frac{\Theta_m - \Theta_{m-1} + \frac{r_{\rm s}}{N}}{\Theta_{n+1} - \Theta_n + \frac{r_{\rm s}}{N}}}\cdot\cos\Big(\sum_{k=\min\{m,n+1\}}^{\max\{m-1,n\}}\varphi_k\Big)\right],$$

where the nuclear DOFs obeys Eq. 98a-Eq. 98b. The two-state special case of the above EOMs are provided in Eq. E13. The above EOMs share a similar form in those original Meyer-Miller mapping EOMs expressed in the action-angle variables[9] (see Eq. 127a), because the conjugate variables $\{\Theta_n, \varphi_n\}$ are closely related to the Meyer-Miller action-angle variables (see Eq. 124 and Eq. 125). The advantage of using the conjugate variable relationship between Θ_n and φ_n in Eq. 104, instead of the EOMs expressed in Eq. 98c with $\{\Omega_j\}$ is that in the former case there are $2N-2$ variables to explicitly propagate, as opposed to the N^2-1 variables of the latter.

B. Equations of Motion with the Generalized Euler Angles

Similarly, one can formulate the EOMs in terms of the generalized Euler angles $\{\theta_n, \varphi_n\}$. The EOMs with these variables are a bit more complicated and non-linear in terms of $\{\theta_n, \varphi_n\}$, as oppose to the case of $\{\Theta_n, \varphi_n\}$. This is because θ_n is not the conjugate variable of φ_n, but Θ_n is. To this end, we express the EOMs in Eq. 102 in terms of $\{\Omega_k\}$, which in turn depends on $\{\theta_n, \varphi_n\}$ (see Eq. B2-Eq. B4). To obtain $\partial H_{\rm s}/\partial\varphi_n$, we use the expression of $H_{\rm s}$ in Eq. 86 and explicitly take the derivative with respect to φ_n. Note that only $\Omega_{\alpha_{jk}}$ and $\Omega_{\beta_{jk}}$ contain φ_n, whereas Ω_{γ_k} only contains $\{\theta_j\}$. Using the detailed expressions of $\Omega_{\alpha_{jk}}$ (Eq. B2) and $\Omega_{\beta_{jk}}$ (Eq. B3), we have

$$-\frac{\partial H_{\rm s}}{\partial \varphi_n} = r_{\rm s}\sum_{j=n+1}^{N}\sum_{k=1}^{n}\big(\mathcal{H}_{\alpha_{jk}}\Omega_{\beta_{jk}} - \mathcal{H}_{\beta_{jk}}\Omega_{\alpha_{jk}}\big). \tag{105}$$

To obtain the time derivative of φ_n, we try to[93] find an expression in terms of the generators that have a well defined time derivative in Eq. 96. From the expressions of $\Omega_{\alpha_{nm}}$ (Eq. B2) and $\Omega_{\beta_{nm}}$ (Eq. B3), we know that

$$\tan\varphi_n = \frac{\Omega_{\beta_{n+1,n}}}{\Omega_{\alpha_{n+1,n}}}, \tag{106}$$

which leads to the expression of the time derivative of φ_n

as

$$\begin{aligned}\dot{\varphi}_n &= \frac{\mathrm{d}}{\mathrm{d}t}\Big(\arctan\frac{\Omega_{\beta_{n+1,n}}}{\Omega_{\alpha_{n+1,n}}}\Big) \\ &= \frac{\dot{\Omega}_{\beta_{n+1,n}}\Omega_{\alpha_{n+1,n}} - \Omega_{\beta_{n+1,n}}\dot{\Omega}_{\alpha_{n+1,n}}}{\Omega^2_{\alpha_{n+1,n}} + \Omega^2_{\beta_{n+1,n}}}.\end{aligned} \tag{107}$$

Using the analytical expressions of the $\mathfrak{su}(N)$ structure constants (Appendix A), we can obtain the closed analytic expression of $\dot{\Omega}_{\alpha_{n+1,n}}$ (Eq. D5) and $\dot{\Omega}_{\beta_{n+1,n}}$ (Eq. D6). Thus, using the transform between $\{\mathbf{\Omega}\}$ and $\{\varphi_n, \Theta_n\}$ as follows

$$\Theta_n = n \cdot r_{\mathrm{s}} \sum_{j=n+1}^{N} \sqrt{\frac{2}{j(j-1)}}\Omega_{\gamma_j}, \tag{108a}$$

$$\varphi_n = \tan^{-1}\frac{\Omega_{\beta_{n+1,n}}}{\Omega_{\alpha_{n+1,n}}}, \tag{108b}$$

the EOMs in Eq. 102 (which is equivalent to Eq. 98) are expressed with the conjugate variables $\{\Theta_n, \varphi_n\}$ as

$$\dot{\Theta}_n = -\frac{\partial H_{\mathrm{s}}}{\partial \varphi_n} = r_{\mathrm{s}} \sum_{j=n+1}^{N}\sum_{k=1}^{n}\left(\mathcal{H}_{\alpha_{jk}}\Omega_{\beta_{jk}} - \mathcal{H}_{\beta_{jk}}\Omega_{\alpha_{jk}}\right) \tag{109a}$$

$$\dot{\varphi}_n = \frac{\partial H_{\mathrm{s}}}{\partial \Theta_n} = \frac{\dot{\Omega}_{\beta_{n+1,n}}\Omega_{\alpha_{n+1,n}} - \Omega_{\beta_{n+1,n}}\dot{\Omega}_{\alpha_{n+1,n}}}{\Omega^2_{\alpha_{n+1,n}} + \Omega^2_{\beta_{n+1,n}}}, \tag{109b}$$

where H_{s} is expressed in Eq. 86, and the nuclear DOFs obeys Eq. 98a-Eq. 98b.

Further, one can also express the EOMs in Eq. 102 directly in terms of the generalized Euler angles $\{\theta_n, \varphi_n\}$, without using the conjugated variables $\{\Theta_n, \varphi_n\}$. To this end, we use the expression of $\Theta_n(\{\theta_k\})$ in Eq. 74 and directly work out its time derivative (through the chain rule with θ_n) as follows

$$\dot{\Theta}_n = -\frac{\partial H_{\mathrm{s}}}{\partial \varphi_n} = -\sum_{j=1}^{n} r_{\mathrm{s}}\dot{\theta}_j \frac{\sin\theta_j}{2}\prod_{\substack{k=1\\k\neq j}}^{n}\sin^2\frac{\theta_k}{2}. \tag{110}$$

The above equation can be expressed as an equivalent

but recursive expression as follows

$$-\frac{\partial H_{\rm s}}{\partial \varphi_n} = -\frac{\partial H_{\rm s}}{\partial \varphi_{n-1}} \sin^2\frac{\theta_n}{2} - r_{\rm s}\dot{\theta}_n \frac{\sin\theta_n}{2}\prod_{j=1}^{n-1}\sin^2\frac{\theta_j}{2}. \tag{111}$$

The above equation gives a numerically efficient recursive expression of $\dot{\theta}_n$ as follows

$$\dot{\theta}_n = \Big(\frac{\partial H_{\rm s}}{\partial \varphi_n}\frac{2}{\sin\theta_n} - \frac{\partial H_{\rm s}}{\partial \varphi_{n-1}}\tan\frac{\theta_n}{2}\Big)\Big/\Big(r_{\rm s}\prod_{j=1}^{n-1}\sin^2\frac{\theta_j}{2}\Big), \tag{112}$$

where for $n = 1$ the denominator is replaced by $r_{\rm s}$ because there is no θ_0 variable and the numerator only has the term that includes $\frac{\partial H_{\rm s}}{\partial \varphi_n}$ as there is no φ_{n-1}.

Thus, the EOMs in Eq. 98 can be expressed with the generalized Euler angles $\{\theta_n, \varphi_n\}$ as

$$\dot{\theta}_n = \Big(\frac{\partial H_{\rm s}}{\partial \varphi_n}\frac{2}{\sin\theta_n} - \frac{\partial H_{\rm s}}{\partial \varphi_{n-1}}\tan\frac{\theta_n}{2}\Big)\Big/\Big(r_{\rm s}\prod_{j=1}^{n-1}\sin^2\frac{\theta_j}{2}\Big), \tag{113a}$$

$$\dot{\varphi}_n = \frac{\dot{\Omega}_{\beta_{n+1,n}}\Omega_{\alpha_{n+1,n}} - \Omega_{\beta_{n+1,n}}\dot{\Omega}_{\alpha_{n+1,n}}}{\Omega^2_{\alpha_{n+1,n}} + \Omega^2_{\beta_{n+1,n}}}, \tag{113b}$$

where the nuclear DOFs obeys Eq. 98a-Eq. 98b. To solve Eq. 113b, one can use the expressions of $\dot{\Omega}_{\alpha_{n+1,n}}$ and $\dot{\Omega}_{\beta_{n+1,n}}$ in Eq. D5 and Eq. D6, respectively, which are only functions of Ω_k (Eq. B2-Eq. B4) that depends on $\{\theta_n, \varphi_n\}$. For a two-level system, it is straightforward to show that Eqs. 112-107 reduce back to Eqs. E9a-E9b, which are the EOMs for the $SU(2)$ mapping formalism derived in the previous work of spin mapping non-adiabatic ring polymer molecular dynamics.[35]

One can evolve each Θ_n, or equivalently θ_n by using the chain rule in Eq. 110, and φ_n using a velocity Verlet algorithm ($\{\Theta_n\}$ being the *generalized conjugate momenta* of $\{\varphi_n\}$), which does not require using the derivative of the potential.

C. Equations of Motion with the MMST mapping Variables

Instead of using conjugated variables $\{\varphi_n, \Theta_n\}$ (Eq. 109), one uses $\{q_n, p_n\}$ defined in Eq. 49, which are also conjugated variables.[43] Here, we explicitly show this using the EOMs. The electronic EOMs in Eq. 98c under the linearization approximation are equivalent to the following equation

$$i\hbar\frac{\partial}{\partial t}\hat{w}_{\rm s} = \big[\hat{V}_{\rm e}(R), \hat{w}_{\rm s}\big], \tag{114}$$

where $\hat{V}_{\rm e}(R)$ is defined as

$$\hat{V}_{\rm e}(R) = \frac{1}{\hbar}\sum_{k=1}^{N^2-1}\mathcal{H}_k \cdot \hat{\mathcal{S}}_k, \tag{115}$$

and $\mathcal{H}_k(R) = \frac{2}{\hbar}\mathrm{Tr}_\mathrm{e}\big[\hat{H}\cdot\hat{\mathcal{S}}_k\big] = \frac{2}{\hbar}\mathrm{Tr}_\mathrm{e}\big[\hat{V}_\mathrm{e}(R)\cdot\hat{\mathcal{S}}_k\big]$. Plugging the expression of $\hat{V}_\mathrm{e}(R)$ (Eq. 115) as well as the expression of $\hat{w}_\mathrm{s}$ (Eq. 26) into Eq. 114, one can easily verify its equivalence with Eq. 98c.

We then re-express Eq. 114 using the kernel expressed in Eq. 52, leading to

$$i\hbar\frac{\partial}{\partial t}(\sum_{na} c_n c_a^*|n\rangle\langle a|) = \big[\hat{V}_\mathrm{e}(R), \sum_{mb} c_m c_b^*|m\rangle\langle b|\big],$$

which can be used to derive

$$i\hbar\dot{c}_n = \sum_m V_{nm}(R)\cdot c_m \tag{116}$$

and its complex conjugate equation. This means that Eq. 96 is equivalent to the Ehrenfest dynamics for the electronic DOFs. The nuclear force described in Eq. 98b, on the other hand, differs from the Ehrenfest dynamics if $r_\mathrm{s} \neq 1$ ($\mathrm{s} \neq \mathrm{Q}$).

Using the transformation defined in Eq. 46, one can rewrite the EOMs in Eq. 116 as the coupled equations for the conjugated variables $\{q_n, p_n\}$ as follows[94]

$$\dot{q}_n = \sum_m V_{nm}(R)\cdot p_m = \frac{\partial\mathcal{H}}{\partial p_n}, \tag{117a}$$

$$\dot{p}_n = -\sum_m V_{nm}(R)\cdot q_m = -\frac{\partial\mathcal{H}}{\partial q_m}. \tag{117b}$$

Thus, Eq. 117 can be viewed as the mapping equation for the time-dependent Schrödinger's equation, which is equivalent to the mapping equation for the Quantum Liouville-von Neumann equation in Eq. 98c (also see Eq. 15). In Eq. 117, the MMST mapping Hamiltonian is

$$\begin{aligned}\mathcal{H} =& \frac{P^2}{2M} + U_0(R) + \sum_n \frac{1}{2}V_{nn}(R)(q_n^2 + p_n^2 - \gamma) \\ &+ \sum_{n<m} V_{nm}(R)(q_n q_m + p_n p_m),\end{aligned} \tag{118}$$

where $\mathcal{H}$ (Eq. 118) is equivalent to $H_\mathrm{s}(R,P)$ (Eq. 86) through the transform defined in Eq. 49 (or equivalently in Eq. 46). The Hamiltonian $\mathcal{H}$ in Eq. 118 can be viewed as Eq. 50 with the Wigner transform over only the nuclear DOFs. Further, using the transformation defined in Eq. 49, the nuclear EOMs in Eq. 98 can be expressed as

$$\dot{R} = \frac{\partial\mathcal{H}}{\partial P}, \quad \dot{P} = -\frac{\partial\mathcal{H}}{\partial R}. \tag{119}$$

Note that Eq. 117 are the classical Hamilton's EOMs of $\mathcal{H}$ (Eq. 118), with the conjugated variables $\{q_n, p_n\}$.

Similarly, Eq. 104 is also the Hamilton's EOMs of H_s, with the conjugate variables $\{\Theta_n, \varphi_n\}$. Thus, the transformation that convert $H_\mathrm{s}(\Theta_n, \varphi_n)$ (Eq. 103) to $\mathcal{H}(q_n, p_n)$ (Eq. 118) is a canonical transform that preserves the form of Hamilton's EOMs. More specifically, this canonical transformation that connects the generalized conjugate

variables $\{\Theta_n, \varphi_n\}$ to the conjugate position and momentum is expressed as

$$\Theta_n = \Big(\frac{1}{n} - \frac{1}{N}\Big) \sum_{m=1}^{n} \frac{1}{2}(q_m^2 + p_m^2) - \frac{n}{N} \sum_{m=n+1}^{N} \frac{1}{2}(q_m^2 + p_m^2), \tag{120a}$$

$$\varphi_n = \tan^{-1}\Big(\frac{p_{n+1} \cdot q_n - q_{n+1} \cdot p_n}{q_{n+1} \cdot q_n + p_{n+1} \cdot p_n}\Big), \tag{120b}$$

where we have used the transform defined in Eq. 49 to convert Eq. 101 into Eq. 120a, and convert Eq. 106 into Eq. 120b. The inverse transform from $\{\varphi_n, \theta_n\}$ to the MMST mapping variables $\{q_n, p_n\}$ (based on Eq. 46) are

$$q_n = \sqrt{2r_s} \cdot \mathrm{Re}[\langle n|\mathbf{\Omega}\rangle \cdot e^{i\Phi}], \tag{121a}$$

$$p_n = \sqrt{2r_s} \cdot \mathrm{Im}[\langle n|\mathbf{\Omega}\rangle \cdot e^{i\Phi}], \tag{121b}$$

where the explicit expression of $\langle n|\mathbf{\Omega}\rangle$ as a function of $\{\varphi_n, \theta_n\}$ can be found in Eq. 18.

Though this mapping is surely one-to-one, this kind of mapping just could not lead to correct canonical Hamilton's equations in Meyer-Miller framework.

Note that the EOMs in Eq. 117 and Eq. 119 are identical to the EOMs commonly used in the MMST mapping formalism.[23,41] These EOMs are also used in the spin-LSC approach,[43] by the argument[43] that they are Hamilton's EOMs of $\mathcal{H}$ (Eq. 118). Here, we rigorously prove that they are equivalent to the EOMs in Eq. 98, thus can be derived as the linearization approximation from the exact quantum Liouvillian (Eq. 85 and Eq. 87). The $2N$ MMST mapping variables are subject to a constraint given in Eq. 56. Further, there is an overall phase factor among the $\{q_n, p_n\}$ variables which does not influence the dynamics (see Eq. 46). Thus, there are still $2N-2$ truly independent variables, in agreement with the $2N-2$ generalized Euler angle variables $\{\varphi_n, \theta_n\}$ or the $2N-2$ conjugate variables $\{\varphi_n, \Theta_n\}$. The EOMs with $\{q_n, p_n\}$ in Eq. 117 are indeed analytically simpler than the EOMs with $\{\varphi_n, \theta_n\}$ in Eq. 113, making them more appealing for practical implementations.

For these MMST variables, one often define action-angle variables[7,23,41] $\{\eta_n, \phi_n\}$ associated with the phase space mapping variables as follows

$$\eta_n = \frac{1}{2}(q_n^2 + p_n^2 - \gamma), \tag{122a}$$

$$\phi_n = \tan^{-1}\Big(\frac{p_n}{q_n}\Big), \tag{122b}$$

or the inverse transform

$$q_n = \eta_n \cdot \cos\phi_n; \quad p_n = \eta_n \cdot \sin\phi_n. \tag{123}$$

Thus, Θ_n in Eq. 120a is a function of the action variables $\{\eta_n\}$ (as we already expected from the expression in Eq. 103), and φ_n in Eq. 120b is a function of the MMST angle variables $\{\phi_n\}$. In fact, using Eq. 75 and Eq. 54 (as well as the definition of η_n in Eq. 122a), we have

$$\eta_n = \Theta_n - \Theta_{n-1} + \frac{1}{N}. \tag{124}$$

Further, we can plug Eq. 123 into Eq. 120b and obtain

$$\begin{aligned}\varphi_n &= \tan^{-1}\Big(\frac{\sin\phi_{n+1}\cdot\cos\phi_n - \cos\phi_{n+1}\cdot\sin\phi_n}{\cos\phi_{n+1}\cdot\cos\phi_n + \sin\phi_{n+1}\cdot\sin\phi_n}\Big)\\ &= \tan^{-1}\Big(\frac{\sin(\phi_{n+1}-\phi_n)}{\cos(\phi_{n+1}-\phi_n)}\Big) = \phi_{n+1}-\phi_n. \end{aligned} \tag{125}$$

Thus, the meaning of φ_n is the phase difference for state $|n\rangle$ and state $|n+1\rangle$ in the angle variables of the MMST mapping formalism. This explains why numerically one can also uniformly sample the angle ϕ_n in the MMST mapping,[43] which is equivalent to the uniform sampling of φ_n.

Moreover, it is well-known that the MMST Hamiltonian (Eq. 118) can also be expressed as the action-angle variables (Eq. 122 or Eq. 123) as[9,23]

$$\begin{aligned}\mathcal{H} &= \frac{P^2}{2M} + U_0(R) + \sum_n V_{nn}(R)\cdot\eta_n \\ &+ 2\sum_{m<n} V_{nm}(R)\sqrt{\Big(\eta_n+\frac{\gamma}{2}\Big)\Big(\eta_m+\frac{\gamma}{2}\Big)}\cos(\phi_n-\phi_m),\end{aligned} \tag{126}$$

and the corresponding EOMs as[9]

$$\begin{aligned}\dot\eta_n &= -\frac{\partial\mathcal{H}}{\partial\phi_n} \\ &= 2\sum_{m<n}\sqrt{\Big(\eta_n+\frac{\gamma}{2}\Big)\Big(\eta_m+\frac{\gamma}{2}\Big)}\cdot\sin(\phi_n-\phi_m)\cdot V_{nm}(R)\end{aligned} \tag{127a}$$

$$\begin{aligned}\dot\phi_n &= \frac{\partial\mathcal{H}}{\partial\eta_n} \\ &= \sum_{m<n}\sqrt{\frac{\eta_m+\frac{\gamma}{2}}{\eta_n+\frac{\gamma}{2}}}\cdot\cos(\phi_n-\phi_m)\cdot V_{nm}(R)\end{aligned} \tag{127b}$$

Though "related", it is never hand-waving to start from eq (127) to recover the canonical Hamilton's equations of motion of Meyer-Miller variables in (117).

These EOMs are closely related to those in Eq. 104 which are expressed in $\{\Theta_n, \varphi_n\}$ variables. Actually, using Eq. 124 and Eq. 125, one can easily verify that $\mathcal{H}(\boldsymbol{\Theta}, \boldsymbol{\varphi})$ of Eq. 103 is equivalent to $\mathcal{H}(\boldsymbol{\eta}, \boldsymbol{\phi})$ of Eq. 126 (by noticing $r_s = 1 + N\gamma/2$, see Eq. 51).

VII. SIMULATION DETAILS

Here, we document the computational method as well as the initial conditions. Details of the model systems are provided in Appendix G.

Computational Method. Using the EOMs expressed in Eq. 113 or Eq. 104 and the out-of-equilibrium TCF expressions that we derived in Eq. 73, we use the spin mapping approach under the linearized approximation to study the non-adiabatic dynamics of model systems. Here, we briefly summarize the details of the propagation algorithm. In this paper, we present numerical results with both sampled and focused initial conditions. The sampling of $\{\theta_n\}$ or $\{\Theta_n\}$ and $\{\varphi_n\}$ is done over the phase space volume element $\int d\boldsymbol{\Omega}$ defined in Eqs. 21-22, through a Metropolis-Hasting algorithm. The results are

presented using $r_{\rm s} = r_{\bar{\rm s}} = r_{\rm W}$. The focused initial condition are described in Eq. 81 and the procedure in Sec. IV. To propagate the dynamics, we use the simple Verlet algorithm because of the conjugate relation between Θ_n and φ_n (see Eq. 109), as well as the relation between $\dot{\Theta}_n$ and $\dot{\theta}_n$ in Eq. 109a (to use the EOMs in Eq. 113).

First, the generalized conjugate variables $\{\varphi_n, \Theta_n\}$ are propagated by a half time-step, which is done using the Verlet algorithm as follows

$$\Theta_n\big(t + \frac{\Delta t}{4}\big) = \Theta_n(t) + \dot{\Theta}_n(t)\frac{\Delta t}{4}, \tag{128a}$$

$$\varphi_n\big(t + \frac{\Delta t}{2}\big) = \varphi_n(t) + \dot{\varphi}_n\big(t + \frac{\Delta t}{4}\big)\frac{\Delta t}{2}, \tag{128b}$$

$$\Theta_n(t + \frac{\Delta t}{2}) = \Theta_n\big(t + \frac{\Delta t}{4}\big) + \dot{\Theta}_n\big(t + \frac{\Delta t}{2}\big)\frac{\Delta t}{4}, \tag{128c}$$

or equivalently with θ_n instead of Θ_n, where $\dot{\theta}_n$ and $\dot{\varphi}_n$ are expressed in Eq. 113a-113b and $\dot{\Theta}_n$ and $\dot{\varphi}_n$ in Eq. 104a-104b. In theory it is possible to have a singular value for $\dot{\theta}_n$ (Eq. 113a) or $\dot{\varphi}_n$ (Eq. 104b) due to a possible zero value of the denominator. In practice, for the calculations performed in this study, this situation *rarely* occurs for the sampled initial condition for s = W approach, but may happen for the first time-step of the focused initial conditions with the choice of s = Q. Nevertheless, for the time-step where this situation occurs, one can switch back to Eq. 98c to avoid these rare numerical singularities in $\dot{\theta}_n$. In this case, one can switch to use a Verlet algorithm with $\dot{\Omega}_i$ and $\ddot{\Omega}_i = \frac{1}{\hbar}\sum_{j,k=1}^{N^2-1} f_{ijk}\mathcal{H}_j\dot{\Omega}_k$, or to the MMST variables by propagating Eq. 117.

The above half-propagation step for the electronic DOFs is followed by a propagation of the nuclear variables using the Verlet algorithm,

$$P\big(t + \frac{\Delta t}{2}\big) = P(t) + \dot{P}(t)\frac{\Delta t}{2}, \tag{129a}$$

$$R\big(t + \Delta t\big) = R(t) + \dot{R}\big(t + \frac{\Delta t}{2}\big)\Delta t, \tag{129b}$$

$$P(t + \Delta t) = P\big(t + \frac{\Delta t}{2}\big) + \dot{P}\big(t + \Delta t\big)\frac{\Delta t}{2}, \tag{129c}$$

and finally by the second half time-step of the mapping variables $\{\varphi_n, \theta_n\}$ with a similar Verlet scheme as outlined in Eq. 128. Thus, in principle, the non-adiabatic mapping dynamics in the $SU(N)$ representation does not need the MMST mapping variables.

On the other hand, an *alternative* but *numerically simpler* way (compared to propagating $\{\varphi_n, \theta_n\}$) to propagate dynamics is to obtain the initial values of the angles for $\{\varphi_n, \theta_n\}$ through either the sampling or focusing approach described in Sec. IV, then transform them into the MMST Cartesian mapping variables $\{q_n, p_n\}$ through Eq. 121, and directly propagate the EOMs with these MMST variables through Eq. 117 and Eq. 119. This is an *easier approach to implement into computer code*, because these equations are much simpler than the corresponding EOMs in Eq. 113. In addition, there are several

previously developed symplectic integrators[21,95] to propagate these EOMs, which one can take advantage of. Our numerical tests suggest that identical numerical accuracy of the results are generated from this approach and the approach in Eq. 128.

Initial Conditions. The initial conditions for all of the model calculations are $\hat{\rho}(0) = |n\rangle\langle n| \otimes \hat{\rho}_{\mathbf{R}}$, where $|n\rangle$ indicates the initial electronic diabatic state (as described in each Model Hamiltonian section) and $\hat{\rho}_{\mathbf{R}}$ represents the initial nuclear density operator. For the spin-boson model calculations (presented in Figs. 1-2), we assume that each nuclear DOF has a canonical thermal density $\hat{\rho}_{\mathbf{R}} = \frac{1}{\mathcal{Z}} e^{-\beta[\sum_\nu \hat{P}_\nu^2/2M_\nu + \frac{1}{2}M_\nu\omega_\nu^2\hat{R}_\nu^2)]}$, where $\beta = 1/k_{\rm B}T$, and $\mathcal{Z}$ is the partition function. The corresponding nuclear Wigner density is then

$$[\hat{\rho}_{\mathbf{R}}]_{\rm w} \tag{130}$$
$$= \prod_{\nu=1}^{F} \frac{1}{\pi} \tanh\frac{\beta\hbar\omega_\nu}{2} \exp[-\tanh\frac{\beta\hbar\omega_\nu}{2}(\frac{P_\nu^2}{\hbar m_\nu\omega_\nu} + \frac{m_\nu\omega_\nu}{\hbar}R_\nu^2)].$$

For the LVC models and the photo-dissociation calculations of Morse Potential (presented in Fig. 3-5), we use $\hat{\rho}_{\mathbf{R}} = |\chi\rangle\langle\chi|$, where $\langle\mathbf{R}|\chi\rangle = \left(\frac{2\Gamma}{\pi}\right)^{1/4} e^{-(\Gamma/2)(\mathbf{R}-\mathbf{R}_0)^2 + \frac{i}{\hbar}\mathbf{P}_0(\mathbf{R}-\mathbf{R}_0)}$ represents a Gaussian wavepacket centered around $\mathbf{R_0}$ and $\mathbf{P_0}$. For the LVC models, $\mathbf{R_0} = \mathbf{P_0} = 0$ with a width $\Gamma = 2$. The corresponding nuclear Wigner density is

$$[\hat{\rho}_{\mathbf{R}}]_{\rm w} = \prod_{\nu=1}^{F} \frac{1}{\pi} e^{-\Gamma(\mathbf{R}-\mathbf{R_0})^2 - (\mathbf{P}-\mathbf{P_0})^2/\Gamma}. \tag{131}$$

For the coupled Morse potential models, we use the same nuclear Wigner density in Eq. 131 with only one nuclear DOF, and $\Gamma = \frac{1}{m\omega}$ where the mass of the nuclear DOF is set to be $m = 20\ 000$ a.u., $\omega = 0.005$, and the values of R_0 are 2.1, 3.3 and 2.9 for models IA, IB and IC, respectively, and $P_0 = 0$ for all three models.

VIII. RESULTS AND DISCUSSIONS

In this section, we refer to the linearized method in the $SU(N)$ mapping formalism as the spin mapping (SM) approach, with the EOMs described in Eq. 98, or equivalently, in Eq. 113 or in Eq. 117. Here, we compare the numerical results obtained from the spin mapping formalism with other methods, including the LSC-IVR[11,90,91] as well as the simple trajectory Ehrenfest method.[96–98] The connection of these other method to the current formalism in the $SU(N)$ mapping formalism is discussed in Sec. F. Note that the current Spin Mapping approach is derived entirely based on the $SU(N)$ formalism, without the necessity to convert back to the Cartesian mapping variables of the MMST formalism that spin-LSC uses. Nevertheless, we found that the current approach generates numerically similar results from spin-LSC.[34,43] As

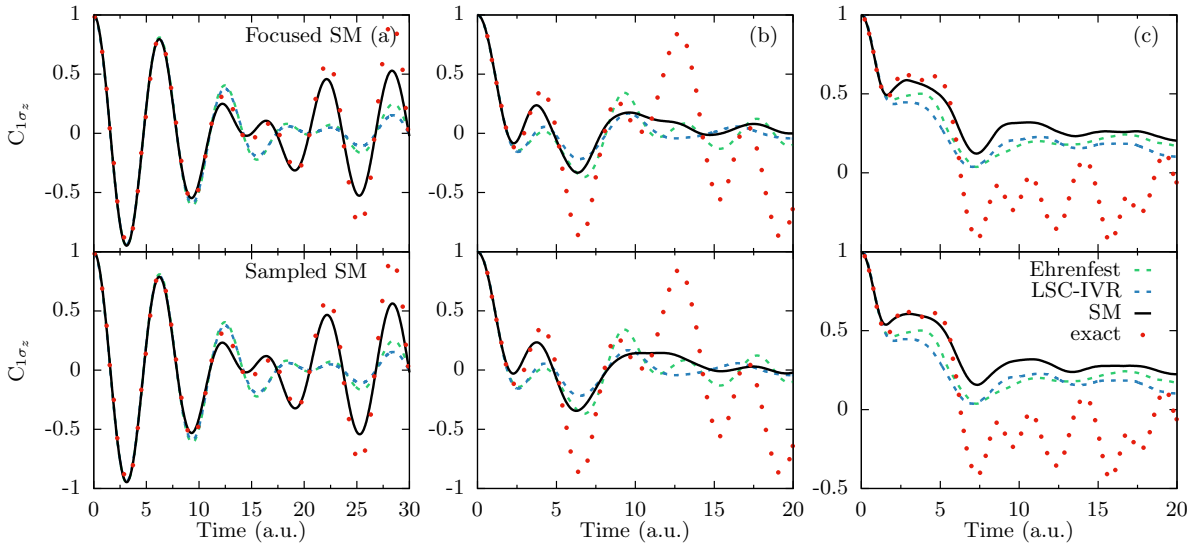

FIG. 1. Population dynamics of the 1-D spin boson models, obtained from focused initial conditions (top panels) and sampled initial conditions (bottom panels). The model parameters are (a) $\xi = 0.1$, (b) $\xi = 0.5$ and (c) $\xi = 1$, the rest of the parameters being provided in Tab. I of Appendix G. The Spin-Mapping results (black solid lines) are compared against the LSC-IVR (blue dashed lines), Ehrenfest (green dashed lines) and exact results (red dots).

we have discussed, the underlying EOMs for the generalized spin mapping approach (within the linearization approximation) are identical to Ehrenfest dynamics and the MMST-based approach under a specific choice of r_s. Nuclear initial conditions for all of these methods are also obtained from the Wigner transform of the initial nuclear density operator. In Appendix G, we connect several previously developed methods with the current method in the language of the $SU(N)$ mapping formalism.

Fig. 1 presents the population dynamics $\langle\sigma_z(t)\rangle = C_{1\sigma_z}(t)$ for a 1-D Spin-Boson model.[99] For the spin mapping simulation, a time-step of $\mathrm{d}t = 0.01$ a.u. is used, and the converged results are obtained with 10^4 trajectories for the focused initial conditions (upper panels) and 10^5 trajectories for the sampled initial conditions (lower panels). The population dynamics of the spin mapping approach are compared to the numerically exact calculations (red dots), LSC-IVR (blue) and Ehrenfest dynamics (green). The SM approach is in a very good agreement with the exact calculations for the model in panel (a), including all of the longer time recurrence of the electronic Rabi oscillations. It is important to note that the sampled and focused initial conditions yield almost exactly the same dynamics for this model. The LSC-IVR approach and the Ehrenfest dynamics, on the other hand, capture the initial electronic oscillations but fail to reproduce the longer time recurrence. This less accurate longer time dynamics from LSC-IVR or Ehrenfest was thought[99] causing by the zero point energy (ZPE) leakage problem associated with the classical Wigner dynamics of the nuclear DOF,[100,101] which is typical for linearized path-integral approaches based on the classical Wigner dynamics.[80,89,102] The ZPE leakage origi-

nates from the fact that classical dynamics does not preserve the ZPE incorporated in the nuclear initial Wigner distribution,[100,101] causing an incorrect energy flow from the nuclear DOF to the electronic DOFs,[71] equalizing the longer time populations and giving $\langle\sigma_z(t)\rangle$=0. In our previous work on non-adiabatic ring polymer molecular dynamics,[99] we have shown that quantizing the nuclear DOF with a ring polymer can effectively incorporate nuclear quantum distribution and alleviate ZPE leaking problem, even when using the MMST mapping formalism. Here, our numerical results suggest that by using the $SU(N)$ mapping formalism which exactly preserves the size of the electronic Hilbert space, this problem can be largely alleviated, compare to the traditional MMST mapping formalism which can get outside of the singly excited oscillator (SEO) mapping subspace, even though the classical Wigner type of dynamics is used for the nuclear DOF.

Fig. 1b-c presents the population dynamics for stronger electron-phonon couplings. We can see that the Spin Mapping method reproduces the exact result reasonably well up to t=5 a.u. At a longer time, however, this approach becomes less accurate compared to the exact results, missing the recurrence of the electronic Rabi oscillations. Nevertheless, as an independent trajectory-based approach, the Spin Mapping approach still outperforms both LSC-IVR and Ehrenfest for all model calculations presented here.

Fig. 2 presents the dynamics of three different spin-boson models, where LSC-IVR and Ehrenfest dynamics are known to provide less accurate results. This includes the electronic asymmetry in models presented in panels (a) and (b), as well as the strong system-bath coupling

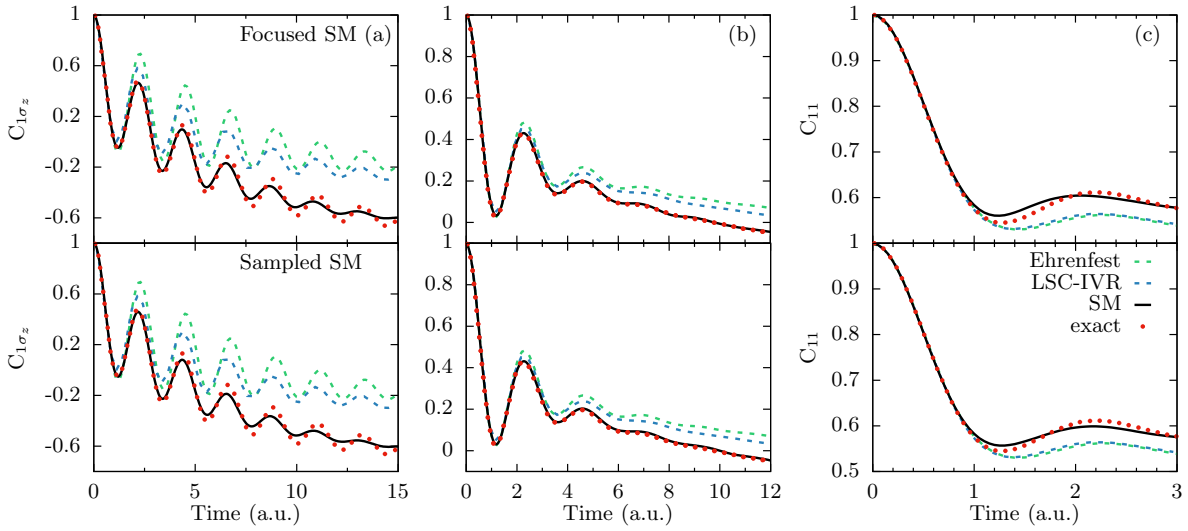

FIG. 2. Population dynamics $\langle\sigma_z(t)\rangle = C_{1\sigma_z}(t)$ (panels a-b) and time-correlation function $C_{11}(t)$ (panel c) from focused initial conditions (top panels) and sampled initial conditions (bottom panels) for the spin-boson models. The details of the parameters are described in Tab. I of Appendix G. The Spin Mapping results (black solid lines) are compared to LSC-IVR (blue dashed lines), Ehrenfest (green dashed lines) and exact results (red dots).

in the model presented in panel (c). The details of the parameters are provided in Tab. I of Appendix G. The Spin Mapping results (black solid lines) are compared to LSC-IVR (blue dashed lines), Ehrenfest (green dashed lines) and exact results (red dots). We used the same time-step and number of trajectories that has been used in the previous model. The s = W choice of the spin mapping method slightly underestimates the oscillations in the population dynamics at low temperature, but gives more accurate results compared to the LSC-IVR method (blue dashed line) or Ehrenfest Dynamics (green dashed line). Both the sampled and the focused initial conditions provide almost identical results.

Fig. 3 presents the population dynamics of state $|2\rangle$ in the pyrazine model.[104] The results are obtained from the current Spin Mapping approach (red solid) with both focused and sampled initial conditions, and compared to Ehrenfest dynamics (green dash), as well as to the recently developed Generalized Discrete Truncated Wigner Approximation (GDTWA)[51] approach (blue dashed line). The Spin Mapping approach generates very accurate population dynamics compared to the exact results, regardless of the initial conditions of the mapping variables, although the early dynamics is slightly more accurate when focusing the initial conditions, while the long-time dynamics seems closer to the exact result when using the sampled initial conditions. Interestingly, the current Spin Mapping approach almost coincides with the GDTWA approach. It was claimed[51] that in the GDTWA approach, the discrete sampling of the phase space is the key to provide more accurate results compared to the spin mapping formalism, when comparing the population dynamics generated from

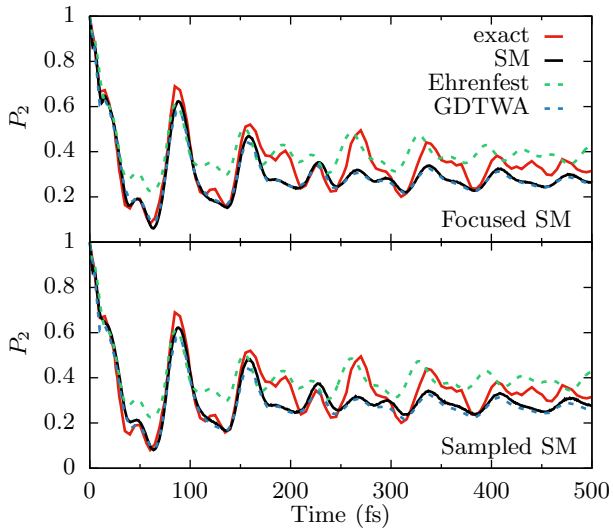

FIG. 3. Population dynamics of the pyrazine model with focused (upper panel) and sampled initial conditions (lower panel) for the Spin Mapping approach. The results obtained from Spin Mapping (black solid lines) are compared to the Ehrenfest method (green dashed line), the GDTWA approach[51] (blue dashed line), and exact results (red solid line).

GDTWA and spin-PLDM.[105,106] However, it seems that this is because the spin-PLDM is less accurate than the current spin mapping approach or spin-LSC for the LVC model, even though the former is more accurate than the latter for spin-boson type problems.[105,106] Future work

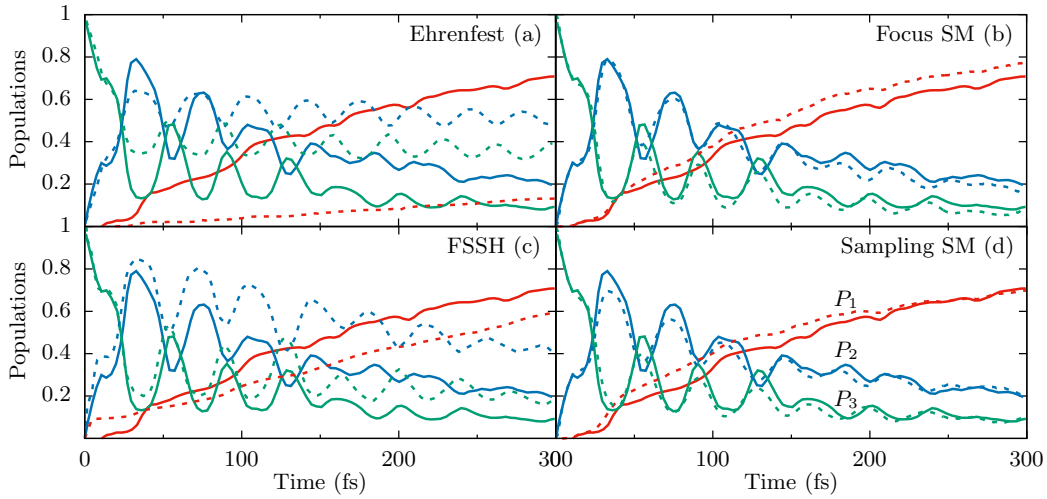

FIG. 4. Electronic populations of the benzene cation model, obtained from (a) Ehrenfest dynamics, (b) Spin Mapping formalism with focused initial condition, (c) fewest switches surface hopping (FSSH) as obtained from Ref. 103, and (d) Spin Mapping with sampled initial conditions. The population dynamics of state 1 (red), state 2 (blue) and state 3 (green) are presented (dashed lines) and compared to exact dynamics (solid lines).

is needed to further explore the numerical performance of these approaches.

Fig. 4 presents the numerical results of a three-state model for the benzene radical cation.[107,108] This is a particularly challenging model due to the multi-state dynamics and the presence of conical intersection, especially for traditional mixed quantum-classical methods such as Ehrenfest (panel a) and Fewest Switches Surface Hopping[3] (panel c), both of which generate less accurate population dynamics.[103] The spin mapping formalism, on the other hand, gives almost quantitatively accurate dynamics for this challenging system. For the Spin Mapping results presented here, we used 10^5 trajectories for the sampled initial condition and 10^4 for the focused initial condition, and a nuclear time-step of $\mathrm{d}t = 0.5$ a.u. as well as a mapping time-step of $\mathrm{d}t_{\mathrm{map}} = \mathrm{d}t_{\mathrm{nuc}}/16$. While the focused initial conditions provide slightly more accurate short-time dynamics up to 150 fs (panel b), the sampled initial conditions seem to generate population closer to the exact result at a longer time.

Fig. 5 presents the results of population dynamics in the three-state coupled Morse potential.[12] Here, we present the Spin Mapping results only using focused initial conditions (solid lines). A time-step of 1 a.u., and 10^5 to 5×10^5 trajectories were used. The sampled initial conditions for spin mapping variables generates less accurate population as the initial nuclear force does not respect the physical occupancy of the electronic states.[73] This has been extensively discussed in the recent work on trajectory-adjusted electronic zero point energy in classical Meyer-Miller vibronic dynamics.[73] Nevertheless, the population dynamics of the Spin Mapping method with the focused initial conditions give almost exact results compared to the numerically exact calculations (dots),

and outperform Ehrenfest dynamics (dashed lines). The Spin Mapping approach generates both accurate short time branching dynamics among three states as well as long time plateau value of the population, that is almost exact for models presented in panel (a) and (c). For the model presented in panel (b), the spin mapping formalism slightly outperforms the state-of-the-art $\gamma-$SQC approach,[73] as well as the non-adiabatic ring polymer molecular dynamics approach.[99]

IX. CONCLUSION

We present the rigorous analytical derivation of the non-adiabatic dynamics using the generators (generalized spin matrices) of the $\mathfrak{su}(N)$ Lie algebra. Applying the S-W transform on the $SU(N)$-based mapping Hamiltonian provides the continuous variables (generalized spin coherence states) that can be viewed as the angle variables on a multi-dimensional Bloch sphere (or so-called general Euler angles[48,49]), hence establishing a mapping between discrete electronic states and continuous variables. The main advantage of the $SU(N)$ representation is that the corresponding S-W transform exactly preserves the identity operator in the N dimensional Hilbert space,[43] as opposed to the MMST formalism where the identity is not preserved through the mapping and there is an ambiguity of how to evaluate it.[22] This is because the MMST representation has a larger size of Hilbert space (that contains other states outside the single excitation manifold of the mapping oscillators) compared to the original electronic subspace, which then requires a projection back to the single excitation subspace of the mapping oscillators to obtain accurate results. The $SU(N)$ representation, on

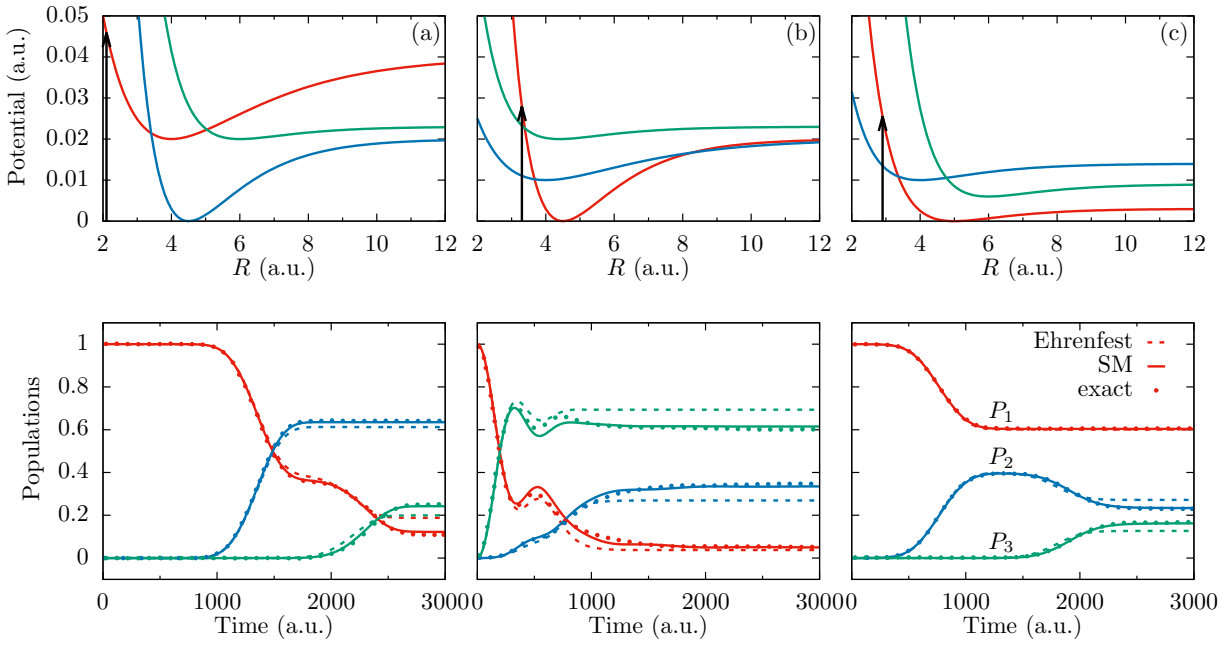

FIG. 5. Diabatic Potential Energy Surfaces (top panels) and the population dynamics (bottom panels) for the three-state coupled Morse models (a) IA, (b) IB and (c) IC, described in Tab. IV of Appendix G. The vertical black arrows in top panels indicate the Franck-Condon vertical photo-excitations. State 1 (red), state 2 (blue) and state 3 (green) populations are calculated with the focused spin-mapping approach (solid lines), and compared with the Ehrenfest dynamics (dashed lines) as well as the exact results (dots).

the other hand, completely alleviates these problems and is the most natural way to map a N-level system into a classical phase space. More discussions can be found in Appendix F.

Using a mixed Wigner/S-W formalism, we derive a general expression of the time-correlation function, where the Wigner representation is used for the nuclear DOFs, and the S-W transform is applied to the generalized spin matrices associated to the electronic DOFs. We obtain the expression of the exact quantum Liouvillian in this formalism. Further making a linearization approximation, we obtain a set of EOMs that describe the coupled dynamics between the electronic and nuclear DOFs. We further connect EOMs with different mapping variables, including the spin coherence state variables, generalized Bloch spherical coordinates, as well as the MMST mapping variables. We formally establish the equivalence of these EOMs with different mapping variables. We also connect a variety of previously developed methods with the current formalism in the language of the $SU(N)$ mapping formalism.

Finally, we perform numerical simulations to assess the accuracy of the generalized spin mapping approach under the linearization approximation. We compute the population dynamics of systems with multiple electronic states coupled to the nuclear DOFs, including a condensed phase spin-boson model system, two conical intersection models, and an anharmonic three-state Morse

model for photo-dissociation dynamics. The current formalism provides an excellent agreement compared to the numerically exact results, and a significant improvement compared to the Ehrenfest dynamics or LSC-IVR which is based on the MMST mapping formalism. Interestingly, the current formalism produces very similar numerical results compared to two recently developed approaches, Spin-LSC and GDTWA, both of which are based on the $SU(N)$ mapping formalism.

Despite that our work is inspired by the recent spin mapping formalism,[43,51] we do want to clearly emphasize the unique theoretical contribution of the current work.

(1) It provides the **exact** expression of the quantum Liouvillian for the $SU(N)$ mapping framework, summarized in Eq. 85-89. To the best of our knowledge, these expressions are derived for the first time in the literature, and will provide an invaluable theoretical foundation for understanding or developing approximate methods.

(2) This general and powerful framework in (1) provides the rigorous theoretical foundation to derive approximate methods, such as the Linearized spin-mapping approach (Eq. 94 and Eq. 96), which can be used to derive the EOMs *proposed* in the previous approaches GDTWA (Eq. 98) or Spin-LSC (Eq. 117). It turns out that these two EOMs are identical, just with different dynamical mapping variables. Our work provides the theoretical insights into how seemingly different approaches can be unified into a consistent and rigorous theoretical frame-

work.

(3) It provides new theoretical insights into improving the approximate method beyond the existing ones. For example, Eq. 94 and Eq. 97, despite being a Linearized approximate approach, should be in principle exact for linear vibronic couplings Hamiltonian (such as the spin-boson problem).

(4) It provides further theoretical insights for several previously proposed *ad hoc* choices made in the Spin-LSC algorithm,[43] such as the procedure to randomly sample the mapping angle variables (Eq. 125). It also provides a rigorous initial condition sampling procedure through the $SU(N)$ mapping formalism, which is naturally connected to the distribution of the generalized Euler angle variables $\mathrm{d}\mathbf{\Omega}$ (Eq. 21), as well as new insights into the choice of the focused initial conditions that connects with the angle variables (Eq. 80 and Eq. 81).

(5) It addresses the potential confusions[25,109] that "the MMST mapping Hamiltonian is a necessary and essential ingredient in the generalized spin mapping formalism". Our theoretical framework clearly shows that one can propagate dynamics with alternative choice of mapping variables, and it is not necessary to introduce the MMST formalism, even though numerically, it might be the most convenient one to implement. The fundamental difference between the $SU(N)$ mapping and the MMST mapping formalism is also extensively discussed in Appendix F.

Even though our focus in this paper is not on mathematical physics, we indeed discovered several valuable analytic formalism of the $\mathfrak{su}(N)$ Lie algebra during our derivation of the mapping dynamics, including:

(i) The analytic expressions of the structure constants of the $\mathfrak{su}(N)$ Lie algebra (see Appendix A), which could be extremely valuable and useful for modern physical science. To the best of our knowledge, there is no available analytic expression for these structure constants, despite their extensive usage and the crucial role they play in modern physics.

(ii) A convenient expression (Eq. 27) of the S-W kernel in terms of the spin coherent state projection operator. Even though it is straightforward to prove its equivalence to the original expression[50] in Eq. 26, this new expression in Eq. 27 can drastically simplify a lot of derivations, such as deriving the identity property of the kernel (Eq. 28), the S-W kernel in the diabatic representation (Eq. 52), the S-W transform of projection operator (Eq. 53), and can be potentially useful for future theoretical derivations. It also drastically simplified the proof of the equivalence (see Sec. VI C) between the EOMs used in GDTWA approach (Eq. 98c) and the EOMs in the MMST variables (Eq. 117).

(iii) The discovery of the conjugate variables (Eq. 101 and Eq. 102) in terms of the generalized Euler angles in spin coherent state , which leads to the corresponding EOMs with these variables (Eq. 109). It turns out that this set of conjugate variables plays a similar role in the $SU(N)$ mapping formalism (see Eq. 103 and Eq. 104) as

the action-angle variable[9,23] play in the MMST formalism (see Eq. 126 and Eq. 127a).

Overall, the theoretical framework presented in this work provides a rigorous foundation to formally derive non-adiabatic quantum dynamics approaches with continuous mapping variables.

ACKNOWLEDGMENTS

This work was supported by the National Science Foundation CAREER Award under Grant No. CHE-1845747. Computing resources were provided by the Center for Integrated Research Computing (CIRC) at the University of Rochester. We would like to thank Braden M. Weight for valuable discussions.

CONFLICT OF INTEREST

The authors have no conflicts to disclose.

AVAILABILITY OF DATA

The data that support the findings of this study are available from the corresponding author upon a reasonable request.

Appendix A: Analytic expression of the structure constants

Despite the extensive usage and the crucial role these structure constants play in modern physics, to the best of our knowledge,[110] there is no analytic expression (closed formulas) of f_{ijk} and d_{ijk}. Here, we derive closed analytic formulas for these structure constants without requiring any matrix multiplication or involving the generator expressions. Their analytic expressions are listed in Eq. A5 (for f_{ijk}) and Eq. A14 (for d_{ijk}).

1. The Totally Anti-symmetric Structure Constants f_{ijk}

The commutation relation between two symmetric generators is

$$\begin{aligned}
\big[\hat{\mathcal{S}}_{\alpha_{nm}}, \hat{\mathcal{S}}_{\alpha_{n'm'}}\big] &= i\hbar \sum_{k=1}^{N^2-1} f_{\alpha_{nm}\alpha_{n'm'}k}\hat{\mathcal{S}}_k \qquad \text{(A1)}\\
&= \frac{\hbar^2}{4}\Big[\delta_{nm'}\big(|m\rangle\langle n'| - |n'\rangle\langle m|\big) + \delta_{nn'}\big(|m\rangle\langle m'| - |m'\rangle\langle m|\big)\\
&\quad + \delta_{mm'}\big(|n\rangle\langle n'| - |n'\rangle\langle n|\big) + \delta_{mn'}\big(|n\rangle\langle m'| - |m'\rangle\langle n|\big)\Big]\\
&= i\frac{\hbar}{2}\Big[\delta_{nm'}\hat{\mathcal{S}}_{\beta_{n'm}} + \delta_{nn'}\big(\hat{\mathcal{S}}_{\beta_{m'm}} - \hat{\mathcal{S}}_{\beta_{mm'}}\big)\\
&\quad + \delta_{mm'}\big(\hat{\mathcal{S}}_{\beta_{n'n}} - \hat{\mathcal{S}}_{\beta_{nn'}}\big) - \delta_{mn'}\hat{\mathcal{S}}_{\beta_{nm'}}\Big].
\end{aligned}$$

With constraints from δ_{ij}, we can identify the indices of each generator, and hence obtain the analytic expressions of non-zero $f_{\alpha_{nm}\alpha_{n'm'}k}$, which are summarized in the first line of Eq. A1 of the main text.

For a symmetric and an anti-symmetric generator, the commutation relation is

$$\begin{aligned}
&\big[\hat{\mathcal{S}}_{\alpha_{nm}}, \hat{\mathcal{S}}_{\beta_{n'm'}}\big] = i\hbar \sum_{k=1}^{N^2-1} f_{\alpha_{nm}\beta_{n'm'}k}\hat{\mathcal{S}}_k \qquad \text{(A2)}\\
&= i\frac{\hbar^2}{4}\Big[\delta_{nn'}\big(|m\rangle\langle m'| + |m'\rangle\langle m|\big) - \delta_{nm'}\big(|m\rangle\langle n'| + |n'\rangle\langle m|\big)\\
&\quad + \delta_{mn'}\big(|n\rangle\langle m'| + |m'\rangle\langle n|\big) - \delta_{mm'}\big(|n\rangle\langle n'| + |n'\rangle\langle n|\big)\Big]\\
&= i\frac{\hbar}{2}\Big[\delta_{nn'}\big(\hat{\mathcal{S}}_{\alpha_{m'm}} + \hat{\mathcal{S}}_{\alpha_{mm'}}\big) - \delta_{nm'}\hat{\mathcal{S}}_{\alpha_{n'm}} + \delta_{mn'}\hat{\mathcal{S}}_{\alpha_{nm'}}\\
&- \delta_{mm'}\big(\hat{\mathcal{S}}_{\alpha_{n'n}} + \hat{\mathcal{S}}_{\alpha_{nn'}}\big) + \frac{\hbar}{2}\delta_{mm'}\delta_{nn'}\big(2|m\rangle\langle m| - 2|n\rangle\langle n|\big)\Big].
\end{aligned}$$

The first two lines of the last equality in Eq. A2 directly give several structure constants. The last line of Eq. A2 contains diagonal elements, hence we know it will be a combination of diagonal generators. We can prove (see Supporting Information) that

$$\begin{aligned}
&i\frac{\hbar^2}{2}(|m\rangle\langle m| - |n\rangle\langle n|) \qquad \text{(A3)}\\
&= i\hbar\Big(\sqrt{\frac{n}{2(n-1)}}\hat{\mathcal{S}}_{\gamma_n} + \sum_{k>m}^{n-1}\frac{\hat{\mathcal{S}}_{\gamma_k}}{\sqrt{2k(k-1)}} - \sqrt{\frac{m-1}{2m}}\hat{\mathcal{S}}_{\gamma_m}\Big).
\end{aligned}$$

This helps to determine the rest of the structure constants $f_{\alpha_{nm}\beta_{n'm'}k}$. The commutation relations between symmetric and diagonal generators are not required as we have already obtained all the non-zero structure constants involving diagonal and symmetric generators (and we know that we cannot obtain a diagonal matrix through the commutator of a symmetric and a diagonal generator).

Between two anti-symmetric generators, the commutation relation is

$$\begin{aligned}
&\big[\hat{\mathcal{S}}_{\beta_{nm}}, \hat{\mathcal{S}}_{\beta_{n'm'}}\big] = i\hbar \sum_{k=1}^{N^2-1} f_{\beta_{nm}\beta_{n'm'}k}\hat{\mathcal{S}}_k \qquad \text{(A4)}\\
&= \frac{\hbar^2}{4}\Big[\delta_{nm'}\big(|n'\rangle\langle m| - |m\rangle\langle n'|\big) + \delta_{nn'}\big(|m\rangle\langle m'| - |m'\rangle\langle m|\big)\\
&\quad + \delta_{mm'}\big(|n\rangle\langle n'| - |n'\rangle\langle n|\big) + \delta_{mn'}\big(|m'\rangle\langle n| - |n\rangle\langle m'|\big)\Big]\\
&= i\frac{\hbar}{2}\Big[-\delta_{nm'}\hat{\mathcal{S}}_{\beta_{n'm}} + \delta_{nn'}\big(\hat{\mathcal{S}}_{\beta_{m'm}} - \hat{\mathcal{S}}_{\beta_{mm'}}\big)\\
&\quad + \delta_{mm'}\big(\hat{\mathcal{S}}_{\beta_{n'n}} - \hat{\mathcal{S}}_{\beta_{nn'}}\big) + \delta_{mn'}\hat{\mathcal{S}}_{\beta_{nm'}}\Big],
\end{aligned}$$

which helps to determine the structure constants involving all anti-symmetric generators (second line of Eq. A1 of the main text). The remaining totally anti-symmetric structure constants are computed through the commutator between two diagonal generators, which is $[\hat{\mathcal{S}}_{\gamma_n}, \hat{\mathcal{S}}_{\gamma_{n'}}] = i\hbar\sum_{k=1}^{N^2-1} f_{\gamma_n\gamma_{n'}k}\hat{\mathcal{S}}_k = 0$, indicating a zero

value for all $f_{\gamma_n\gamma_{n'}k}$. This was a known fact, as the diagonal matrices are generators of the Cartan subalgebra of $\mathfrak{su}(N)$, and they commute by definition[31].

All of the non-zero totally anti-symmetric structure constants are expressed as follows

$$
\begin{aligned}
&f_{\alpha_{nm}\alpha_{kn}\beta_{km}} = f_{\alpha_{nm}\alpha_{nk}\beta_{km}} = f_{\alpha_{nm}\alpha_{km}\beta_{kn}} = \frac{1}{2}, \qquad \text{(A5)}\\
&f_{\beta_{nm}\beta_{km}\beta_{kn}} = \frac{1}{2},\\
&f_{\alpha_{nm}\beta_{nm}\gamma_m} = -\sqrt{\frac{m-1}{2m}}, \quad f_{\alpha_{nm}\beta_{nm}\gamma_n} = \sqrt{\frac{n}{2(n-1)}},\\
&f_{\alpha_{nm}\beta_{nm}\gamma_k} = \sqrt{\frac{1}{2k(k-1)}},\ m<k<n.
\end{aligned}
$$

The structure constants derived here are within the basis of the GGM matrices $\hat{\mathcal{S}}$. Another choice of basis of $\hat{\mathcal{S}}'$ is also possible, which is related to the GGM basis through the following transformation

$$\hat{\mathcal{S}}_i = \sum_j [\mathcal{A}]_{ij}\hat{\mathcal{S}}'_j, \qquad \text{(A6)}$$

where $\mathcal{A}$ is the transformation matrix, and $[\mathcal{A}]_{ij}$ is its ij_{th} matrix element of $\mathcal{A}$. Within the new basis $\hat{\mathcal{S}}'$, one can always directly obtain the expressions of the structure constants through the following relation (see Chapter 4 of Ref. 111)

$$f'_{lmn} = \sum_{i,j,k} [\mathcal{A}^{-1}]_{li}[\mathcal{A}^{-1}]_{mj} f_{ijk} [\mathcal{A}]_{kn}, \qquad \text{(A7)}$$

where $\mathcal{A}^{-1}$ is the inverse matrix of $\mathcal{A}$. With the analytic expressions of f_{ijk} in the GGM basis, this transformation becomes useful for obtaining structure constants in any basis of generators of $\mathfrak{su}(N)$.

2. The Totally Symmetric Structure Constants d_{ijk}

The anti-commutation relation between two symmetric generators is

$$\{\hat{\mathcal{S}}_{\alpha_{nm}}, \hat{\mathcal{S}}_{\alpha_{n'm'}}\} = \frac{\hbar^2}{N}\delta_{\alpha_{nm}\alpha_{n'm'}}\hat{\mathcal{I}} + \hbar\sum_{k=1}^{N^2-1} d_{\alpha_{nm}\alpha_{n'm'}k}\hat{\mathcal{S}}_k \qquad \text{(A8)}$$

$$
\begin{aligned}
&= \frac{\hbar^2}{4}\Big[\delta_{nm'}\big(|m\rangle\langle n'| + |n'\rangle\langle m|\big) + \delta_{nn'}\big(|m\rangle\langle m'| + |m'\rangle\langle m|\big)\\
&\quad + \delta_{mm'}\big(|n\rangle\langle n'| + |n'\rangle\langle n|\big) + \delta_{mn'}\big(|n\rangle\langle m'| + |m'\rangle\langle n|\big)\Big]\\
&= \frac{\hbar}{2}\Big[\delta_{nm'}\hat{\mathcal{S}}_{\alpha_{n'm}} + \delta_{nn'}\big(\hat{\mathcal{S}}_{\alpha_{m'm}} + \hat{\mathcal{S}}_{\alpha_{mm'}}\big)\\
&\quad + \delta_{mm'}\big(\hat{\mathcal{S}}_{\alpha_{n'n}} + \hat{\mathcal{S}}_{\alpha_{nn'}}\big) + \delta_{mn'}\hat{\mathcal{S}}_{\alpha_{nm'}}\\
&\quad + \delta_{nn'}\delta_{mm'}\frac{\hbar}{2}\big(2|m\rangle\langle m| + 2|n\rangle\langle n|\big)\Big].
\end{aligned}
$$

We know that the last line of Eq. A8 only involves diagonal matrices. In fact we have (see proof in Supporting Information)

$$\begin{aligned}&\frac{\hbar^2}{2}(|m\rangle\langle m| + |n\rangle\langle n|) \qquad \text{(A9)}\\ &= \frac{\hbar^2}{N}\hat{\mathcal{I}} + \hbar\Big(\sum_{k>n}^{N}\sqrt{\frac{2}{k(k-1)}}\hat{\mathcal{S}}_{\gamma_k} + \frac{2-n}{\sqrt{2n(n-1)}}\hat{\mathcal{S}}_{\gamma_n}\\ &\quad + \sum_{k>m}^{n-1}\frac{1}{\sqrt{2k(k-1)}}\hat{\mathcal{S}}_{\gamma_k} - \sqrt{\frac{m-1}{2m}}\hat{\mathcal{S}}_{\gamma_m}\Big).\end{aligned}$$

Thus, we can extract all the non-zero $d_{\alpha_{nm}\alpha_{n'm'}k}$.

Between a symmetric and an anti-symmetric generator, the anti-commutation relation reads

$$\begin{aligned}&\{\hat{\mathcal{S}}_{\alpha_{nm}}, \hat{\mathcal{S}}_{\beta_{n'm'}}\} = \hbar\sum_{k=1}^{N^2-1} d_{\alpha_{nm}\beta_{n'm'}k}\hat{\mathcal{S}}_k \qquad \text{(A10)}\\ &= i\frac{\hbar^2}{4}\Big[\delta_{nm'}\big(|n'\rangle\langle m| - |m\rangle\langle n'|\big) + \delta_{nn'}\big(|m\rangle\langle m'| - |m'\rangle\langle m|\big)\\ &\quad + \delta_{mm'}\big(|n'\rangle\langle n| - |n\rangle\langle n'|\big) + \delta_{mn'}\big(|n\rangle\langle m'| - |m'\rangle\langle n|\big)\Big]\\ &= \frac{\hbar}{2}\Big[\delta_{nm'}\hat{\mathcal{S}}_{\beta_{n'm}} + \delta_{nn'}\big(\hat{\mathcal{S}}_{\beta_{mm'}} - \hat{\mathcal{S}}_{\beta_{m'm}}\big)\\ &\quad + \delta_{mm'}\big(\hat{\mathcal{S}}_{\beta_{n'n}} - \hat{\mathcal{S}}_{\beta_{nn'}}\big) + \delta_{mn'}\hat{\mathcal{S}}_{\beta_{nm'}}\Big],\end{aligned}$$

from which one can extract $d_{\alpha_{nm}\beta_{n'm'}k}$. Note that based on Eq. A10, there is no diagonal component $\hat{\mathcal{S}}_\gamma$, thus all $d_{\alpha\beta\gamma} = 0$. Computing the anti-commutator between symmetric and diagonal generators is not necessary as we already obtained the structure constants involving those generators by permutation, because $d_{\alpha\gamma\gamma'}$ will be same as $d_{\gamma\gamma'\alpha}$, $d_{\alpha\gamma\alpha'}$ will be same as $d_{\alpha\alpha'\gamma}$, and $d_{\alpha\gamma\beta}$ will be same as $d_{\alpha\beta\gamma}$.

Computing the anti-commutators between two anti-symmetric generators gives

$$\{\hat{\mathcal{S}}_{\beta_{nm}}, \hat{\mathcal{S}}_{\beta_{n'm'}}\} = \frac{\hbar^2}{N}\delta_{\beta_{nm}\beta_{n'm'}}\hat{\mathcal{I}} + \hbar\sum_{k=1}^{N^2-1} d_{\beta_{nm}\beta_{n'm'}k}\hat{\mathcal{S}}_k \qquad \text{(A11)}$$

$$\begin{aligned}&= \frac{\hbar^2}{4}\Big[\delta_{nn'}\big(|m\rangle\langle m'| + |m'\rangle\langle m|\big) - \delta_{nm'}\big(|m\rangle\langle n'| + |n'\rangle\langle m|\big)\\ &\quad + \delta_{mm'}\big(|n\rangle\langle n'| + |n'\rangle\langle n|\big) - \delta_{mn'}\big(|n\rangle\langle m'| + |m'\rangle\langle n|\big)\Big]\\ &= \frac{\hbar}{2}\Big[\delta_{nn'}\big(\hat{\mathcal{S}}_{\alpha_{m'm}} + \hat{\mathcal{S}}_{\alpha_{mm'}}\big) - \delta_{nm'}\hat{\mathcal{S}}_{\alpha_{n'm}}\\ &\quad + \delta_{mm'}\big(\hat{\mathcal{S}}_{\alpha_{n'n}} + \hat{\mathcal{S}}_{\alpha_{nn'}}\big) - \delta_{mn'}\hat{\mathcal{S}}_{\alpha_{nm'}}\\ &\quad + \delta_{nn'}\delta_{mm'}\frac{\hbar}{2}\big(2|m\rangle\langle m| + 2|n\rangle\langle n|\big)\Big],\end{aligned}$$

where we recognize that the last line of Eq. A11 is identical to the last line of Eq. A8, which can be expressed as generators in Eq. A9. We do not need to compute the anti-commutator between an asymmetric and a diagonal

generator as we already have the result by permutation from Eq. A11 (and Eqs. A10 indicates $d_{\alpha\beta\gamma} = 0$).

The remaining d_{ijk} values are obtained through the anti-commutator between two diagonal generators

$$\{\hat{\mathcal{S}}_{\gamma_n}, \hat{\mathcal{S}}_{\gamma_{n'}}\} = \frac{\hbar^2}{N}\delta_{\gamma_n\gamma_{n'}}\hat{\mathcal{I}} + \hbar\sum_{k=1}^{N^2-1} d_{\gamma_n\gamma_{n'}k}\hat{\mathcal{S}}_k \tag{A12}$$

$$\begin{aligned}
&= \frac{\hbar^2}{\sqrt{2n(n-1)2n'(n'-1)}}\Big[\sum_{k=1}^{n-1}\sum_{k'=1}^{n'-1}\delta_{kk'}\big(|k\rangle\langle k'| + |k'\rangle\langle k|\big) \\
&\quad + \delta_{kn'}\big(1-n'\big)\big(|k\rangle\langle n'| + |n'\rangle\langle k|\big) \\
&\quad + \delta_{nk'}\big(1-n\big)\big(|n\rangle\langle k'| + |k'\rangle\langle n|\big) \\
&\quad + \delta_{nn'}\big(1-n\big)(1-n')\big(|n\rangle\langle n'| + |n'\rangle\langle n|\big)\Big] \\
&= \frac{\hbar}{\sqrt{2n(n-1)}}2\delta_{kn'}\hat{\mathcal{S}}_{\gamma_{n'}} + \frac{\hbar}{\sqrt{2n'(n'-1)}}2\delta_{nk'}\hat{\mathcal{S}}_{\gamma_n} \\
&\quad + \delta_{nn'}\frac{\hbar^2}{n(n-1)}\Big(\sum_{k=1}^{n-1}|k\rangle\langle k| + (1-n)^2|n\rangle\langle n|\Big).
\end{aligned}$$

One can see that only diagonal matrices are involved in the last line of Eq. A12 and there is no off-diagonal element. We show in Supporting Information that

$$\begin{aligned}
&\frac{\hbar^2}{n(n-1)}\Big(\sum_{k=1}^{n-1}|k\rangle\langle k| + (1-n)^2|n\rangle\langle n|\Big) \\
&= \frac{\hbar^2}{N}\hat{\mathcal{I}} + \hbar\Big(\sum_{k>n}^{N}\sqrt{\frac{2}{k(k-1)}}\hat{\mathcal{S}}_{\gamma_k} + (2-n)\sqrt{\frac{2}{n(n-1)}}\hat{\mathcal{S}}_{\gamma_n}\Big),
\end{aligned} \tag{A13}$$

which helps to determine all $d_{\gamma_n\gamma_{n'}k}$.

We summarize all the non-zero totally symmetric structure constants as follows

$$\begin{aligned}
&d_{\alpha_{nm}\alpha_{kn}\alpha_{km}} = d_{\alpha_{nm}\beta_{kn}\beta_{km}} = d_{\alpha_{nm}\beta_{mk}\beta_{nk}} = \frac{1}{2}, \\
&d_{\alpha_{nm}\beta_{nk}\beta_{km}} = -\frac{1}{2}, \\
&d_{\alpha_{nm}\alpha_{nm}\gamma_m} = d_{\beta_{nm}\beta_{nm}\gamma_m} = -\sqrt{\frac{m-1}{2m}}, \\
&d_{\alpha_{nm}\alpha_{nm}\gamma_k} = d_{\beta_{nm}\beta_{nm}\gamma_k} = \sqrt{\frac{1}{2k(k-1)}},\ m<k<n, \\
&d_{\alpha_{nm}\alpha_{nm}\gamma_n} = d_{\beta_{nm}\beta_{nm}\gamma_n} = \frac{2-n}{\sqrt{2n(n-1)}}, \\
&d_{\alpha_{nm}\mathrm{S}_{nm}\gamma_k} = d_{\beta_{nm}\beta_{nm}\gamma_k} = \sqrt{\frac{2}{k(k-1)}},\ n<k, \\
&d_{\gamma_n\gamma_k\gamma_k} = \sqrt{\frac{2}{n(n-1)}},\ k<n, \\
&d_{\gamma_n\gamma_n\gamma_n} = (2-n)\sqrt{\frac{2}{n(n-1)}}.
\end{aligned} \tag{A14}$$

Similarly to the totally anti-symmetric structure constants, the analytical expression of totally symmetric

structure constants can be obtained in any basis of generators of $\mathfrak{su}(N)$ by mean of the transformation presented in Eq. A7.

Appendix B: Coherent state basis and expectation value of the spin operator

The expansion coefficients of the coherent state basis in the N-level diabatic basis are[43,47]

$$\langle n|\mathbf{\Omega}\rangle_N = \begin{cases} \langle n|\mathbf{\Omega}\rangle_{N-1}, & 1 \le n < N-1, \\ \langle N-1|\mathbf{\Omega}\rangle_{N-1}\cos\frac{\theta_{N-1}}{2}, & n = N-1, \\ \langle N-1|\mathbf{\Omega}\rangle_{N-1}\sin\frac{\theta_{N-1}}{2}, & n = N, \end{cases} \tag{B1}$$

where $\langle 1|\mathbf{\Omega}\rangle_1 = 1$, and for $N > 1$ the spin coherent states are defined recursively. This is equivalent to the expression in Eq. 18.

Using the definition of the spin coherent states presented here (or defined in Eq. 18), and the definition of the generators of $\mathfrak{su}(N)$ in Eqs. 2-4, we can derive a general expression of the expectation value of the spin operators. The expression of the expectation value of the symmetric spin operator is

$$\begin{aligned} &\hbar\Omega_{\alpha_{nm}} \equiv \langle\mathbf{\Omega}|\hat{\mathcal{S}}_{\alpha_{nm}}|\mathbf{\Omega}\rangle \\ &= \frac{\hbar}{2}\Big(\cos\frac{\theta_m}{2}\prod_{j=1}^{m-1} e^{-i\varphi_j}\sin\frac{\theta_j}{2}\cos\frac{(1-\delta_{nN})\theta_n}{2}\prod_{k=1}^{n-1} e^{i\varphi_k} \\ &\quad\times\sin\frac{\theta_k}{2} + \cos\frac{\theta_m}{2}\prod_{j=1}^{m-1} e^{i\varphi_j}\sin\frac{\theta_j}{2}\cos\frac{(1-\delta_{nN})\theta_n}{2} \\ &\quad\times\prod_{k=1}^{n-1} e^{-i\varphi_k}\sin\frac{\theta_k}{2}\Big) \\ &= \hbar\prod_{j=1}^{m-1}\sin^2\frac{\theta_j}{2}\cos\frac{\theta_m}{2}\prod_{k=m}^{n-1}\sin\frac{\theta_k}{2}\cos\frac{(1-\delta_{nN})\theta_n}{2} \\ &\quad\times\cos\Big(\sum_{l=m}^{n-1}\varphi_l\Big), \end{aligned} \tag{B2}$$

where $1 \le m < n \le N$. When $m = 1$, $\prod_{j=1}^{m-1}\sin^2\frac{\theta_j}{2}$ is replaced by 1.

Similarly, for the anti-symmetric spin operator, we have

$$\begin{aligned} &\hbar\Omega_{\beta_{nm}} \equiv \langle\mathbf{\Omega}|\hat{\mathcal{S}}_{\beta_{nm}}|\mathbf{\Omega}\rangle \\ &= \hbar\prod_{j=1}^{m-1}\sin^2\frac{\theta_j}{2}\cos\frac{\theta_m}{2}\prod_{k=m}^{n-1}\sin\frac{\theta_k}{2}\cos\frac{(1-\delta_{nN})\theta_n}{2} \\ &\quad\times\sin\Big(\sum_{l=m}^{n-1}\varphi_l\Big), \end{aligned} \tag{B3}$$

and when $m = 1$, the term $\prod_{j=1}^{m-1}\sin^2\frac{\theta_j}{2}$ is replaced by 1.

For the diagonal spin operator there is only one index $1 < n \leq N$ and the expression is

$$\begin{aligned}\hbar\Omega_{\gamma_n} &\equiv \langle \mathbf{\Omega}|\hat{\mathcal{S}}_{\gamma_n}|\mathbf{\Omega}\rangle \\ &= \frac{\hbar}{\sqrt{2n(n-1)}}\Big(\sum_{j=1}^{n-1}\cos^2\frac{\theta_j}{2}\prod_{k=1}^{j-1}\sin^2\frac{\theta_k}{2} \\ &\quad + (1-n)\cos^2\frac{(1-\delta_{nN})\theta_n}{2}\prod_{j=1}^{n-1}\sin^2\frac{\theta_j}{2}\Big),\end{aligned} \tag{B4}$$

where $\prod_{k=1}^{j-1}\sin^2\frac{\theta_k}{2}$ is replaced by 1 when $n = 2$ (or $j = 1$).

Appendix C: Differential Phase-Space Volume Element of $SU(N)$

The volume element defined in Eq. 21, which is expressed as

$$\mathrm{d}\mathbf{\Omega} = \frac{N!}{(2\pi)^{N-1}}\prod_{n=1}^{N-1}\cos\frac{\theta_n}{2}\Big(\sin\frac{\theta_n}{2}\Big)^{2(N-n)-1}\mathrm{d}\theta_n\mathrm{d}\varphi_n. \tag{C1}$$

is different than the expression defined in Ref. 43. Here, we justify our choice.

The differential phase-space volume element is normalized as[50]

$$\int \mathrm{d}\mathbf{\Omega} = N, \tag{C2}$$

which can be easily proved as follows. To compute the integral over a given θ_n we express it as

$$\begin{aligned}&\int_0^{\pi}\cos\frac{\theta_n}{2}\Big(\sin\frac{\theta_n}{2}\Big)^{2(N-n)-1}\mathrm{d}\theta_n \\ &= 2\int_0^{\frac{\pi}{2}}\cos\theta_n'\Big(\sin\theta_n'\Big)^{2(N-n)-1}\mathrm{d}\theta_n', \quad \theta_n' = \frac{\theta_n}{2} \\ &= 2\int_0^1 y_n(1-y_n^2)^{N-n-1}\mathrm{d}y_n, \quad y_n = \cos\theta_n' \\ &= \int_0^1(1-t_n)^{N-n-1}\mathrm{d}t_n, \quad t_n = y_n^2.\end{aligned} \tag{C3}$$

We recognize the expression of the beta function, $B(x,y) = \int_0^1 t^{x-1}(1-t)^{y-1}\mathrm{d}t = \frac{\Gamma(x)\Gamma(y)}{\Gamma(x+y)}$, with $\Gamma(x)$ as the gamma function, and when x is a positive integer, $\Gamma(x) = (x-1)!$. We identify x and y leading to

$$\begin{aligned}\int_0^{\pi}\cos\frac{\theta_n}{2}\Big(\sin\frac{\theta_n}{2}\Big)^{2(N-n)-1}\mathrm{d}\theta_n &= B(1, N-n) \\ &= \frac{1}{N-n}.\end{aligned} \tag{C4}$$

Considering the product over all the angles we have

$$\prod_{n=1}^{N-1}\int_0^{\pi}\cos\frac{\theta_n}{2}\Big(\sin\frac{\theta_n}{2}\Big)^{2(N-n)-1}\mathrm{d}\theta_n = \frac{1}{(N-1)!}, \tag{C5}$$

hence we have the normalization condition

$$\int \mathrm{d}\mathbf{\Omega} = \frac{N!}{(2\pi)^{N-1}} \frac{1}{(N-1)!} (2\pi)^{N-1} = N. \tag{C6}$$

Further, one can show the following identity

$$\int |\mathbf{\Omega}\rangle\langle\mathbf{\Omega}| \mathrm{d}\mathbf{\Omega} = \hat{\mathcal{I}}, \tag{C7}$$

and we provide a concise proof below. The starting point is to prove that

$$\int \langle n|\mathbf{\Omega}\rangle\langle\mathbf{\Omega}|m\rangle \mathrm{d}\mathbf{\Omega} = \int c_n c_m^* \mathrm{d}\mathbf{\Omega} = \delta_{nm}. \tag{C8}$$

where $\langle n|\mathbf{\Omega}\rangle$ is expressed in Eq. 17, and c_n is defined in Eq. 46. For all the non-diagonal elements in Eq. C8, c_n and c_m^* include at least one angle φ_l (see Eq. 18), such that

$$\int_0^{2\pi} e^{\pm i\varphi_l} \mathrm{d}\varphi_l = 0, \tag{C9}$$

hence $\int c_n c_m^* \mathrm{d}\mathbf{\Omega} = 0$ for $n \neq m$.

Next, we consider the diagonal components of the integral, and separate them in three cases, $\int c_1 c_1^* \mathrm{d}\mathbf{\Omega}$, $\int c_n c_n^* \mathrm{d}\mathbf{\Omega}$ with $1 < n < N$, and $\int c_N c_N^* \mathrm{d}\mathbf{\Omega}$, due to the separate expressions of c_n in Eq. 18. For the θ_1 integral of the $\int c_1 c_1^* \mathrm{d}\mathbf{\Omega}$, we have

$$\begin{aligned}\int_0^{\pi} \Big(\cos\frac{\theta_1}{2}\Big)^3 \Big(\sin\frac{\theta_1}{2}\Big)^{2N-3} \mathrm{d}\theta_1 &= B(2, N-1) \\ &= \frac{1}{N(N-1)},\end{aligned} \tag{C10}$$

whereas for the integral related to $\theta_n,\ n > 1$ we have

$$\prod_{n=2}^{N-1} \int_0^{\pi} K(\theta_n) \mathrm{d}\theta_n = \frac{1}{(N-2)!}. \tag{C11}$$

Combining these results, we have

$$\frac{N!}{(2\pi)^{N-1}} \frac{1}{N(N-1)} \prod_{n=2}^{N-1} \int_0^{\pi} K(\theta_n) \mathrm{d}\theta_n \int_0^{2\pi} \mathrm{d}\varphi_n = 1. \tag{C12}$$

For the $\int c_N c_N^* \mathrm{d}\mathbf{\Omega}$ integral, each angle is integrated as

$$\begin{aligned}\int_0^{\pi} \cos\frac{\theta_l}{2} \Big(\sin\frac{\theta_l}{2}\Big)^{2(N-l)+1} \mathrm{d}\theta_l &= B(1, N-l+1) \\ &= \frac{1}{N-l+1},\end{aligned} \tag{C13}$$

leading to

$$\prod_{l=1}^{N-1} \int_0^{\pi} \cos\frac{\theta_l}{2} \Big(\sin\frac{\theta_l}{2}\Big)^{2(N-l)+1} \mathrm{d}\theta_l = \frac{1}{N!}. \tag{C14}$$

Finally for the remaining components $\int c_n c_n^* \mathrm{d}\mathbf{\Omega}$, with $1 < n < N$, the θ_n dependent integral is

$$\int \cos^2 \frac{\theta_n}{2} \prod_{l=1}^{n-1} \sin^2 \frac{\theta_l}{2} \mathrm{d}\mathbf{\Omega}. \tag{C15}$$

For the angles with indices l lower than n, the integral along θ_l is evaluated as

$$\int_0^\pi \cos \frac{\theta_l}{2} \Big(\sin \frac{\theta_l}{2} \Big)^{2(N-l)+1} \mathrm{d}\theta_l = \frac{1}{N-l+1}, \tag{C16}$$

which is equivalent to Eq. C13, while for indices l higher than n, the integral with θ_l is evaluate as

$$\int_0^\pi \cos \frac{\theta_l}{2} \Big(\sin \frac{\theta_l}{2} \Big)^{2(N-l)-1} \mathrm{d}\theta_l = \frac{1}{N-l}, \tag{C17}$$

equivalent to Eq. C4. For the index $l = n$, the integral related to θ_l is

$$\begin{aligned} \int_0^\pi \Big(\cos \frac{\theta_n}{2} \Big)^3 \Big(\sin \frac{\theta_n}{2} \Big)^{2(N-n)-1} \mathrm{d}\theta_n &= B(2, N-n) \\ &= \frac{1}{(N-n+1)(N-n)}, \end{aligned} \tag{C18}$$

which leads for any $|n\rangle\langle n|$ component to be

$$\int \cos^2 \frac{\theta_n}{2} \prod_{l=1}^{n-1} \sin^2 \frac{\theta_l}{2} \mathrm{d}\mathbf{\Omega} = \frac{1}{N!}. \tag{C19}$$

Summarizing all of the above results for the diagonal elements, we have

$$\frac{N!}{(2\pi)^{N-1}} \prod_{n=1}^{N-1} \int_0^\pi K(\theta_n) \mathrm{d}\theta_n \int_0^{2\pi} \mathrm{d}\varphi_n \langle l|\mathbf{\Omega}\rangle\langle\mathbf{\Omega}|l\rangle = 1, \tag{C20}$$

for $1 \leq l \leq N$. Combining with the result of the off-diagonal elements in Eq. C8, we have the identity

$$\frac{N!}{(2\pi)^{N-1}} \prod_{n=1}^{N-1} \int_0^\pi K(\theta_n) \mathrm{d}\theta_n \int_0^{2\pi} \mathrm{d}\varphi_n |\mathbf{\Omega}\rangle\langle\mathbf{\Omega}| = \hat{\mathcal{I}}, \tag{C21}$$

which is Eq. 20 of the main text.

Fig. 6 presents a system with $N = 5$ electronic states on the four Bloch spheres (for the s = W case), and the distribution of θ_i with the solid curves. As a comparison, the distribution used in Ref. 43 is shown with dashed curves. For a general N states system, we can see that the last Bloch sphere (here $n = 4$ in Fig. 6) always contains only the last two electronic states, hence requiring a distribution of the last angle, θ_{N-1}, to be symmetric around $\frac{\pi}{2}$ (for any choice of s index). On the contrary, the first Bloch sphere ($n = 1$ in Fig. 6) always puts the first electronic state on the north hemisphere, and all the other electronic states on the south hemisphere, requiring a distribution centered on the south hemisphere. As

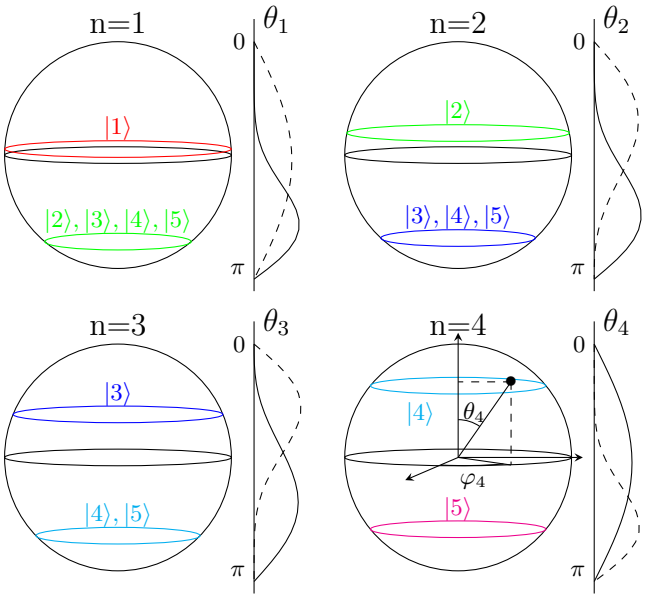

FIG. 6. Schematic representation of the Bloch spheres for a $N = 5$ system (with $\mathrm{s} = \bar{\mathrm{s}} = \mathrm{W}$). On the $n = 4$ sphere are represented θ_4 and φ_4. On the right of each sphere, the θ_n distribution is sketched from the differential phase space volume element in Eq. 21 (solid lines), and the distribution from the volume element previously derived in the literature[43,48,49] (dashed lines).

the index of the Bloch sphere increases (here, for example, $n = 2$ and $n = 3$ in Fig. 6), less states are present on the south hemisphere, and the distribution slowly shifts toward the center. This means that the previously used distribution[43,49] (dashed curves in Fig. 6) could potentially have an inconsistent labeling of the angles (the θ_1 distribution belongs to θ_{N-1} and inversely), as well as an inconsistent distributions for $1 < \theta_n < N - 1$ which does not have the right peak on the hemisphere of the Bloch spheres. This demonstrates that the differential phase-space volume element in Eq. 21 is the proper one to consider for the spin coherent state representation of $SU(N)$, as opposed to the one presented in Ref. 43, which gives incorrect distribution of the θ_n variables.

Appendix D: Derivation of the conjugate relationship between φ and Θ

We begin with the proposed conjugate relation

$$r_{\bar{\mathrm{s}}} \sum_{j=1}^{N} C_n(j) \frac{\mathrm{d}}{\mathrm{d}t} \Omega_{\gamma_j} = -\frac{\partial H_{\bar{\mathrm{s}}}}{\partial \varphi_n} \tag{D1a}$$

$$r_{\bar{\mathrm{s}}} \frac{\mathrm{d}}{\mathrm{d}t} \varphi_n = \frac{\partial H_{\bar{\mathrm{s}}}}{\partial \sum_{j=1}^{N} C_n(j) \Omega_{\gamma_j}}, \tag{D1b}$$

and compute $-\frac{\partial H_{\bar{\mathbb{s}}}}{\partial \varphi_n}$ (using Eq. B2 and Eq. B3) as follows

$$-\frac{\partial H_{\bar{\mathbb{s}}}}{\partial \varphi_n} = r_{\bar{\mathbb{s}}} \sum_{j=n+1}^{N} \sum_{k=1}^{n} \big(\mathcal{H}_{\alpha_{jk}} \Omega_{\beta_{jk}} - \mathcal{H}_{\beta_{jk}} \Omega_{\alpha_{jk}}\big), \quad \text{(D2)}$$

and compare it to $r_{\bar{\mathbb{s}}} \sum_{j=1}^{N} C_n(j) \frac{\mathrm{d}}{\mathrm{d}t} \Omega_{\gamma_j}$ (using Eq. 96) to determine the coefficients $C_n(j)$. We derived in Appendix A the closed formulas for the structure constants of $\mathfrak{su}(N)$ and hence can explicitly express the derivatives of Eq. 96 as

$$\begin{aligned}\frac{\mathrm{d}}{\mathrm{d}t}\Omega_{\gamma_j} = \frac{1}{\hbar}\Big[&\sqrt{\frac{j}{2(j-1)}} \sum_{k=1}^{j} \big(\mathcal{H}_{\alpha_{jk}} \Omega_{\beta_{jk}} - \mathcal{H}_{\beta_{jk}} \Omega_{\alpha_{jk}}\big) \\ &- \sqrt{\frac{j-1}{2j}} \sum_{k=j+1}^{N} \big(\mathcal{H}_{\alpha_{kj}} \Omega_{\beta_{kj}} - \mathcal{H}_{\beta_{kj}} \Omega_{\alpha_{kj}}\big) \\ &+ \sqrt{\frac{1}{2j(j-1)}} \sum_{k=j+1}^{N} \sum_{l=1}^{j-1} \big(\mathcal{H}_{\alpha_{kl}} \Omega_{\beta_{kl}} - \mathcal{H}_{\beta_{kl}} \Omega_{\alpha_{kl}}\big)\Big].\end{aligned} \quad \text{(D3)}$$

Starting from $\varphi_n,\ n = 1$, and solving iteratively Eq. D1a for every element $\mathcal{H}_{\alpha_{kl}} \Omega_{\beta_{kl}} - \mathcal{H}_{\beta_{kl}} \Omega_{\alpha_{kl}}$ (from $k = 2,\ l = 1$ and ascending) until deducing the expression of the coefficients $C_1(j)$, then using the same approach for $n > 1$, we obtain a formula that can be generalized, hence an expression for any coefficient

$$C_n(j \le n) = 0; \quad C_n(j > n) = n\sqrt{\frac{2}{j(j-1)}}. \quad \text{(D4)}$$

Further, the analytical expression of the time derivative of the symmetric generators is (we write $n+1 \equiv k$ for convenience)

$$\begin{aligned}\frac{\mathrm{d}}{\mathrm{d}t}\Omega_{\alpha_{k,n}} = \frac{1}{\hbar}\Big[&\sqrt{\frac{n-1}{2n}}\big(\mathcal{H}_{\gamma_n} \Omega_{\beta_{kn}} - \mathcal{H}_{\beta_{kn}} \Omega_{\gamma_n}\big) \\ &- \sqrt{\frac{n+1}{2n}}\big(\mathcal{H}_{\gamma_k} \Omega_{\beta_{kn}} - \mathcal{H}_{\beta_{kn}} \Omega_{\gamma_k}\big) \\ &+ \frac{1}{2}\sum_{j=1}^{n-1} \big(\mathcal{H}_{\beta_{nj}} \Omega_{\alpha_{kj}} - \mathcal{H}_{\alpha_{kj}} \Omega_{\beta_{nj}} - \mathcal{H}_{\alpha_{nj}} \Omega_{\beta_{kj}} + \mathcal{H}_{\beta_{kj}} \Omega_{\alpha_{nj}}\big) \\ &+ \frac{1}{2}\sum_{l=n+2}^{N} \big(\mathcal{H}_{\alpha_{ln}} \Omega_{\beta_{lk}} - \mathcal{H}_{\beta_{lk}} \Omega_{\alpha_{ln}} - \mathcal{H}_{\beta_{ln}} \Omega_{\alpha_{lk}} + \mathcal{H}_{\alpha_{lk}} \Omega_{\beta_{ln}}\big)\Big].\end{aligned} \quad \text{(D5)}$$

and the time derivative of anti-symmetric generators are

$$\begin{aligned}\frac{\mathrm{d}}{\mathrm{d}t}\Omega_{\beta_{kn}} = \frac{1}{\hbar}\Big[&\sqrt{\frac{n+1}{2n}}\big(\mathcal{H}_{\gamma_k} \Omega_{\alpha_{kn}} - \mathcal{H}_{\alpha_{kn}} \Omega_{\gamma_k}\big) \\ &- \sqrt{\frac{n-1}{2n}}\big(\mathcal{H}_{\gamma_n} \Omega_{\alpha_{kn}} - \mathcal{H}_{\alpha_{kn}} \Omega_{\gamma_n}\big) \\ &+ \frac{1}{2}\sum_{j=1}^{n-1} \big(\mathcal{H}_{\alpha_{nj}} \Omega_{\alpha_{kj}} - \mathcal{H}_{\alpha_{kj}} \Omega_{\alpha_{nj}} + \mathcal{H}_{\beta_{nj}} \Omega_{\beta_{kj}} - \mathcal{H}_{\beta_{kj}} \Omega_{\beta_{nj}}\big) \\ &+ \frac{1}{2}\sum_{l=n+2}^{N} \big(\mathcal{H}_{\alpha_{ln}} \Omega_{\alpha_{lk}} - \mathcal{H}_{\alpha_{lk}} \Omega_{\alpha_{ln}} + \mathcal{H}_{\beta_{ln}} \Omega_{\beta_{lk}} - \mathcal{H}_{\beta_{lk}} \Omega_{\beta_{ln}}\big)\Big],\end{aligned} \quad \text{(D6)}$$

where the elements of the sum are null when the conditions cannot be satisfied.

Using Eq. 75 and Eq. 77, the mapping Hamiltonian in Eq. 86 can be expressed as

$$\begin{aligned} H_{\mathrm{s}} &= \mathcal{H}_0 \\ &+ \sum_{n=2}^{N}\sum_{m=1}^{n-1}\sqrt{\Big(\Theta_n - \Theta_{n-1} + \frac{r_{\mathrm{s}}}{N}\Big)\Big(\Theta_m - \Theta_{m-1} + \frac{r_{\mathrm{s}}}{N}\Big)} \\ &\qquad \times \Big(\mathcal{H}_{\alpha_{nm}} \cos\big(\sum_{k=m}^{n-1}\varphi_k\big) + \mathcal{H}_{\beta_{nm}} \sin\big(\sum_{k=m}^{n-1}\varphi_k\big)\Big) \\ &+ \sum_{n=2}^{N}\mathcal{H}_{\gamma_n}\Big(\sqrt{\frac{n}{2(n-1)}}\Theta_{n-1} - \sqrt{\frac{n-1}{2n}}\Theta_n\Big). \end{aligned} \tag{D7}$$

Under the special case of a purely real Hamiltonian ($\mathcal{H}_{\beta_{nm}} = 0$), the above mapping Hamiltonian is expressed as Eq. 103 of the main text.

Appendix E: Mapping of Two-Level Systems under the $SU(2)$ Representation

For a two-level system $\hat{H} = \frac{\hat{P}^2}{2M}\hat{\mathcal{I}} + U_0(\hat{R})\hat{\mathcal{I}} + \hat{V}_e(\hat{R})$ where $\hat{\mathcal{I}}$ is the 2×2 identity matrix, and

$$\hat{V}_{\mathrm{e}}(\hat{R}) = \begin{pmatrix} V_{11}(\hat{R}) & V_{12}(\hat{R}) \\ V_{21}(\hat{R}) & V_{22}(\hat{R}) \end{pmatrix}. \tag{E1}$$

For this special case, $f_{ijk} = \varepsilon_{ijk}$ and $d_{ijk} = 0$, all of the equations in the main text remain general. Nevertheless, it will be beneficial to explicitly give several key equations under this special limit, whereas more detailed discussion of the $SU(2)$ can be found in the previous work of Spin-LSC[34] and spin-mapping non-adiabatic RPMD (SM-NRPMD).[35]

Using the $SU(2)$ representation, one can express the original two-states Hamiltonian as follows

$$\hat{H} = \mathcal{H}_0\hat{\mathcal{I}} + \frac{1}{\hbar}\mathbf{H}\cdot\hat{\mathbf{S}} = H_0\hat{\mathcal{I}} + \frac{1}{\hbar}(\mathcal{H}_x\cdot\hat{\mathcal{S}}_x + \mathcal{H}_y\cdot\hat{\mathcal{S}}_y + \mathcal{H}_z\cdot\hat{\mathcal{S}}_z), \tag{E2}$$

where $\hat{S}_i = \frac{\hbar}{2}\hat{\sigma}_i$ (for $i\in\{x,y,z\}$) is the quantum spin operator, with $\hat{\sigma}_i$ as the Pauli matrices expressed in Eq. 2, and $\mathcal{H}_0 = \frac{\hat{P}^2}{2m} + U_0(\hat{R}) + \frac{1}{2}(V_{11}(\hat{R}) + V_{22}(\hat{R}))$, $\mathcal{H}_x = 2\mathrm{Re}(V_{12}(\hat{R}))$, $\mathcal{H}_y = 2\mathrm{Im}(V_{12}(\hat{R}))$, $\mathcal{H}_z = V_{11}(\hat{R}) - V_{22}(\hat{R})$, which are the $N=2$ limit of Eq. 12.

Using the spin coherent state for $N=2$ (Eq. 16), the expectation value of the spin operator is

$$\hbar\Omega_i(\mathbf{u}) = \langle\mathbf{u}|\hat{S}_i|\mathbf{u}\rangle = \frac{\hbar}{2}u_i, \qquad i\in\{x,y,z\}, \tag{E3}$$

where $u_x = \sin\theta\cos\varphi$, $u_y = \sin\theta\sin\varphi$, $u_z = \cos\theta$ as the special case of Eqs. B2-B4. The identity in Eq. 20 becomes $\hat{\mathcal{I}} = \int \mathrm{d}\mathbf{u}|\mathbf{u}\rangle\langle\mathbf{u}|$, where $\int\mathrm{d}\mathbf{u} = \frac{1}{2\pi}\int_0^{\pi}\mathrm{d}\theta\sin\theta\int_0^{2\pi}\mathrm{d}\varphi$ is the $N=2$ limit of Eq. 21.

Under the $\mathfrak{su}(2)$ Lie algebra, the S-W kernel in Eq. 26 becomes

$$\hat{w}_{\rm s} = \frac{1}{2}\hat{\mathcal{I}} + r_{\rm s}\boldsymbol{\Omega}\cdot\hat{\boldsymbol{\sigma}}, \tag{E4}$$

where $\boldsymbol{\Omega}\cdot\hat{\boldsymbol{\sigma}} = \Omega_x\cdot\hat{\sigma}_x + \Omega_y\cdot\hat{\sigma}_y + \Omega_z\cdot\hat{\sigma}_z$. Note that the $r_{\rm s}$ used in this paper is twice the one defined in the previous work,[34,35] (see the factor between $\boldsymbol{\Omega}$ and $\mathbf{u}$ in Eq. E3).

The S-W transform of the Hamiltonian becomes

$$\begin{aligned}[\hat{H}]_{\rm s}(\boldsymbol{\Omega}) &= \mathcal{H}_0 + r_{\rm s}\mathcal{H}\cdot\boldsymbol{\Omega} \\ &= \frac{P^2}{2m} + U_0 + (\frac{1}{2} + \frac{r_{\rm s}}{2}\cos\theta)\cdot V_{11}(\hat{R}) \\ &+ (\frac{1}{2} - \frac{r_{\rm s}}{2}\cos\theta)\cdot V_{22}(\hat{R}) + r_{\rm s}\sin\theta\cos\varphi\cdot{\rm Re}[V_{12}(\hat{R})] \\ &+ ir_{\rm s}\sin\theta\sin\varphi\cdot{\rm Im}[V_{12}(\hat{R})],\end{aligned} \tag{E5}$$

and the projection operators are transformed as

$$\begin{aligned}[|1\rangle\langle 1|]_{\rm s} &= [\frac{1}{2}\hat{\mathcal{I}} + \frac{1}{\hbar}\hat{S}_z]_{\rm s} = \frac{1}{2} + \frac{r_{\rm s}}{2}\cos\theta, \\ [|2\rangle\langle 2|]_{\rm s} &= [\frac{1}{2}\hat{\mathcal{I}} - \frac{1}{\hbar}\hat{S}_z]_{\rm s} = \frac{1}{2} - \frac{r_{\rm s}}{2}\cos\theta, \\ [|1\rangle\langle 2| + |2\rangle\langle 1|]_{\rm s} &= 2[\frac{1}{\hbar}\hat{S}_x]_{\rm s} = r_{\rm s}\sin\theta\cos\varphi \\ [|1\rangle\langle 2| - |2\rangle\langle 1|]_{\rm s} &= 2i[\frac{1}{\hbar}\hat{S}_y]_{\rm s} = ir_{\rm s}\sin\theta\sin\varphi.\end{aligned}$$

The derivation procedure of the TCF and exact Liouvillian are same as outlined in the main text. The electronic EOMs under the linearization approximation is

$$\frac{\rm d}{{\rm d}t}\Omega_i = \frac{1}{\hbar}\sum_{j,k=1}^{3}\varepsilon_{ijk}H_j(R)\Omega_k, \tag{E7}$$

which is the $N = 2$ limit of Eq. 98c. This is commonly written as[32,33]

$$\frac{d}{dt}\boldsymbol{\Omega} = \frac{1}{\hbar}\mathbf{H}(\hat{R})\times\boldsymbol{\Omega}. \tag{E8}$$

For a two-level system, Eq. 113 reduce back to[35]

$$\dot{\theta} = -\mathcal{H}_x\sin\varphi + \mathcal{H}_y\cos\varphi, \tag{E9a}$$

$$\dot{\varphi} = \mathcal{H}_z - \mathcal{H}_x\frac{\cos\varphi}{\tan\theta} - \mathcal{H}_y\frac{\sin\varphi}{\tan\theta}, \tag{E9b}$$

It is interesting to note[35] that the above equations are equivalent to the following

$$\dot{\theta} = \frac{1}{\frac{1}{2}r_{\rm s}\sin\theta}\frac{\partial H_{\rm s}}{\partial\varphi} \tag{E10a}$$

$$\dot{\varphi} = -\frac{1}{\frac{1}{2}r_{\rm s}\sin\theta}\frac{\partial H_{\rm s}}{\partial\theta} \tag{E10b}$$

from which we obtain the conjugate variables $\dot{\varphi}$ and $\frac{1}{2}r_{\rm s}\cos\theta$ related to the spin mapping representation,

where the latter plays the role of conjugate momentum[92] to φ as

$$\frac{d}{dt}(\frac{1}{2}r_{\rm s}\cos\theta) = -\frac{\partial H_{\rm s}}{\partial \varphi} \tag{E11a}$$

$$\dot{\varphi} = \frac{\partial H_{\rm s}}{\partial(\frac{1}{2}r_{\rm s}\cos\theta)}. \tag{E11b}$$

This helps to inspire the relation we conjectured in Eq. 99, and one notice that when $N = 2$, the expression of Θ (Eq. 74) indeed reduces to $\Theta = r_{\rm s}(\frac{2-1}{2} - \sin^2\frac{\theta}{2}) = \frac{1}{2}r_{\rm s}\cos\theta$, which is the conjugate variable of φ.

Finally, under the two level special case, the mapping Hamiltonian (Eq. 103) with $\{\Theta, \varphi\}$ as the natural variables is expressed as

$$\begin{aligned} H_{\rm s} =& \frac{P^2}{2M} + U_0(R) \\ &+ \Big(\Theta + \frac{1}{2}\Big)\cdot V_{11}(R) + \Big(-\Theta + \frac{1}{2}\Big)\cdot V_{22}(R) \\ &+ 2V_{12}(R)\sqrt{\Big(\Theta + \frac{r_{\rm s}}{2}\Big)\Big(-\Theta + \frac{r_{\rm s}}{2}\Big)}\cdot\cos\varphi, \end{aligned} \tag{E12}$$

and the corresponding EOMs in Eq. 104 becomes

$$\begin{aligned} \dot{\Theta}_n &= -\frac{\partial H_{\rm s}}{\partial \varphi_n} \\ &= 2V_{12}(R)\sqrt{\Big(\Theta + \frac{r_{\rm s}}{2}\Big)\Big(-\Theta + \frac{r_{\rm s}}{2}\Big)}\cdot\sin\varphi, \end{aligned} \tag{E13a}$$

$$\begin{aligned} \dot{\varphi} = \frac{\partial H_{\rm s}}{\partial \Theta} &= V_{11}(R) - V_{22}(R) \\ &+ V_{12}(R)\left[\sqrt{\frac{-\Theta + \frac{r_{\rm s}}{N}}{\Theta + \frac{r_{\rm s}}{N}}} - \sqrt{\frac{\Theta + \frac{r_{\rm s}}{N}}{-\Theta + \frac{r_{\rm s}}{N}}}\right]\cos\varphi. \end{aligned} \tag{E13b}$$

Appendix F: Connections with Previous Methods

Note that historically, the MMST mapping Hamiltonian (Eq. 50) is established through the Stock-Thoss mapping procedure[8,10] by representing the N-level system with N harmonic oscillators' singly excited states

$$|n\rangle \to |0_1, \cdots, 1_n, \cdots, 0_N\rangle = \hat{a}_n^\dagger |0_1, \cdots, 0_n, \cdots, 0_N\rangle, \tag{F1}$$

where $\hat{a}_n^\dagger = \frac{1}{\sqrt{2}}(\hat{q}_n - i\hat{p}_n)$, $\hat{a}_n = \frac{1}{\sqrt{2}}(\hat{q}_n + i\hat{p}_n)$ are harmonic oscillator's raising and lowering operators, and the commutator $[\hat{q}_n, \hat{p}_m] = i\delta_{nm}$ is valid in the complete Hilbert space of the mapping oscillator. This can be viewed as a generalized Schwinger's bosonization approach.[10] Using the mapping relation

$$\sum_{nm} V_{nm}(\hat{R})|n\rangle\langle m| \to \sum_{nm} V_{nm}(\hat{R})\hat{a}_n^\dagger \hat{a}_m, \tag{F2}$$

the Stock-Thoss mapping Hamiltonian is expressed as

$$\begin{aligned} \hat{H}_{\rm MMST} =& \hat{T}_R + U_0(\hat{R}) + \sum_n \frac{1}{2}V_{nn}(\hat{R})(\hat{q}_n^2 + \hat{p}_n^2 - 1) \\ &+ \sum_{n<m} V_{nm}(\hat{R})(\hat{q}_n\hat{q}_m + \hat{p}_n\hat{p}_m). \end{aligned} \tag{F3}$$

This argument leads to the ZPE parameter $\gamma = 1$, and without the constraint provided in Eq. 57, even though $\sum_{n=1}^{N} \frac{1}{2}(q_n^2 + p_n^2 - \gamma)$ is a constant of motion. Most of the existing mapping approaches are based upon this mapping procedure,[11,14] or a modified one that constraint the operators within the SEO subspace. One can further down-grade these mapping operators into classical variables, for example, using the Wigner transform through the mixed quantum-classical approximation,[112] linearization approximation,[11,91] or the Husimi representation (coherent state basis) for these mapping variables through the semi-classical approximation[8,10,12,13,88,113] or the partial linearization approximation.[15,16,114,115]

The MMST mapping formalism should be viewed as a fundamentally different mapping procedure compared to the $SU(N)$ formalism. This is because that the MMST mapping operators $\hat{a}_n^\dagger$ and $\hat{a}_n$ (or $\hat{q}_n$, $\hat{p}_n$) live in a *larger* Hilbert space than the electronic Hilbert space of the original Hamiltonian.[10,20,21] Truncating the larger Hilbert space to include only SEO subspace[24] ruins the simple commutation relation between $\hat{p}_n$ and $\hat{q}_n$, such that $[\hat{q}_n, \hat{p}_n] \neq i$ in the truncated Hilbert space.[24,116] A detailed expression of $[\hat{q}_n, \hat{p}_n]$ in the truncated SEO mapping space can be found in Eq. 17 of Ref. 109. Thus, when applying truncation of the mapping Hilbert space (such as done for the mapping formalism in Ref. 24), this additional commutator $[\hat{q}_n, \hat{p}_n]$ need to be explicitly included to replace $\gamma = 1$ in $\hat{H}_{\text{MMST}}$ Hamiltonian (Eq. F3), and is required to be evaluated through additional approximations.[25]

As opposed to the Stock-Thoss mapping procedure, the starting point of the $SU(N)$ mapping formalism is completely different. The $SU(N)$ mapping formalism uses the generators of the $\mathfrak{su}(N)$ Lie algebra (more specifically, the GGM basis in Eq. 2-Eq. 4), which exactly preserves the commutation relations among operators as well as the original electronic Hilbert space. As a result, there is no need for additional Hilbert space truncation that ruins commutation relations, nor necessity of projecting back to the subspace as required by MMST formalism.[20,21] The exact quantum Liouvillian from the current $SU(N)$ mapping formalism (see Sec. V) is also different than the exact Liouvillian of the MMST formalism.[76–78]

It is interesting that despite a completely different mapping procedure, the same mapping Hamiltonian (Eq. 50) can be obtained upon a variable transformation (Eq. 49) of the mapping Hamiltonian $\left[\hat{H}(\hat{R})\right]_{\text{s}}(\mathbf{\Omega})$ in the $SU(N)$ formalism. In the context of the $SU(N)$ mapping formalism, these conjugated mapping variables $\{q_n, p_n\}$ do not have the meaning of position and momentum of mapping oscillators as suggested in the Stock-Thoss mapping procedure;[8,10] they are simply the real and imaginary components of the expansion coefficients[69] of the generalized spin coherent states in the diabatic basis (up to a global phase) as indicated in Eq. 46.

Next, we connect several previously developed methods with the current approach in the language of the

$SU(N)$ mapping formalism. As we have discussed, the underlying EOMs for the $SU(N)$ approach (within the linearization approximation) are identical to Ehrenfest dynamics and the MMST-based approach under a specific choice of $r_{\rm s}$. Nuclear initial conditions for all of these methods are also obtained from the Wigner transform of the initial nuclear density operator.

(1). Ehrenfest Dynamics is equivalent to use $r_{\rm s} = 1$ (s = Q method) for the EOMs (Eq. 118 and Eq. 119), and the focused initial conditions in Eq. 82 with $\gamma = 0$ (corresponding to $r_{\rm s} = 1$). The original Ehrenfest dynamics also enforces all angles ϕ_n in Eq. 122 to be zero. However, having a random distribution in ϕ_n (Eq. 122) or in φ_n Eq. 120b does not influence the numerical results, based on the calculations of model systems we explored in this work.

(2). LSC-IVR[11,90,91] uses $\gamma = 1$ (corresponding to $r_{\rm s} = \frac{N}{2} + 1$) in the EOMs (Eq. 118 and Eq. 119). The estimator based on the Stock-Thoss mapping procedure[8,10] is $|n\rangle\langle n| \to |1_n\rangle\langle 1_n|$ (mapped onto the singly excited oscillator state $|1_n\rangle \equiv |0_1, ..., 1_n ..., 0_N\rangle$), and the Wigner transform (defined in the mapping oscillator phase space) of this operator is $[|1_n\rangle\langle 1_n|]_{\rm w} = G(\mathbf{q},\mathbf{p})(q_n^2 + p_n^2 - \frac{1}{2})$, where the Gaussian function is $G(\mathbf{q},\mathbf{p}) = 2^{N+1} \cdot \exp[-\sum_{l=1}^{N}(q_l^2 + p_l^2)]$. In LSC-IVR,[11,90,91] both operator $\hat{A}$ and $\hat{B}$ in $C_{AB}(t)$ (Eq. 73) use the expression $[|1_n\rangle\langle 1_n|]_{\rm w}$. For the closely related Poisson Bracket Mapping Equation (PBME),[14,21,117] method, the choice of the operator $\hat{A}$ is the same, but the estimator $\hat{B}$ is chosen to be $[\hat{a}_n^\dagger \hat{a}_n]_{\rm w} = \frac{1}{2}(q_n^2 + \hat{p}_n^2 - 1)$, which is identical to Eq. 54 when using $\gamma = 1$. Both methods are more accurate than Ehrenfest,[34] but less accurate than Spin-LSC.[43] Using an identity trick[22,67] which forces the identity operator's Wigner transform to be 1, the accuracy of the linearized MMST methods can be significantly improved.[22,67] Note that with the spin mapping formalism, the identity is naturally forced to be one[34,43] through the basic property of the S-W transform (Eq. 30b).

(3). Spin-LSC[34,43] is similar to the linearized method derived in this work (Eq. 117 and Eq. 119) and we provide here a proof from first principle. The EOMs are justified through the quantum-classical Liouville equation,[43] resulting in the EOMs in Eq. 117 and Eq. 119. The difference between spin-LSC and the current formalism are the initial conditions. In our current formalism, the sampling of the mapping variables is determined by the expression of $\mathrm{d}\mathbf{\Omega}$ in Eq. 21, whereas in spin-LSC, the mapping variables $\{q_n, p_n\}$ are randomly sampled from a Gaussian distribution, then universally scaled such that Eq. 57 (total population constraint) is satisfied.[43] For the focused initial conditions, both the current formalism and spin-LSC use Eq. 82. Numerically, we found that our current formalism and spin-LSC produce similar initial conditions, for both the sampled and the focused procedures.

(4). Generalized Discrete Truncated Wigner Approximation (GDTWA)[51] is also based upon the $SU(N)$ mapping formalism, and uses the *effective* value of $r_{\rm s}$ =

$\sqrt{N+1}$ or $\gamma = \frac{2}{N}(\sqrt{N+1}-1)$ (s = W), although it is only possible to rigorously connect[51] to Spin-LSC when $N = 2$. The EOMs of GDTWA are *proposed* to be Eq. 98, which is the classical limit of the Heisenberg EOMs of $\hat{\mathcal{S}}$, $\hat{R}$ and $\hat{P}$. Thus, the EOMs are equivalent to the current linearized approach and Spin-LSC (Eq. 117 and Eq. 119). The initial conditions for the generalized coherent state variables Ω_i are chosen[51] to be *eigenvalues* of $\hat{\mathcal{S}}_i$ (with the expressions in Eq. 2-4), which is in principle different than both the focused and the sampled procedure of the current linearized method or Spin-LSC.[34,43] However, the detailed expressions of estimators in GDTWA require the quasi-phase point operator in Wootters's discrete phase space representation,[118,119] and future work is needed to establish a formal connection between the current work/Spin-LSC and GDTWA.

This is dull repeat of what we had published in Ref. 74.

(5). The eCMM is based on the MMST formalism, and uses a γ parameter that can take values within the range $r_s \in (-\frac{2}{N}, \infty)$, which can in principle be negative,[74] as discussed under Eq. 51. The choice of the population estimator is $[|n\rangle\langle n|]_s$ (Eq. 54) for operator $\hat{A}$ and $[|n\rangle\langle n|]_{\bar{s}}$ (Eq. 55) for operator $\hat{B}$. The EOMs are proposed to be Eq. 117 and Eq. 119, with the same choice of r_s used in estimator for $\hat{A}$. The initial mapping variables are randomly sampled within the constraint given in Eq. 57. Even though eCMM and spin-LSC are seemingly derived from very different perspectives, where eCMM is formulated with the MMST Hamiltonian with a total population constraint and spin-LSC is developed based on the $SU(N)$ mapping formalism, the kernel of eCMM approach to evaluate the expectation value of the electronic operator turns out to be the Cartesian coordinates ($\{q_n, p_n\}$) expression of the S-W kernel expressed in Eq. 52. In addition, the EOMs used in Spin-LSC and eCMM are identical as well. Considering all of the above, eCMM[25] is an identical approach compared to Spin-LSC.[43]

It is mentioned in Ref. 25, 74, 109 that the P/Q/W versions of spin-LSC are just three special cases of eCMM, while here try to confuse the relations between these two methods. It is no reason to say that eCMM with continuous \gamma parameter is identical to spin-LSC that only involves three special versions. Moreover, it is never "identical" between EOMs in Spin-LSC and eCMM because in Ref.43 they just use the EOMs of eCMM to evolve the so-called spin-mapping variables. And it is sure that the EOMs of eCMM is NOT identical to those of Stratonovich-Weyl phase space due to the evolving global phase, as mentioned in WIREs. Comput. Mol. Sci. e1619 (2022).

(6). The Symmetric Quasi-Classical (SQC) method[17,23] uses $\gamma = (\sqrt{3}-1)/2$ for the square window[23], $\gamma = 1/3$ for the triangle window[72], or a state- and trajectory-specific γ to enforce initial electronic population[73] to be 1 or 0. The initial conditions for the action variable η_n (Eq. 122a) is uniformly sampled within a window function, and the angle variable ϕ_n (Eq. 122b) is randomly sampled. The EOMs are identical to Eq. 118 and Eq. 119 with the above mentioned specific choice of γ. Note that the SQC approach assumes the same γ parameter for both window estimators of $\hat{A}$ and $\hat{B}$, as well as in the EOM.

Appendix G: Details of the Model systems

One dimensional spin-boson model. We use a one dimensional spin-boson model[99,120] to investigate the accuracy of the non-adiabatic dynamics for various meth-

ods. The Hamiltonian is expressed as

$$\hat{H} = \Big(\frac{\hat{P}^2}{2m} + \frac{1}{2}m\omega^2\hat{R}^2\Big)\hat{\mathcal{I}} + \sqrt{2}\zeta\hat{R}\hat{\sigma}_z + \Delta\hat{\sigma}_x, \tag{G1}$$

where $\hat{\sigma_x}$ and $\hat{\sigma}_z$ are the Pauli matrices, $\hat{\mathcal{I}}$ is a 2×2 identity matrix, $\hat{R}$ and $\hat{P}$ are the position and momentum operators of the boson mode. The parameter ζ controls the electronic-nuclear coupling, and Δ is the electronic coupling between two electronic states. We choose $2\Delta = \omega = m = 1$ and increasing values of the coupling strength parameter, the temperature is chosen in order to have $\beta = 16$. The initial electronic state is prepared on state $|1\rangle$.

Spin-Boson model. The spin-boson model[121] is a commonly used two-level benchmark model for non-adiabatic dynamics.[23,34,122] It consists in two electronic states, coupled to a harmonic bath of F-nuclear modes. The Hamiltonian of the model system is

$$\hat{H} = \sum_{\nu=1}^{F}\Big(\frac{\hat{P}_\nu^2}{2m_\nu} + \frac{1}{2}m_\nu\omega_\nu^2\hat{R}_\nu^2\Big)\hat{\mathcal{I}} + \Big(\varepsilon + \sum_{\nu=1}^{F} c_\nu\hat{R}_\nu\Big)\hat{\sigma}_z + \Delta\cdot\hat{\sigma}_x, \tag{G2}$$

where m_ν is the nuclear masse set to be 1, Δ is the diabatic electronic coupling set to be 1, and ε is the energy bias between two electronic states. The F nuclear modes each have their frequency ω_ν and vibronic coupling coefficient c_ν, determined through the spectral density of the bath $J(\omega)$. Here, we use an Ohmic spectral density

$$J(\omega) = \frac{\pi}{2}\sum_{\nu=1}^{F}\frac{c_\nu^2}{\omega_\nu}\delta(\omega - \omega_\nu) = \frac{\pi\xi}{2}\omega e^{-\omega/\omega_c}, \tag{G3}$$

where ξ is the Kondo parameter and ω_c the cut-off frequency for the bath. We perform simulations with three sets of model parameters, from a low to a high temperature and different system-bath coupling strengths (through the Kondo parameter), with parameters listed in Tab. I. We discretize the Ohmic spectral density with F discrete nuclear modes Ref. 123 as follows

$$\omega_\nu = -\omega_c \ln\Big(\frac{\nu - 1/2}{F}\Big), \tag{G4a}$$

$$c_\nu = \omega_\nu\sqrt{\frac{\xi\omega_c m_\nu}{F}}. \tag{G4b}$$

The initial electronic state is prepared on state $|1\rangle$.

Two- and Three-States Linear Vibronic Coupling Models. The linear vibronic coupling (LVC) models describe conical intersections in molecules. The Hamiltonian is expressed as

$$\hat{H} = \frac{1}{2}\sum_\nu \omega_\nu\hat{P}_\nu^2 + \sum_{k,l}|k\rangle H_{kl}(\hat{\mathbf{R}})\langle l|, \tag{G5a}$$

$$H_{kk}(\hat{\mathbf{R}}) = E_k + \frac{1}{2}\sum_\nu \omega_\nu\hat{R}_\nu^2 + \sum_\nu \kappa_\nu^k\hat{R}_\nu, \tag{G5b}$$

$$H_{kl}(\hat{\mathbf{R}}) = \sum_\nu \lambda_\nu^{kl}\hat{R}_\nu, \tag{G5c}$$

where ω_ν is the frequency of the ν-th nuclear normal mode, E_k is the vertical transition energy of state k, and the electronic-nuclear coupling is λ_ν^{kl}. Here, we investigate two widely tested LVC models: the pyrazine model,[104] and the benzene cation radical model.[107,108] The pyrazine model is a standard conical intersection model used to study non-adiabatic dynamics.[51,124–126] It is a three-modes two-states model, with two tuning coordinates, $\hat{R}_1$ and $\hat{R}_2$, and one coupling coordinate, $\hat{R}_3$. The parameters are given in Tab. II of Appendix G. The initial electronic state is prepared on state $|2\rangle$. The benzene radical cation model is a five-modes three-states model with three tuning coordinates, $\hat{R}_1$, $\hat{R}_2$ and $\hat{R}_3$, and two coupling coordinates, $\hat{R}_4$ and $\hat{R}_5$. The parameters are given in Tab. III of Appendix G. The initial electronic state[51] is prepared on state $|3\rangle$.

Three-state Morse model. Finally, we consider an anharmonic model. We compute the population dynamics of a three-state Morse potential,[12] which is used to model photo-dissociation dynamics with three sets of parameters. The Hamiltonian is expressed as

$$\hat{H} = \frac{\hat{P}^2}{2m}\hat{\mathcal{I}} + \sum_{ij} V_{ij}(\hat{R})|i\rangle\langle j|, \tag{G6a}$$

$$V_{ii}(\hat{R}) = D_{ii}(1 - e^{-\alpha_{ii}(\hat{R}-R_{ii})})^2 - c_{ii}, \tag{G6b}$$

$$V_{ij}(\hat{R}) = A_{ij}e^{-\alpha_{ij}(\hat{R}-R_{ij})^2},\ i \neq j, \tag{G6c}$$

where the mass is set to be $m = 20\,000$ a.u. and the rest of the parameters are specified in Tab. IV of Appendix G for the three models IA, IB and IC. The system is initially excited onto state $|1\rangle$.

TABLE I. Parameters for the spin-boson models presented in Fig. 2, in a.u.

Model	ϵ	ξ	β	ω_c
(a)	1.0	0.1	5.0	2.5
(b)	1.0	0.1	0.25	1.0
(c)	0.0	2.0	1.0	1.0

TABLE II. Parameters for the pyrazine model presented in top panels of Fig. 3, given in eV.

ν/k	E_k	ω_ν	$\kappa_\nu^{(1)}$	$\kappa_\nu^{(2)}$	λ_ν^{12}
1	3.94	0.126	0.037	-0.254	0.0
2	4.84	0.074	-0.105	0.149	0.0
3		0.118	0.0	0.0	0.262

[1] J. C. Tully, J. Chem. Phys. **137**, 22A301 (2012).
[2] J. C. Tully and R. K. Preston, J. Chem. Phys. **55**, 562 (1971).
[3] J. C. Tully, J. Chem. Phys. **93**, 1061 (1990).
[4] J. E. Subotnik, A. Jain, B. Landry, A. Petit, W. Ouyang, and N. Bellonzi, Annu. Rev. Phys. Chem. **67**, 387 (2016).
[5] L. Wang, A. Akimov, and O. V. Prezhdo, J. Phys. Chem. Lett. **7**, 2100 (2016).
[6] R. Crespo-Otero and M. Barbatti, Chem. Rev. **118**, 7026 (2018).

TABLE III. Parameters for the benzene radical cation model presented in bottom panels of Fig. 4, given in eV.

ν/k	E_k	ω_ν	$\kappa_\nu^{(1)}$	$\kappa_\nu^{(2)}$	$\kappa_\nu^{(3)}$	λ_ν^{12}	λ_ν^{23}
1	9.75	0.123	-0.042	-0.042	-0.301	0.0	0.0
2	11.84	0.198	-0.246	0.242	0.0	0.0	0.0
3	12.44	0.075	-0.125	0.1	0.0	0.0	0.0
4		0.088	0.0	0.0	0.0	0.164	0.0
5		0.12	0.0	0.0	0.0	0.0	0.154

TABLE IV. Parameters for the three-state Morse potential presented in Fig. 5, in a.u.

	IA			IB			IC		
i	1	2	3	1	2	3	1	2	3
D_{ii}	0.02	0.02	0.003	0.02	0.01	0.003	0.003	0.004	0.003
α_{ii}	0.4	0.65	0.65	0.65	0.4	0.65	0.65	0.6	0.65
R_{ii}	4.0	4.5	6.0	4.5	4.0	4.4	5.0	4.0	6.0
c_{ii}	0.02	0.0	0.02	0.0	0.01	0.02	0.0	0.0	0.006
ij	12	13	23	12	13	23	12	13	23
A_{ij}	0.005	0.005	0.0	0.005	0.005	0.0	0.002	0.0	0.002
α_{ij}	32.0	32.0	0.0	0.005	0.005	0.0	0.002	0.0	0.002
R_{ij}	3.4	4.97	0.0	3.66	3.34	0.0	3.4	0.0	4.8

[7] H.-D. Meyer and W. H. Miller, J. Chem. Phys. **71**, 2156 (1979).
[8] G. Stock and M. Thoss, Phys. Rev. Lett. **78**, 578 (1997).
[9] H.-D. Meyer and W. H. Miller, J. Chem. Phys. **70**, 3214 (1979).
[10] M. Thoss and G. Stock, Phys. Rev. A **59**, 64 (1999).
[11] X. Sun and W. H. Miller, J. Chem. Phys. **106**, 916 (1997).
[12] E. A. Coronado, J. Xing, and W. H. Miller, Chem. Phys. Lett. **349**, 521 (2001).
[13] S. Bonella and D. F. Coker, J. Chem. Phys. **114**, 7778 (2001).
[14] H. Kim, A. Nassimi, and R. Kapral, J. Chem. Phys. **129**, 084102 (2008).
[15] P. Huo and D. F. Coker, J. Chem. Phys. **135**, 201101 (2011).
[16] P. Huo and D. F. Coker, J. Chem. Phys. **137**, 22A535 (2012).
[17] W. H. Miller and S. J. Cotton, Faraday Discuss. **195**, 9 (2016).
[18] J. O. Richardson, P. Meyer, M.-O. Pleinert, and M. Thoss, Chem. Phys. **482**, 124 (2017).
[19] J. O. Richardson and M. Thoss, J. Chem. Phys. **139**, 031102 (2013).
[20] N. Ananth and T. F. Miller, J. Chem. Phys. **133**, 234103 (2010).
[21] A. Kelly, R. van Zon, J. Schofield, and R. Kapral, J. Chem. Phys. **136**, 084101 (2012).
[22] M. A. C. Saller, A. Kelly, and J. O. Richardson, J. Chem. Phys. **150**, 071101 (2019).
[23] S. J. Cotton and W. H. Miller, J. Chem. Phys. **139**, 234112 (2013).
[24] J. Liu, J. Chem. Phys. **145**, 204105 (2016).
[25] X. He, B. Wu, Z. Gong, and J. Liu, J. Phys. Chem. A **125**, 6845 (2021).
[26] Y. Gu, Phys. Rev. A **32**, 1310 (1985).
[27] C. Brif and A. Mann, Phys. Rev. A **59**, 971 (1999).
[28] A. B. Klimov and S. M. Chumakov, *A Group-Theoretical Approach to Quantum Optics: Models of Atom-Field Interactions* (John Wiley & Sons, 2009).
[29] B. C. Hall, *GTM222: Lie Groups, Lie Algebras, and Representations, An Elementary Introduction, 2nd Ed.* (Springer, Switzerland, 2015).
[30] See Page 71 corollary 3.47 of Ref. 29.
[31] H. Georgi, *Lie Algebras In Particle Physics: from Isospin To Unified Theories* (CRC Press, 2000).
[32] C. Cohen-Tannoudji, B. Diu, and F. Laloe, *Quantum Mechanics, Volume 1* (Wiley, 1997).
[33] R. P. Feynman, F. L. Vernon, and R. W. Hellwarth, J. App. Phys. **28**, 49 (1957).
[34] J. E. Runeson and J. O. Richardson, J. Chem. Phys. **151**, 044119 (2019).
[35] D. Bossion, S. N. Chowdhury, and P. Huo, J. Chem. Phys. **154**, 184106 (2021).
[36] F. T. Hioe and J. H. Eberly, Phys. Rev. Lett. **47**, 838 (1981).
[37] M. A. Marchiolli and D. Galetti, J. Phys. A: Math. Theor. **52**, 405305 (2019).
[38] C. W. McCurdy, H. D. Meyer, and W. H. Miller, J. Chem. Phys. **70**, 3177 (1979).
[39] H. Meyer and W. H. Miller, J. Chem. Phys. **72**, 2272 (1980).
[40] See Appendix C of Ref. 43 for a detailed discussion.
[41] S. J. Cotton and W. H. Miller, J. Phys. Chem. A **119**, 12138 (2015).
[42] It turns out that this mapping approach does not generate the exact results for an isolated quantum system, see discussions in Sec VI of Ref. 24.
[43] J. E. Runeson and J. O. Richardson, J. Chem. Phys. **152**, 084110 (2020).
[44] R. L. Stratonovich, Sov. Phys. JETP **4** (1957).
[45] J. C. Várilly and J. M. Gracia-Bondía, Ann. Phys. **190**, 107 (1989).
[46] J. M. Radcliffe, J. Phys. A: Gen. Phys. **4**, 313 (1971).
[47] K. Nemoto, J. Phys. A: Math. Gen. **33**, 3493 (2000).
[48] T. Tilma and E. C. G. Sudarshan, J. Phys. A: Math. Gen. **35**, 10467 (2002).
[49] T. Tilma and E. Sudarshan, J. Geom. Phys. **52**, 263 (2004).
[50] T. Tilma and K. Nemoto, J. Phys. A: Math. Theor. **45**, 015302 (2011).
[51] H. Lang, O. Vendrell, and P. Hauke, J. Chem. Phys. **155**, 024111 (2021).
[52] F. Halzen and A. Martin, *Quarks and Leptons: An Introductory Course in Modern Particle Physics* (Wiley, 1984).
[53] W. Pfeifer, *The Lie Algebras SU(N): An Introduction* (Springer, 2003).
[54] M. Gell-Mann, Phys. Rev. **125**, 1067 (1962).
[55] R. A. Bertlmann and P. Krammer, J. Phys. A: Math. Theor. **41**, 235303 (2008).
[56] Note that the usual way to write down this state is $|\mathbf{u}\rangle = \cos\frac{\theta}{2}e^{-i\varphi/2}|1\rangle + \sin\frac{\theta}{2}\cdot e^{i\varphi/2}|2\rangle$. This specific choice of splitting phase φ does not influence any physical expectation values we aim to calculate.
[57] More generally, for a given n-dimensional Lie algebra $\mathfrak{g}$, there is an associated simply connected n-dimensional Lie group G (which is also a manifold) whose Lie algebra is isomorphic to $\mathfrak{g}$. This is referred to as the Lie's third theorem. See Ref. 29 or 58.
[58] D. Bump, *GTM225: Lie Groups, 2nd Ed.* (Springer, Switzerland, 2013).
[59] Note that in the work of Tilma and Nemoto[50], the main focus is to get the correct integrated value over all the Euler angles, which is not sensitive to the peak of the distribution. However, to make a consistent phase space volume with the choice of the coherence state we used in Eq. 18 that gives the correct peak position along θ_n (see Fig. 6), we need to make this specific choice of $d\mathbf{\Omega}$ in Eq. 21.
[60] C. Brif and A. Mann, J. Phys. A: Math. Gen. **31**, L9 (1998).
[61] F. Bloch, Phys. Rev. **70**, 460 (1946).
[62] R. K. Wangsness and F. Bloch, Phys. Rev. **89**, 728 (1953).
[63] I. I. Rabi, N. F. Ramsey, and J. Schwinger, Rev. Mod. Phys. **26**, 167 (1954).
[64] To the best of our knowledge, we do not see this expression in the previous literature. We also made an incorrect statement in our previous work in Ref. 35 by suggesting that for s≠Q, there is no simple relation between $\hat{w}_s$ and $|\mathbf{\Omega}\rangle\langle\mathbf{\Omega}|$, which is not true because of Eq. 27.
[65] E. Wigner, Phys. Rev. **40**, 749 (1932).
[66] J. E. Moyal, Math. Proc. Camb. Philos. Soc. **45**, 99–124 (1949).
[67] M. A. C. Saller, A. Kelly, and J. O. Richardson, Faraday Discuss. **221**, 150 (2020).

Since the cos\theta_n and sin\theta_n are of different sequences in Tilma and Nemoto's work and this manuscript, the meaning of theta_n are obviously different, and should be treated differently when one wants to talk about distributions. Thus, 59 is very strange, seemingly have failure in understanding the literature. And for 64, same expressions just are here in WIREs. Comput. Mol. Sci. e1619 (2022).

The authors of Ref. 43 are clearly aware of this issue. They omit this phase for sake of convenience, not ignoring it.

[68] M. A. C. Saller, J. E. Runeson, and J. O. Richardson, Path-integral approaches to non-adiabatic dynamics, in *Quantum Chemistry and Dynamics of Excited States* (John Wiley & Sons, 2020) Chap. 20, pp. 629–653.

[69] A. Heslot, Phys. Rev. D **31**, 1341 (1985).

[70] The original definitions of $\{q_n, p_n\}$ in Eq. 27-28 of Ref. 43 are missing this phase $e^{i\Phi}$.

[71] U. Müller and G. Stock, J. Chem. Phys. **111**, 77 (1999).

[72] S. J. Cotton and W. H. Miller, J. Chem. Phys. **145**, 144108 (2016).

[73] S. J. Cotton and W. H. Miller, J. Chem. Phys. **150**, 194110 (2019).

[74] X. He, Z. Gong, B. Wu, and J. Liu, J. Phys. Chem. Lett. **12**, 2496 (2021).

[75] W.-M. Zhang and D. H. Feng, Phys. Rep. **252**, 1 (1995).

[76] A. N. S. Bonella and R. Kapral, J. Chem. Phys. **133**, 134115 (2010).

[77] T. J. H. Hele and N. Ananth, Faraday Discuss. **195**, 269 (2016).

[78] S. N. Chowdhury and P. Huo, J. Chem. Phys. **154**, 124124 (2021).

[79] X. Sun, H. Wang, and W. H. Miller, J. Chem. Phys. **109**, 7064 (1998).

[80] J. A. Poulsen, G. Nyman, and P. J. Rossky, J. Chem. Phys. **119**, 12179 (2003).

[81] Q. Shi and E. Geva, J. Chem. Phys. **118**, 8173 (2003).

[82] T. J. H. Hele, M. J. Willatt, A. Muolo, and S. C. Althorpe, J. Chem. Phys. **142**, 134103 (2015).

[83] M. Hillery, R. O'Connell, M. Scully, and E. Wigner, Phys. Rep. **106**, 121 (1984).

[84] W. B. Case, American Journal of Physics **76**, 937 (2008).

[85] See Fig. 7 in Ref. 34.

[86] H. Groenewold, Physica **12**, 405 (1946).

[87] K. Imre, E. Özizmir, M. Rosenbaum, and P. F. Zweifel, J. Math. Phys. **8**, 1097 (1967).

[88] S. Bonella and D. Coker, J. Chem. Phys. **118**, 4370 (2003).

[89] Q. Shi and E. Geva, J. Phys. Chem. A **108**, 6109 (2004).

[90] H. Wang, X. Sun, and W. H. Miller, J. Chem. Phys. **108**, 9726 (1998).

[91] X. Sun, H. Wang, and W. H. Miller, J. Chem. Phys. **109**, 7064 (1998).

[92] J. R. Klauder, Phys. Rev. D **19**, 2349 (1979).

[93] One can use the conjugate relationship between φ_n and Θ_n to get $\dot{\varphi}_n = \frac{\partial H_\mathrm{s}}{\partial \Theta_n} = \sum_{j=1}^{n} \frac{\partial H_\mathrm{s}}{\partial \theta_j} \frac{\partial \theta_j}{\partial \Theta_n} = \sum_{j=1}^{n} \frac{\partial H_\mathrm{s}}{\partial \theta_j} \left(\frac{\partial \Theta_n}{\partial \theta_j} \right)^{-1}$, but the detailed expression obtained from the above equation is long and tedious to use.

[94] One can, in principle, directly derive Eq. 117 from Eq. 98c using the transformation in Eq. 49 and the expressions of the structure constant f_{ijk} in Eq. A5, through a rather tedious process.

[95] M. S. Church, T. J. H. Hele, G. S. Ezra, and N. Ananth, J. Chem. Phys. **148**, 102326 (2018).

[96] P. Ehrenfest, Z. Phys. **45**, 455 (1927).

[97] A. D. McLachlan, Mol. Phys. **8**, 39 (1964).

[98] R. Grunwald, A. Kelly, and R. Kapral, Quantum dynamics in almost classical environments, in *Energy Transfer Dynamics in Biomaterial Systems*, edited by I. Burghardt, V. May, D. A. Micha, and E. R. Bittner (Springer Berlin Heidelberg, Berlin, Heidelberg, 2009) pp. 383–413.

[99] S. N. Chowdhury and P. Huo, J. Chem. Phys. **150**, 244102 (2019).

[100] J. Liu and W. H. Miller, J. Chem. Phys. **134**, 104101 (2011).

[101] S. Habershon and D. E. Manolopoulos, J. Chem. Phys. **131**, 244518 (2009).

[102] W. H. Miller, J. Phys. Chem. A **113**, 1405 (2009).

[103] G. Stock and M. Thoss, Mixed quantum-classical description of the dynamics at conical intersections, in *Conical Intersections* (World Scientific Publishing, 2004) pp. 619–695.

[104] R. Schneider and W. Domcke, Chem. Phys. Lett. **150**, 235 (1988).

[105] J. R. Mannouch and J. O. Richardson, J. Chem. Phys. **153**, 194109 (2020).

[106] J. R. Mannouch and J. O. Richardson, J. Chem. Phys. **153**, 194110 (2020).

[107] H. Köppel, L. S. Cederbaum, and W. Domcke, J. Chem. Phys. **89**, 2023 (1988).

[108] H. Köppel, Chem. Phys. Lett. **205**, 361 (1993).

[109] J. Liu, X. He, and B. Wu, Acc. Chem. Res. **54**, 4215 (2021).

[110] On page 106 of Ref. 53 (Chapter 6), the author suggested that "In order to determine the structure constants of $\mathfrak{su}(N)$, no closed formulas are known, they have to be calculated by means of performing matrix multiplications [Eq. 9 in the current note].".

[111] R. Gilmore, *Lie Groups, Physics, and Geometry: An Introduction for Physicists, Engineers and Chemists* (Cambridge University Press, 2008).

[112] H. Kim, Chem. Phys. Lett. **436**, 111 (2007).

[113] S. Bonella and D. F. Coker, Chem. Phys. **268**, 189 (2001).

[114] C. Hsieh and R. Kapral, J. Chem. Phys. **137**, 22A507 (2012).

[115] C. Hsieh and R. Kapral, J. Chem. Phys. **138**, 134110 (2013).

[116] D. T. Pegg and S. M. Barnett, Phys. Rev. A , **39**, 1665 (1989).

[117] A. Nassimi, S. Bonella, and R. Kapral, J. Chem. Phys. **133**, 134115 (2010).

[118] W. K. Wootters, Ann. Phys **176**, 1 (1987).

[119] K. S. Gibbons, M. J. Hoffman, and W. K. Wootters, Phys. Rev. A **70**, 062101 (2004).

[120] S. A. Sato, A. Kelly, and A. Rubio, Phys. Rev. B **97**, 134308 (2018).

[121] A. Garg, J. N. Onuchic, and V. Ambegaokar, J. Chem. Phys. **83**, 4491 (1985).

[122] A. Kelly, N. Brackbill, and T. E. Markland, J. Chem. Phys. **142**, 094110 (2015).

[123] I. R. Craig and D. E. Manolopoulos, J. Chem. Phys. **122**, 084106 (2005).

[124] R. Schneider and W. Domcke, Chem. Phys. Lett. **159**, 61 (1989).

[125] G. Stock, J. Chem. Phys. **103**, 2888 (1995).

[126] A. Mandal, S. S. Yamijala, and P. Huo, J. Chem. Theory Comput. **14**, 1828 (2018).